

Certification

**Quantification of Bacterial RubisCO Genes and Their Expression in Soil Adjacent to H₂
Releasing Legume Nodules**

by

Bryan CJ Flynn

**A Thesis Submitted to Saint Mary's University, Halifax, Nova Scotia,
in Partial Fulfillment of the Requirements for
the Degree of Masters of Applied Science**

May, 2011, Halifax, Nova Scotia

Copyright Bryan Flynn, 2011

**Approved: Dr. Zhongmin Dong
Supervisor
Department of Biology**

**Approved: Dr. Yantai Gan
External Examiner
Research Scientist, Agriculture and Agri-food Canada**

**Approved: Dr. Kevin Vessey,
Supervisory Committee Member
Department of Biology**

**Approved: Dr. Adam Sarty,
Supervisory Committee Member
Department of Astronomy and Physics**

**Approved: Dr. Jeremy Lundholm
Program Representative**

**Approved: Dr. Diane Crocker
Graduate Studies Representative**

Date: May 19, 2011



Library and Archives
Canada

Published Heritage
Branch

395 Wellington Street
Ottawa ON K1A 0N4
Canada

Bibliothèque et
Archives Canada

Direction du
Patrimoine de l'édition

395, rue Wellington
Ottawa ON K1A 0N4
Canada

Your file *Votre référence*
ISBN: 978-0-494-81323-2
Our file *Notre référence*
ISBN: 978-0-494-81323-2

NOTICE:

The author has granted a non-exclusive license allowing Library and Archives Canada to reproduce, publish, archive, preserve, conserve, communicate to the public by telecommunication or on the Internet, loan, distribute and sell theses worldwide, for commercial or non-commercial purposes, in microform, paper, electronic and/or any other formats.

The author retains copyright ownership and moral rights in this thesis. Neither the thesis nor substantial extracts from it may be printed or otherwise reproduced without the author's permission.

In compliance with the Canadian Privacy Act some supporting forms may have been removed from this thesis.

While these forms may be included in the document page count, their removal does not represent any loss of content from the thesis.

AVIS:

L'auteur a accordé une licence non exclusive permettant à la Bibliothèque et Archives Canada de reproduire, publier, archiver, sauvegarder, conserver, transmettre au public par télécommunication ou par l'Internet, prêter, distribuer et vendre des thèses partout dans le monde, à des fins commerciales ou autres, sur support microforme, papier, électronique et/ou autres formats.

L'auteur conserve la propriété du droit d'auteur et des droits moraux qui protègent cette thèse. Ni la thèse ni des extraits substantiels de celle-ci ne doivent être imprimés ou autrement reproduits sans son autorisation.

Conformément à la loi canadienne sur la protection de la vie privée, quelques formulaires secondaires ont été enlevés de cette thèse.

Bien que ces formulaires aient inclus dans la pagination, il n'y aura aucun contenu manquant.


Canada

ABSTRACT

Quantification of Bacterial RubisCO Genes and Their Expression in Soil Adjacent to H₂ Releasing Legume Nodules

By Bryan CJ Flynn

The release of H₂ from legume nodules has many positive effects on soil health; H₂ has been shown to increase CO₂ fixation in soils. RubisCO plays an important role in bacterial CO₂ fixation. The effect of H₂ on CO₂ fixation was determined by quantifying the copies and expression of the RubisCO large subunit gene, *cbbL*. *cbbL* gene copies and expression were quantified from soil surrounding H₂ releasing (Hup⁻) and H₂ conserving (Hup⁺) nodules and from controlled H₂ and air treated soils with varying times of exposure. A significant increase in *cbbL* gene copies and expression was found in H₂ treated soils compared to air treated soils. A trend was noted, that higher gene copies and expression were found in soil adjacent to Hup⁻ nodules compared to Hup⁺ nodules; however, there was no significant difference between the two.

May 19, 2011

Acknowledgements

First, I would like to extend my deepest gratitude to my supervisor, Dr. Zhongmin Dong. His support, guidance, encouragement and knowledge has made this work possible, and helped me in developing the skills required for this research.

I would like to thank external examiner, Dr. Yantai Gan, and my committee members, Dr. Kevin Vessey and Dr. Adam Sarty. Their support and knowledge was a great help throughout my research and it was an honor to have them review my work and provide me with valuable feedback.

I would like to thank everyone at the German Research Centre for Environmental Health, particularly, Dr. Anton Hartmann, Dr. Michael Schloter, Dr. Felix Haessler and Ms. Sylvia Hanyka. Their support helped greatly in the development of my methods and provided me with valuable lab experience.

I would like to thank Xiang (Nancy) He, Sarah Hall, Andrew Weseen, and Amber Leigh-Golding for all of their support and assistance with my lab work and in the development of my project. I would also like to thank Ms. Carman Cranley, Ms. Heidi de Boer, Ms. Jing Yang, Ms. Lehka Panmanathan, Ms. Elizabeth McLeod, Ms. Darlene Goucher, Ms. Janet White and Ms. Susan Dore for all of their much needed assistance over the last few years.

I would like to thank my partner and best friend, Melanie Mills, for all of her support, patience and love throughout the last few years. You have helped me through some of the toughest times that I've had. I love you.

Thank you to my parents, Marion and Charles Flynn; their love and support has helped me through the last few years. Words cannot express how much I appreciate what you have done for me. Thank you also to my brothers and sister for always being there for me when I needed them.

Finally, thank you to all of my friends and family, for providing me with many laughs and relieving stress. And to everyone else who played any role in helping me get to where I am today, thank you.

TABLE OF CONTENTS

1. INTRODUCTION	1
1.1 SOIL AND ENVIRONMENTAL HEALTH.....	1
1.2 AGRICULTURE AND THE ENVIRONMENT.....	2
1.2.1 The Carbon Cycle.....	2
1.2.2 The Carbon Cycle in Agriculture.....	2
1.2.3 The Nitrogen Cycle and the Nitrogen Fertilizers.....	3
1.3 CROP ROTATION	4
1.3.1 Legume Rotation	4
1.3.2 Effects of Legumes on Crop Production and Soil Health	5
1.4 THE NATURE OF LEGUMES	7
1.4.1 Nodule Formation	7
1.4.2 Hydrogen Production	8
1.4.3 Hydrogenase Uptake.....	8
1.4.4 Nitrogenase Activity vs. Hydrogen Production.....	9
1.5 LEGUMES AND THE SOIL MICROBIAL COMMUNITY	9
1.6 CHANGES IN GAS EXCHANGE IN SOIL.....	12
1.6.1 Hydrogen Oxidation	12
1.6.2 Carbon Dioxide Fixation	12
1.6.2.1 CO ₂ Fixation in Soil and Roots.....	12
1.6.2.2 Enzymes Involved in CO ₂ Fixation.....	13
1.6.2.3 RubisCO	14
1.7 MOLECULAR TECHNIQUES AND APPLICATION	15
1.7.1 Polymerase Chain Reaction	15
1.7.2 Real Time PCR	16
1.7.3 Absolute Quantification using External Calibration.....	18
1.7.4 Real Time PCR in Microbial Studies	19
1.7.5 Real Time PCR in RubisCO Studies	19
1.7.5.1 RubisCO Genes in Non-soil Media	19
1.7.5.2 RubisCO Genes in Soil Bacteria	20
1.8 CONCLUSIONS.....	20
2 MATERIALS AND METHODS	24
2.1 SOIL TREATMENT.....	24
2.1.1 Controlled H ₂ Treatment.....	24
2.1.2 Controlled Air Treatment.....	25
2.2 SOIL GAS EXCHANGE MONITORING	25
2.2.1 Standard Curve for ppm H ₂ Calculation.....	26
2.2.2 H ₂ Uptake Measurements.....	26

2.2.3 Soil Collection for H ₂ and Air Treated Samples	27
2.3 SOYBEAN RHIZOSPHERE SOIL PREPARATION.....	32
2.3.1 Surface Sterilization of Seeds.....	32
2.3.2 Inoculation with Rhizobia Bacteria	32
2.3.3 Soybean Growth.....	33
2.3.4 Soil Collection from Rhizosphere	35
2.3.5 Testing HUP Status.....	35
2.5 RNA EXTRACTION FROM SOIL SAMPLES.....	36
2.6 cDNA PREPARATION	38
2.6.1 RNA Purification	38
2.6.2 Reverse Transcription of RNA to cDNA.....	39
2.7 PCR FOR RUBISCO LARGE SUB-UNIT GENES	40
2.8 PRIMER DESIGN FOR GREEN-LIKE CBBL REAL TIME PCR.....	41
2.9 QUANTIFICATION OF CBBL GENE COPIES AND EXPRESSION	42
2.9.1 Preparation of Standards	42
2.9.1.1 Internal vs. External Standards	42
2.9.1.2 Amplification for Cloning	43
2.9.1.3 Purification of PCR Product.....	44
2.9.2 Cloning.....	44
2.9.2.1 Ligation and Transformation.....	44
2.9.2.2 Plasmid Linearization	46
2.9.3 Generation of Standard Curve	46
2.10 QUANTITY OF CBBL GENES IN UNKNOWN SAMPLES	47
2.10.1 Preparation of Unknown Samples	47
2.10.2 Calculating Quantity of cbbL in Unknowns	48
2.10.3 Limit Detection, Quantification Limit and Undetected Expression	49
2.11 <i>CBBL</i> SEQUENCING.....	50
3 RESULTS	51
3.1 CONTROLLED GAS TREATMENT	51
3.1.1 Standard Curve.....	51
3.1.2 H ₂ Treated Soil Samples	51
3.1.3 Air Treated Soil Samples	53
3.2 RHIZOSPHERE SOIL SAMPLES.....	53
3.3 NUCLEOTIDE EXTRACTION	54
3.3.1 DNA Extraction	54
3.3.2 RNA Extraction	55
3.4 DETECTION AND QUANTIFICATION OF RUBISCO <i>CBBL</i> GENES.....	56
3.4.1 Real Time PCR Primer Testing.....	56
3.4.2 Quantification of RubisCO Genes from Gas Treated Soils	57
3.4.2.1 Primer Set cbbLR1F/cbbLR1intR	57

3.4.2.2 Primer Set cbbLG1F/cbbLG2R1	58
3.4.3 Quantification of RubisCO Genes from Rhizosphere Soil	59
3.4.3.1 Primer Set cbbLR1F/cbbLR1intR	59
3.4.3.2 Primer Set cbbLG1F/cbbLG2R1	59
3.4.4 Statistical Variation in Gene Copies	60
3.4.4.1 Primer Set cbbLR1F/cbbLR1intR	60
3.4.4.2 Primer Set cbbLG1F/cbbLG2R1	61
3.4.5 Quantification of RubisCO Gene Expression from Gas Treated Soils	61
3.4.5.1 Primer Set cbbLR1F/cbbLR1intR	61
3.4.6 Quantification of RubisCO Gene Expression from Rhizosphere	63
3.4.6.1 Primer Set cbbLR1F/cbbLR1intR	63
3.4.6.2 Primer Set cbbLG1F/cbbLG2R1	63
3.4.7 Statistical Variation in Gene Expression	64
3.4.7.1 Primer Set cbbLR1F/cbbLR1intR	64
3.4.7.2 Primer Set cbbLG1F/cbbLG2R1	65
3.5 SEQUENCING RESULTS FOR REAL-TIME PRIMERS.....	65
3.5.1 Cloning for Primer Set cbbLR1F/cbbLR1intR.....	65
3.5.2 Cloning for Primer Set cbbLG1F/cbbLG2R1	66
3.5.3 Cloning for H ₂ vs. Air treated Soils	66
4 DISCUSSION	160
4.1 CONTROLLED GAS TREATMENT	160
4.1.1 H ₂ Uptake	160
4.1.2 CO ₂ Exchange	161
4.2 SOYBEAN TRIALS AND RHIZOSPHERE SOIL SAMPLES.....	161
4.3 NUCLEOTIDE EXTRACTION YIELDS	162
4.3.1 DNA Extraction	162
4.3.2 RNA Extraction	163
4.4 CBBL GENE COPY NUMBERS	163
4.5 CBBL GENE EXPRESSION	167
4.6 INHIBITION	171
4.7 WHY CBBL?	171
4.8 TAQMAN VS. SYBR GREEN PCR CHEMISTRIES.....	172
4.9 <i>CBBL</i> SEQUENCING DATA	172
5 GENERAL CONCLUSIONS.....	174
6 REFERENCES	177

LIST OF FIGURES

Figure M1 – Diagram of controlled H ₂ and air treatment system (Dong and Layzell, 2001).....	28
Figure M2 – Setup for H ₂ uptake measurements using controlled gas flow and Qubit H ₂ sensor. (He, 2009).....	30
Figure 1 – Standard curve for [H ₂] calculations showing [H ₂] in ppm vs. voltage output detected (V). Equation of the exponential trend line was found to be $y = 7.8912e^{1.269x}$, where x is the voltage detected and e is the natural number.	70
Figure 2 – H ₂ uptake plot for treatment H ₂ T1. Treatment lasted for 77 days. Y-axis shows H ₂ uptake rate in μmol absorbed per hour per gram soil and X-axis shows number of days of treatment at time of measurement.....	74
Figure 3 – H ₂ uptake plot for treatment H ₂ T2. Treatment lasted for 47 days. Y-axis shows H ₂ uptake rate in μmol absorbed per hour per gram soil and X-axis shows number of days of treatment at time of measurement.....	78
Figure 4 – CO ₂ exchange plot for treatment H ₂ T1. Treatment lasted for 77 days. Y-axis shows CO ₂ exchange rate in μmol per hour per gram soil and X-axis shows H ₂ uptake rate in μmol absorbed per hour per gram soil.	82
Figure 5 – CO ₂ exchange plot for treatment H ₂ T1. Treatment lasted for 77 days. Y-axis shows CO ₂ exchange rate in μmol per hour per gram soil and X-axis shows number of days of treatment at time of measurement	84
Figure 6 – CO ₂ exchange plot for treatment H ₂ T2. Treatment lasted for 47 days. Y-axis shows CO ₂ exchange rate in μmol per hour per gram soil and X-axis shows H ₂ uptake rate in μmol absorbed per hour per gram soil.	88
Figure 7 – CO ₂ exchange plot for treatment H ₂ T2. Treatment lasted for 47 days. Y-axis shows CO ₂ exchange rate in μmol per hour per gram soil and X-axis shows number of days of treatment at time of measurement	90
Figure 8 - H ₂ uptake plot for treatments H ₂ T3. Treatment lasted for 32 days. Y-axis shows H ₂ uptake rate in μmol absorbed per hour per gram soil and X-axis shows number of days of treatment at time of measurement.	96
Figure 9 – CO ₂ exchange plot for treatments H ₂ T3. Treatment lasted for 47 days. Y-axis shows CO ₂ exchange rate in μmol per hour per gram soil and X-axis shows H ₂ uptake rate in μmol absorbed per hour per gram soil.	98
Figure 10 – CO ₂ exchange plot for treatments H ₂ T3. Treatment lasted for 47 days. Y-axis shows CO ₂ exchange rate in μmol per hour per gram soil and X-axis shows number of days of treatment at time of measurement	100

Figure 11 – H ₂ uptake plot for treatment AT1. Treatment lasted for 47 days. Y-axis shows H ₂ uptake rate in μmol absorbed per hour per gram soil and X-axis shows number of days of treatment at time of measurement	104
Figure 12 – H ₂ uptake plot for treatment AT2. Treatment lasted for 77 days. Y-axis shows H ₂ uptake rate in μmol absorbed per hour per gram soil and X-axis shows number of days of treatment at time of measurement.	108
Figure 13 – CO ₂ exchange plot for treatment AT1. Treatment lasted for 47 days. Y-axis shows CO ₂ exchange rate in μmol per hour per gram soil and X-axis shows number of days of treatment at time of measurement	112
Figure 14 – CO ₂ exchange plot for treatment AT2. Treatment lasted for 77 days. Y-axis shows CO ₂ exchange rate in μmol per hour per gram soil and X-axis shows number of days of treatment at time of measurement	116
Figure 15 – Reference for comparison of H ₂ uptake rates of treatments at time of collection.....	118
Figure 16 – Methylene blue assays for nodules of soybean plants inoculated with JH47	122
Figure 17 – Methylene blue assays for nodules of soybean plants inoculated with JH.	124
Figure 18 – Methylene blue assays for nodules of soybean plants inoculated with volunteer nodules. Nodules were treated as Hup ⁻	126
Figure 19 –DNA/RNA extracted from all soil treatments. Chart displays calculated mean with standard error bars.	132
Figure 20 –PCR result for cbbLR1F/cbbLR1R for red-like <i>cbbL</i> (wells 2-5) and cbbLG1F/cbbLG1R for green-like (wells 8-11). Wells 2, 3, 8 and 9 contain DNA from Air treated soil and 4,5,10 and 11 contain DNA from H ₂ treated soil.	134
Figure 21–Example of PCR result for cbbLR1F/cbbLR1intR. Shows cDNA result for air treated soil (wells 2, 3), rhizosphere soils (wells 4, 5, 6) and plasmid control (well 7). Bottom band of ladder = 250 bp.....	136
Figure 22 –Example of PCR result for cbbLG1F/cbbLG2R1. Shows DNA results for H ₂ treated soil (wells 2-5), rhizosphere (wells 6-9) and negative control (well 10).	138
Figure 23 – Average gene copy number and gene expression for primer set cbbLR1F/cbbLR1intR. Figures show average quantification with standard error bars. Figure 23a shows copies per ng DNA/RNA. Figure 23b shows DNA/RNA copies per g soil.....	148
Figure 24 – Average gene copy number and gene expression for primer set cbbLG1F/cbbLG2R1. Figures show average quantification with standard error bars. Figure 24a shows copies per ng DNA/RNA. Figure 24b shows DNA/RNA copies per g soil.....	150

Figure 25 – Example of real time PCR results. Labels include standards (10^8 , 10^6 , 10^4 and 10^3), unknown sample, inhibition control (unknown+ 10^4) and negative control
..... 152

LIST OF TABLES

Table M1 – Real time PCR primers used in this study.....	42
Table 1 – Standard curve data for H ₂ uptake calculations from controlled gas treated soils.....	68
Table 2 – H ₂ uptake data for treatment H ₂ T1.....	72
Table 3 – H ₂ uptake data for treatment H ₂ T2.....	76
Table 4 – CO ₂ exchange data for treatment H ₂ T1.....	80
Table 5 – CO ₂ exchange data for treatment H ₂ T2.....	86
Table 6 – H ₂ uptake data for two treatments, H ₂ T3.....	92
Table 7 – CO ₂ exchange data for two treatments, H ₂ T3.....	94
Table 8 – H ₂ uptake data for treatment AT1.....	102
Table 9 – H ₂ uptake data for treatment AT2.....	106
Table 10 – CO ₂ exchange data for treatment AT1.....	110
Table 11 – CO ₂ exchange data for treatment AT2.....	114
Table 12 – Reference table for general trends in H ₂ uptake rate and CO ₂ exchange rate in gas treated samples.....	120
Table 13 – DNA extraction data for all treatments. Data includes maximum, minimum and mean DNA extracted for all treatments. Measured in ng DNA per g soil. ..	128
Table 14 – RNA extraction data for all treatments. Data includes maximum, minimum and mean DNA extracted for all treatments. Measured in ng RNA per g soil....	130
Table 15 – cbbLR1F/cbbLR1intR gene copy data for all treatments. Includes copies per ng DNA and copies per g soil. Table 15a shows copies per ng DNA and Table 15b shows copies per g soil. Note: subscript letters with means show significant groupings (p<0.05).....	140
Table 16 – cbbLG1F/cbbLG2R1 gene copy data for all treatments. Includes copies per ng DNA and copies per g soil. Table 16a shows copies per ng DNA and Table 16b shows copies per g soil.....	142
Table 17 – cbbLR1F/cbbLR1intR gene expression data for all treatments. Includes copies per ng RNA and RNA copies per g soil. Table 17a shows copies per ng RNA and Table 17b shows copies per g soil Note: subscript letters with means show significant groupings (p<0.05).....	144

Table 18 – cbbLG1F/cbbLG2R1 gene expression data for all treatments. Includes copies per ng DNA and copies per g soil. Table 18a shows copies per ng RNA and Table 18b shows RNA copies per g soil	146
Table 19 – Sequencing results for primer set cbbLR1F/cbbLR1intR. 186 Cases	154
Table 20 – Sequencing results for primer set cbbLG1F/cbbLG2R1. 74 Cases	156
Table 21 – Sequencing results for primer set cbbLR1F/cbbLR1intR comparing species found in Air and H ₂ treated soils.....	158

1. Introduction

1.1 Soil and Environmental Health

With the ever growing human population of the planet, increased investments to research are being made to ensure that crop production continues to supply enough food for the global community. Soil health is of critical importance when attempting to maintain sustainable agricultural systems, and also in maintaining health of the global environment. Soil health can be a vague term; Doran and Zeiss (2000) define soil health as “the capacity of soil to function as a vital living system, within ecosystem and land-use boundaries, to sustain plant and animal productivity, maintain or enhance water and air quality, and promote plant and animal health”. Generally speaking, healthy soil is a much better medium for the growth of crops than deficient soils. There are many indicators of soils health. Microorganisms are a major contributor to soil quality and health. A good microbiological or biochemical indicator of soil quality and health should be easily measured, be consistent in a wide range of environments and consistently reveal when problems exist (Schloter *et al.*, 2003). Indicators of soil health can include the microbial biomass of the soil (mainly bacterial and fungal), structural microbial diversity (community structural balance of all species of microorganisms present in the soil), the activity of microorganisms in the soil, nitrogen turnover rates (through microbial nitrification and denitrification) and faunal indicators, which are other organisms that play an important role in soil health and quality (such as nematodes)

(Schloter *et al.*, 2003). Many of these indicators are contributors to soil organic carbon which is another indicator of soil health.

1.2 Agriculture and the Environment

1.2.1 The Carbon Cycle

Carbon is well known as the element of life; it is the third most abundant element in the human body (9%) and the fifth most abundant element in the universe (0.021%) (Frieden, 1972). The carbon cycle involves the cycling of carbon through various organic and inorganic compounds through the terrestrial environment, oceans, atmosphere, etc. Shifting land use throughout the world from forestry to agriculture over the past 300 years, increased consumption of fossil fuels and other industrial and agricultural practices have led to dramatic changes in the global carbon cycle, namely by depleting soil carbon stocks and increasing atmospheric carbon levels (Houghton and Skole, 1990).

1.2.2 The Carbon Cycle in Agriculture

One major contributor to soil carbon loss to CO₂ is the agricultural practice of tilling. Tillage systems involve the breaking up of land, bringing more organic matter within the soil to the surface. In the first 24 hours after tilling there is a dramatic increase in the flux of CO₂ from tilled soils when compared to non-tilled soils (Reicosky *et al.*, 2001). Shifting land use can have dramatic effects on the soil organic carbon levels; this effect can be positive or negative. Shifts that can cause a decline in soil

carbon stocks include shifts from land for pasture to plantation, native forest land to plantation, native forest to crop and most dramatically from grassland to crop (Guo and Gifford, 2002). However, due to the depletion of soil organic carbon it has been suggested that depleted agricultural soils can now act as a sink for sequestering atmospheric carbon and mitigating CO₂ emissions (Paustian *et al.*, 1997). For example, new conservation tillage systems focus on reducing soil and water loss that accompany traditional tillage systems and have been found to decrease the loss in soil organic carbon and have been suggested as a method for sequestering carbon within soil (Lal and Kimble, 1997). Conservation tillage systems leave more plant matter and microorganisms undisturbed in the soil so that carbon loss to the atmosphere is reduced.

1.2.3 The Nitrogen Cycle and the Nitrogen Fertilizers

The nitrogen cycle involves the catalytic conversion of nitrogen by organisms through its many forms (N₂, NH₃/NH₄⁺, N₂O, NO, NO₂, HNO₂/NO₂⁻, HNO₃/NO₃⁻). Much of earth's atmosphere consists of N₂; however, due to the large amount of energy necessary to break the dinitrogen bond, the majority of nitrogen used by organic life on earth is recycled from the other forms (Soderlund and Svenson, 1976; Rosswall, 1976).

Another widely used agricultural practice that can be harmful to the environment is the use of inorganic nitrogen fertilizers. Nitrogen is an important nutrient for plant growth and can have dramatic effects on crop yields. However, due to

nitrification and denitrification reactions that occur in the soil, there is a release of nitrous oxide (N_2O), which is an intermediate of these processes, and is a very harmful green house gas. Nitrification involves the enzymatic conversion of ammonium (NH_4^+) to nitrite (NO_2^-). However, at low levels of oxygen the production and evolution of nitrous oxide (N_2O) is increased (Goreau *et al.*, 1980). It has been found that increases in the usage of nitrogen based fertilizer leads to an increase in the emission of N_2O from agricultural crops (Kaiser *et al.*, 1998).

Most nitrogen based fertilizer today is made through the Haber process which catalyses the conversion of atmospheric dinitrogen to ammonia. Between the 1950's and the 1990's the industrial output of synthetic nitrogen based fertilizers has increased 27-fold (Postgate, 1998). Biological nitrogen fixation is still very important even in countries where synthetics are readily available; between 1971 and 1972 synthetic fertilizer in the United States constituted one third of all nitrogen entering soils while in Australia it accounted for less than one percent (Postgate, 1998). Nitrogen can also be introduced to soils through crop rotation which utilizes biological nitrogen fixation.

1.3 Crop Rotation

1.3.1 Legume Rotation

Crop rotation is a long standing practice in agriculture; there is even record of the use of cereal-legume and cereal-fallow rotations occurring in Roman times (White, 1970). In simple terms, crop rotation is the agricultural practice of growing different

crops on a given piece of land in order to maintain productivity. An example of a four crop rotation regime could include two cereal crops (barley, wheat, maize), a root crop (potato, turnip) and a nitrogen fixing crop (legumes such as soybean, alfalfa, or clover).

Crop rotation provides numerous benefits, such as avoiding the diminishing yields of continuous cropping and the control of pest species (Emmond and Ledingham, 1972; Roush *et al.*, 1990). Legume rotation has even been shown to decrease the occurrence of certain crop diseases, when compared to rotation regimes excluding legumes (Peters *et al.*, 2003).

1.3.2 Effects of Legumes on Crop Production and Soil Health

It has been suggested that the use of legume crops world-wide can decrease the amount of nitrogen fertilizer required to optimize growth (Verge *et al.*, 1997). There is dual reasoning behind this suggestion: first, legume crops are able to fix atmospheric nitrogen, which reduces the need for synthetic nitrogen based fertilizer, and second, legume crops are excellent rotational crops and greatly increase yield of crops grown in succession.

Generally speaking, certain types of crops deplete soil nutrients during growth and because of this there is a decrease in yield as these crops are grown continuously in the same soil from season to season. Other crops, however, are able to add needed compounds (i.e. N based compounds) into the soil. Legume crops have been found to increase yields of crops grown in rotation with them. Again, one of the most important

benefits of rotation with legume crops is the addition of nitrogen to the soil. Nitrogen budgets constructed for fields containing alfalfa in 1-, 2- and 3-year stands found that the legumes were able to add an average of 84, 148 and 137 kg of nitrogen per hectare for 1-, 2- and 3-year stands respectively (Kelner *et al.*, 1997). Kelner *et al.* suggested that a legume stand of 2 years is enough to significantly benefit the soil nitrogen status.

There have been many studies that show the benefit of using legumes in rotation with other cereal and grain crops. In a 13 year study on rotation regimes, it was found that a rotation involving two stands of alfalfa with no fertilizer led to an increase in corn yield of an average of 3500 kg ha⁻¹ when compared to continuous corn growth (Bolton *et al.*, 1976). In the same study, even one stand of alfalfa with no fertilizer led to an increase in average corn yield of 1800 kg ha⁻¹ when compared to continuous corn growth. In this study it was concluded that rotations containing 2-year stands of alfalfa were calculated to have an effect equivalent to 110 kg N fertilizer per hectare per year. In another study it was found that inoculating maize plants with soil used to grow legume plants led to a 3 to 4 fold increase in shoot growth in comparison with control plants grown in a nutrient poor medium, while those inoculated with maize soil showed no significant difference in growth (Fyson and Oaks, 1990). In the same study, a variety of tests were conducted in order to discover the nature of the growth promoting factor in the soil. Gamma radiation and sterilization by autoclaving concluded that a large amount of the growth promoting factor is biotic due to diminished growth after treatment (Fyson and Oaks, 1990). Through the application of a bactericide (streptomycin) and fungicides (benomyl

and PCNB), it was concluded that the biotic factor in the soil was fungal, although there is much discussion on this point.

More recent studies have begun to look at the potential of crop rotations with legumes to reduce the carbon footprint of certain field crops. Some crops (such as wheat) have large carbon footprints due to the large amount of resources that go into them (production, harvesting, shipping, marketing, etc.), and crop rotation has shown potential to mitigate these effects (Gan *et al.*, 2011a; Gan *et al.*, 2011b).

1.4 The Nature of Legumes

1.4.1 Nodule Formation

The formation of legume nodules plays a central role in why legumes are able to enrich soil with nutrients. Nodules are the site of nitrogen fixation. Nodules are tumor-like growths found on the roots of legume plants and are the site of a symbiotic relationship that occurs between the legume plant and certain types of bacteria called rhizobia bacteria. Nodulation is a very complex process that can occur in a number of ways involving interaction between both bacteria and plant roots. The general process involves rhizobia bacteria coming into contact with plant roots and using plant exudates to multiply and activate nodulation genes; these bacteria can then infect roots through root hairs, wounds or intact epidermis (Sprent, 1989). Nodule initiation occurs as the infection spreads to other root cells. The end result is the formation of a symbiotic

relationship between the plant and bacteria where plant tissue encapsulates the bacteria into tumor-like growths called nodules.

1.4.2 Hydrogen Production

Hydrogen gas (H_2) is a byproduct of the nitrogen fixation pathway. Hydrogen produced is the result of nitrogen fixation within the root nodules, and the production rate of H_2 is directly related to the rate of nitrogen fixation. In a study involving the measurement of hydrogen gas released from leguminous soil, it was found that actions taken to reduce the nitrogen fixation rate in nodules, such as topping plants, keeping plants in dark so that light reactions could not occur and adding NH_4Cl , all led to a decrease in the release of hydrogen from nodules (Conrad and Seiler, 1980). It was also found that hydrogen production was at a peak during the vegetation phase of plant growth. It has been calculated that the total hydrogen production from all soils containing legume plants was 0.9-1.2 Tg per year and that the global sink strength of soil to hydrogen gas was calculated to be 70-110 Tg per year (Conrad and Seiler, 1980).

1.4.3 Hydrogenase Uptake

One way of classifying the rhizobia forming legume nodules is based on the presence or absence of the enzyme uptake hydrogenase (HUP). Hydrogen uptake positive strains (HUP^+) produce H_2 through metabolic processes but the hydrogen is oxidized within the nodule, while hydrogen uptake negative strains (HUP^-) produce hydrogen and release it into the soil environment surrounding the nodule. In a study

involving the nature of the *Rhizobium japonicum* bacteria that infect major U.S. soybean crops, it was found that more than 75% of the soybean crops in the U.S. were lacking the uptake hydrogenase enzyme (Uratsu *et al.*, 1982). Another study found that almost all (>99.9%) commercially inoculated alfalfa and clover crops tested show low levels of hydrogenase activity (Ruiz-Argueso *et al.*, 1979).

1.4.4 Nitrogenase Activity vs. Hydrogen Production

It is interesting to note that there is no discernable difference in the rate of nitrogen fixation activity and production of hydrogen within HUP⁺ and HUP⁻ nodules (Shubert *et al.*, 1977). This suggests that the release of hydrogen gas from HUP⁻ nodules compared to HUP⁺ nodules is due to the lack of a hydrogen uptake enzyme, and not due to a lack of nitrogen fixation activity producing hydrogen in HUP⁺ nodules. In the same study it was also found that 25-35% of the electron flux through the nitrogenase enzyme was being used in the production of hydrogen; when this hydrogen is released instead of recycled, it represents a large energy expenditure for HUP⁻ plants (Shubert *et al.*, 1977). However, as previously mentioned, these HUP⁻ plants still account for the majority of many legume species.

1.5 Legumes and the Soil Microbial Community

The questions that arise are why HUP⁻ legumes release hydrogen gas and why are they more abundant. The release of hydrogen gas by HUP⁻ strains represents an energy loss equal to about 5% of a crop's net photosynthetic carbon gain for a day (Dong

and Layzell, 2002). One might expect that this loss of energy would favor the more efficient HUP⁺ strains in legume crops, but this is not the case. One explanation is that the release of hydrogen leads to an increase in the bacterial biomass (an indicator of healthy soil) surrounding the root nodules (La Favre and Focht, 1983).

There have been many studies investigating the release of hydrogen from HUP⁻ nodules and the resulting increase in microbial biomass. In an early study of the fate of hydrogen gas released from legume nodules, it was found that the hydrogen uptake rates of soil exposed to HUP⁻ nodules was significantly higher than that of HUP⁺ nodules (La Favre and Focht, 1983). In the same study it was found that, when observing HUP⁻ nodules, the hydrogen uptake rates in soil was inversely related to the distance from the center of the root nodule; as the distance from the nodule increases the hydrogen uptake rate of the soil decreases. Similarly, it was found that the concentration of hydrogen oxidizing bacteria in the soil environment was also inversely related to the distance from the center of the root nodule; as the distance from the center of the nodule increased, the concentration of hydrogen oxidizing bacteria decreased. These findings suggest that the uptake of hydrogen from soil surrounding root nodules is accomplished, at least in part, by bacteria.

There is a relationship between the microbial biomass and H₂-uptake capabilities of soils; there is a significant positive correlation between the biomass carbon and the hydrogen uptake rates in soil; it has been suggested that the hydrogen uptake rate of the soil could be used as an indirect indicator of the soil microbial biomass (a contributor

to soil health) (Popelier *et al.*, 1985). In the same study it was concluded that the uptake of hydrogen from the soil was due to microbial metabolic action, and that there was a positive correlation between the production of hydrogen gas from legume plants and the rate of hydrogen gas uptake in the soil by microorganisms.

There has been much disagreement over the roles of bacteria and fungi in both the plant growth promoting effects of leguminous soil and in the nature of the hydrogen oxidizing entity in the soil. In a study by McLearn and Dong (2002), a variety of tests were used in order to determine if the H₂ oxidizing entity in the soil was bacterial, fungal or abiotic in nature. Sterilization of soil through autoclaving showed that the hydrogen uptake in the soil was biotic in nature. The biotic nature of the H₂ uptake was also supported by the fact that the H₂ uptake rate decreased after the addition of glucose; suggesting sugar was a preferred energy source (McLearn and Dong, 2002). Through the use of various bactericides (streptomycin, neomycin and penicillin) and fungicides (benomyl, nystatin and amphotericin B), it was concluded that the hydrogen uptake in hydrogen treated soils was performed by bacteria and not fungus, as the bactericides had the greatest negative effect of the hydrogen uptake rates.

It is evident that there are changes occurring within the soil bacterial community surrounding the legume nodule. Hydrogen gas is being released from the legume nodule into the soil surrounding it, which can lead to changes in the structure and interactions of the microbial community within that environment. Bacteria which are capable of using hydrogen gas as a source of energy begins to flourish causing

community structure changes. Because of this community structure change, it can be expected that the attributes of the soil community may now begin to change as there is a new flow of energy introduced. Some studies, such as the one previously mentioned, have begun using controlled H₂ to treat soils in order to investigate the effect of H₂ on gas exchange and bacterial community structure.

1.6 Changes in Gas Exchange in Soil

1.6.1 Hydrogen Oxidation

There exists a lag period between the introduction of H₂ gas into the soil and the gradual increase in the H₂ uptake rate (Dong and Layzell, 2001). The H₂ rate increases gradual with maintained H₂ treatment and will eventually peak. The oxidation of hydrogen by bacteria in the soil causes a change in energy flow within the soil microbial community. It was found that when hydrogen is oxidized by soil bacteria, 60% of the electrons produced are used in the consumption of O₂ while 40% of the electrons are used to fix CO₂ (Dong and Layzell, 2001).

1.6.2 Carbon Dioxide Fixation

1.6.2.1 CO₂ Fixation in Soil and Roots

Soil normally has a net CO₂ production; however, as hydrogen uptake rates increase due to hydrogen exposure, there is a gradual increase in the CO₂ fixation rate to a point where a net CO₂ consumption in soil can be observed (Dong and Layzell, 2001,

Stein *et al.*, 2005). There are also shifts in the overall community structure of bacteria within the soil; namely, there is an increase in both beta-proteobacteria and gamma-proteobacteria populations (Stein *et al.*, 2005).

CO₂ fixation has also been noted in the roots and nodules of legumes. Legume roots and nodules have been found to be able to fix CO₂ at rates of 120 and 110 nmol mg⁻¹ h⁻¹ respectively, due to the action of phosphoenolpyruvate (PEP) carboxylase (Coker and Schubert, 1981). The designation of HUP⁺ and HUP⁻ strains can also have an effect on the rate of CO₂ fixation in the nodule due to the presence or absence of hydrogen. (Simpson *et al.*, 1979). It has been suggested that Hup⁺ nodules are capable of higher CO₂ fixation within the nodule than Hup⁻ nodules when nitrogen fixation is occurring. However, Hup⁺ nodules may not elicit the same response in soil dynamics that occurs as a result of the release of hydrogen gas from Hup⁻ nodules. This suggests that both Hup⁺ crops and Hup⁻ crops may be capable of increasing CO₂ fixation in agricultural fields.

1.6.2.2 Enzymes Involved in CO₂ Fixation

Two major enzymes involved in CO₂ fixation are ribulose-1,5-bisphosphate carboxylase/oxygenase (RubisCO) and phosphoenolpyruvate (PEP) carboxylase. The main pathway through which CO₂ is fixed is the Calvin-Benson-Bassham cycle, involving the enzyme RubisCO.

RubisCO is widely believed to be the most abundant protein in the world, as it is the rate limiting enzyme in the Calvin-Benson-Bassham cycle and is found in all plants

and many other chemoautotrophic and photoautotrophic organisms (Ellis, 1979). The enzyme incorporates CO₂ into the Calvin cycle by introducing it to ribulose-1,5-bisphosphate to produce two 3-phosphoglycerate. Through a series of catalyzed reactions involving other important enzymes the Calvin cycle produces glyceraldehyde-3-phosphate which can be converted to glucose and other organic compounds for energy and growth (Garrett and Grisham, 2005).

1.6.2.3 RubisCO

Generally speaking, there are four different forms of RubisCO, forms I-IV, with RubisCO form I being the most abundant since it is found in all plants, algae, cyanobacteria, and many chemoautotrophs (Atomi, 2002). Form II RubisCO is most closely related to form I but it does not contain the small subunits (see next paragraph) (Tabita, 1988). Form II large subunit shares only a 25-30% homology to that of the form I large subunit (Tabita *et al.*, 2008). Form III RubisCO was termed for a RubisCO protein found in the Archaea, which was distinct from forms I and II. Form IV is a RubisCO-like protein which does not catalyze CO₂ fixation (Tabita, 1999; Hanson and Tabita, 2003, Tabita *et al.*, 2008).

The RubisCO form I enzyme consists of 16 subunits; eight large subunits and eight small subunits. The subunits of the RubisCO enzyme are coded for by genes belonging to the *cbb* family of genes; genes in the *cbb* family code for enzymes and proteins involved in the Calvin-Benson-Bassham cycle (Kusian and Bowien, 1997). There

are many genes involved in the production and regulation of RubisCO, including the *cbbL* gene which codes for the large subunit, the *cbbS* gene which codes for the small subunit and other genes such as the *cbbR* and *cbbZ* genes which serve regulatory purposes (Kusian and Bowien, 1997).

The form I RubisCO large subunit can also be split into two groups; red-like and green-like RubisCO (Watson and Tabita, 1996). The difference between these two groups is phylogenetic, with red-like and green-like RubisCO having sequence similarities of 57.8-100% and 60.7-100% respectively, compared to 22-100% combined (Selesi *et al.*, 2005).

Using molecular techniques this study will investigate the role of bacterial RubisCO in the H₂ induced CO₂ fixation that occurs in soils. Using a technique known as real time PCR this study will quantify changes in gene copy numbers and gene expression that occur in H₂ treated soils and in the soils adjacent to Hup⁺ and Hup⁻ nodules.

1.7 Molecular Techniques and Application

1.7.1 Polymerase Chain Reaction

Advances in molecular biology techniques have made studying genes much easier in recent years. The polymerase chain reaction (PCR) allows researchers to work with small amounts of DNA by amplifying specific regions of interest. From taxonomists to geneticists, almost all fields of biology have benefited in some way from the use of

PCR; it is no wonder that Kary Mullis won a Nobel Prize for the invention of the technique in 1984 (Bartlett & Stirling, 2003).

The PCR process can be broken down into a series of cycles: denaturation, primer annealing and primer extension. Denaturation involves the use of heat to separate the double stranded DNA helix into two separate strands. The temperature is then lowered to allow annealing (bonding of primers to DNA template) of forward and reverse primers to the DNA. The primer is a small sequence of DNA which corresponds to a specific sequence in the target DNA so that annealing can occur between the two. The choice of primers will be specific to the gene or DNA sequence which is to be amplified. The temperature is then raised once again for extension, in which an enzyme, the Taq polymerase enzyme, is activated and moves along the DNA template strand, starting from the primer, adding base pairs to match the template strand (Innis & Gelfand, 1990). These cycles are repeated a number of times (commonly 30 to 40), and each repetition will result in replication of the targeted template DNA sequence. Starting with one copy of the DNA sequence of interest, at the end of n cycles, there theoretically should be 2^n copies of the DNA sequence. The new copies of DNA that are created are known as amplicons.

1.7.2 Real Time PCR

Another great advancement in molecular techniques was the creation of the real time quantitative PCR. This process works very similarly to the traditional PCR method

but with one difference; it allows for the quantification of initial copies of the target gene being studied, during the PCR reaction.

Methods for the quantification of DNA and mRNA date back to before the use of detection systems, however currently almost all quantitative PCR (especially for mRNA) is done with the use of detection systems and software (Wang *et al.*, 1989).

A method for performing quantitative PCR involves the use of SYBR Green fluorescent dye. In this method, the PCR reaction proceeds as normal, however, the PCR master mix contains a fluorescent dye called SYBR Green. SYBR Green allows for the detection and quantification of DNA and cDNA samples as it binds to the minor grooves of unspecific double stranded DNA and emits a fluorescence which is measured by a detector (Morrison *et al.*, 1998). Since there are an increasing number of copies of the gene of interest with each round of the PCR, there will also be an increase in fluorescence; with each round of the PCR, the concentration of double stranded DNA will theoretically double. So, with each round of the PCR a higher fluorescence will be detected. The detection system will detect when a sample crosses a set fluorescence level known as a threshold; the PCR amplification cycle at which this occurs is known as the threshold cycle (Ct) (Bustin, 2009). An unknown Ct can be compared to known standards in order to quantify the unknown. The lower the Ct value is, the higher the initial quantity of gene copies.

The primer probe (Taqman) method of quantitative PCR is quite similar to regular PCR as well but with one major difference; the PCR master mix contains a fluorescent labeled probe. The probe anneals between the forward and reverse primers on the template DNA and is tagged with two fluorescent labels: a reporter and a quencher. As the polymerase enzyme moves along the template DNA it will arrive at the probe and cleave off the fluorescent marker. When the marker is cleaved from the probe there will be fluorescence emitted which is measured by a detector. Again, this fluorescence will increase with each round until the threshold is crossed, and a Ct value is obtained (Heid *et al.*, 1996).

1.7.3 Absolute Quantification using External Calibration

Absolute quantification makes use of an internal or external calibration curve in order to calculate initial amounts of DNA or cDNA (Pfaffl, 2001). Absolute quantification uses the calibrator to calculate the absolute quantity of initial gene copies in the reaction. The external calibrator can be made using recombinant RNA or recombinant DNA; while both methods have their advantages and disadvantages, recombinant DNA was used in this study for its larger quantification range, higher reproducibility and better stability within reactions and in storage (Pfaffl and Hageleit, 2001).

1.7.4 Real Time PCR in Microbial Studies

There are many examples of the use of real time quantitative PCR in gene studies. There are many reactions that occur in soil that can be measured through gene studies. Denitrification is the conversion of nitrate (NO_3^-) to nitrous oxide (N_2O) or nitrogen (N_2). There are many enzymes involved in this process such as nitrite reductase which is coded in part by the gene *nirK* which is an example of a gene that has been successfully measured through real time quantitative PCR in agricultural soil (Henry *et al.*, 2004). This is important work as it is through denitrification that much of the nitrous oxide emissions from agricultural soil are produced. Other studies include the quantification of ammonia-oxidizing bacteria in arable soils and the quantification of specific fungal species among many others (Hermansson and Lindgren, 2001; Filion *et al.*, 2003).

1.7.5 Real Time PCR in RubisCO Studies

1.7.5.1 RubisCO Genes in Non-soil Media

There are many examples of PCR and real time quantitative PCR being used in order to study RubisCO presence, abundance and activity. In a study on facultatively lithotrophic aerobic CO-oxidizing bacteria, colorless and purple sulphur-oxidizing microbial mats and DNA extracts from ash deposits from the Kilauea volcano, Nanba *et al.* (2004) were able to develop primers for the detection of the RubisCO large subunit gene. In a study on diatoms and pelagophytes from marine water Wawrick *et al.* (2002)

were able to measure RubisCO large subunit gene activity using real time quantitative PCR and found that the technique was three times more sensitive for measurement than the hybridization method of quantification used for comparison.

1.7.5.2 RubisCO Genes in Soil Bacteria

The RubisCO large subunit gene is widely used as an indicator for the presence of RubisCO in various media. The presence of the RubisCO large subunit gene has been detected in a wide variety of agricultural soils. Primers for the detection of both “red-like” and “green-like” RubisCO *cbbL* genes have been developed, and it was found that green-like *cbbL* showed relatively low levels of diversity while red-like *cbbL* showed higher levels of diversity in fertilized soils (Selesi *et al.*, 2005). Primers have also been developed for the quantification of the red-like RubisCO large subunit gene, *cbbL*, through real time quantitative PCR. It was found that the average gene copy number for the agricultural soils tested ranged from 6.8×10^6 to 3.4×10^8 copies per g soil (Selesi *et al.*, 2007).

1.8 Conclusions

In summary, the benefits of using legumes in agricultural settings are self evident. Legumes have been used for thousands of years in agriculture as rotational crops before the intricate details of their benefits were known, and the result of increased yield in crops grown in rotation was the primary goal. While yield remains a main concern for farmers around the world, other benefits achieved through the use of

legume crops in agriculture have become evident. Beyond the addition of nitrogen to the soil, there are many other benefits to the use of legumes.

There have been many studies performed in order to observe the effects of legume crops in agriculture. Effects such as increased yield of crops grown in rotation, increase in soil nitrogen and increase in soil organic matter are well documented. The increase in soil organic matter can be attributed to not only the increase in plant matter in the soil but also to the increase in microorganisms in the soil environment. The community of microorganisms consists of a wide variety of bacteria, fungus, insects and other organisms.

As previously mentioned, the introduction of hydrogen into the legume rhizosphere (area surrounding roots and nodules) affects the microbial community structure. It has been shown that with exposure to hydrogen there is an increase in the population of hydrogen oxidizing bacteria. Community structure within the microbial environment is altered which leads to changes in the nature of the community.

One notable change within the microbial community is that gas exchange is altered. H_2 treatment has been shown to increase the consumption of O_2 and there is an increase in CO_2 fixation under laboratory conditions, while H_2 is available for oxidation. A link has been found between the oxidation of hydrogen and the fixation of CO_2 as 40% of the electrons produced from oxidation are used up in the fixation of CO_2 (while 60% are used in O_2 consumption) (Dong and Layzell, 2001).

Now that it is established that the fixation of CO₂ is occurring within soils that are exposed to hydrogen, and that bacterial RubisCO genes are detectable and measurable in agricultural soils, it is now possible to determine what changes are occurring on a molecular level in order to allow this fixation to occur.

The *cbbL* gene is well studied and documented, which makes it a good candidate for studying CO₂ fixation in soils. With real time quantitative PCR techniques it will be possible to use DNA and RNA extracted from leguminous and hydrogen treated soils in order to detect changes in bacterial RubisCO gene copy numbers and gene expression that occur. Using cloning and sequencing techniques it will also be possible to identify bacterial species being measured.

The objective of this study is to quantify the bacterial RubisCO genes, red-like and green-like *cbbL*, and their expression in soils and to determine changes that occur in response to H₂ treatment. This study will determine the effects of H₂ treatment on *cbbL* gene copies and expression by quantifying in soils treated in lab with controlled H₂ until the max H₂ uptake rate is reached and in soils with prolonged exposure to H₂ and comparing results to soil treated with air as a control. This study will determine if the HUP status of a nodule has an effect on the gene copies and gene expression of *cbbL* in soil by comparing soil adjacent to HUP⁻ nodules, to soil adjacent to HUP⁺ nodules and non-inoculated roots.

It is expected that soils treated with H₂ will have higher gene copies and gene expression than control soil treated with air, due to the fact that H₂ treatment has been shown to increase CO₂ fixation in soils and it is expected that RubisCO plays a role in this phenomenon. It is also expected that soil adjacent to HUP⁻ nodules will have higher *cbbL* copies and expression than soil adjacent to HUP⁺ nodules or roots since HUP⁻ nodules release greater amounts of H₂ into to soil and a similar response in CO₂ fixation is expected.

This study should provide a better understanding of the changes occurring in the microbial community which leads to the increase in soil CO₂ fixation. A better understanding of this process as well as the other soil processes and benefits provided by legumes may help us in better utilizing the beneficial effects that legumes provide.

2 Materials and Methods

2.1 Soil Treatment

Soil used in this experiment was collected from Truro, Nova Scotia, Canada. Soil used for this experiment was mixed as a sandy clay loam (2:1 clay to sand). Sand was added to clay in order to prevent clumping in soil samples.

2.1.1 Controlled H₂ Treatment

In order to test the effects of H₂ gas exposure in soil on the abundance of RubisCO *cbbL* genes and their expression, soil was treated with a controlled source of H₂ gas. The clay/sand mixture was moistened and placed in 60 ml syringes. H₂ gas was produced through hydrolysis. Two electrodes were immersed in a solution of phosphoric acid. An electrical current was placed across the two electrodes causing the hydrolysis of the acid and the production of hydrogen gas. Air flow was generated from a Maxima air pump; air was pumped into the flask containing the electrodes where it mixes with H₂ gas. The H₂ and air mixture was then passed through a flask containing water to moisten the gas. Finally the gas was pumped through a series of 60 ml syringes containing the soil samples. Soil samples were treated with a controlled and constant concentration of 1000 ppm H₂. H₂ concentration was calculated by converting current (mA) into e⁻ pairs, then into μmol H₂, and flow rate was used to calculate ppm H₂.

Three H₂ treatments were performed. Treatment H₂T1 (long term H₂ treatment) was treated for 77 days; soil samples were collected once the H₂ uptake rate levelled off

after long term treatment. Treatment H₂T2 (midterm H₂ treatment) was treated for 47 days; soil was collected once the H₂ uptake rate reached its peak. Treatment H₂T3 (short term H₂ treatment) was treated for 33 days (soil and data obtained from Sarah Hall); soil was collected during the initial increase phase of the H₂ uptake rate.

2.1.2 Controlled Air Treatment

Air treatment was used as a control as no changes in the H₂ uptake was expected for soil treated with air. Control samples were treated using room air generated from a Maxima air pump. No alterations were made to the room air gas composition. Air was bubbled through water in order to moisten the air to keep soil columns from drying out. H₂ and air treated samples were treated at similar flow rates of about 81 ml/min. H₂ uptake rate and CO₂ exchange rate of soil samples were measured frequently during treatment.

Two air treatments were performed. Treatment AT1 was treated for 47 days; soil samples were collected to correspond with the time of treatment for H₂T2. Treatment AT2 was treated for 77 days; soil was collected to correspond with the time of treatment for H₂T1.

Diagram of the controlled gas treatment setup can be found in Figure M1.

2.2 Soil Gas Exchange Monitoring

The H₂ uptake rate and CO₂ exchange rate were monitored throughout the treatment of the soil columns. The H₂ uptake rate was measured using a Qubit H₂ sensor

(Kingston, ON). A diagram for the H₂ uptake monitoring system can be found in Figure M2. The CO₂ exchange rate was measured using an Infra-Red CO₂ analyzer (Model 225-MK3, Analytical Development Corp., Hoddeson, UK). The same measurement set-up was used for measuring H₂ uptake and CO₂ exchange.

2.2.1 Standard Curve for ppm H₂ Calculation

In order to calculate ppm H₂ from the voltage output of the Qubit H₂ sensor, a standard curve had to be created. The standard curve consisted of H₂ in concentrations of 25 ppm, 50 ppm, 100 ppm, 200 ppm, 500 ppm and 1000 ppm. The voltage detected for each concentration of H₂ was recorded. The measured voltage from each concentration of H₂ was used to produce a standard curve for calculating unknown concentrations (ppm) from a detected voltage.

2.2.2 H₂ Uptake Measurements

H₂ uptake rates were measured using a Qubit H₂ sensor. H₂ gas was produced at a flow rate of 321.4 ml/min and a concentration of 100 ppm. The flow rate of the 100 ppm H₂ gas was then slowed to a rate of 29.9 ml/min using a second flow meter. Three-way valves were placed on both ends of the soil column being measured in order to control the direction of the gas flow. The valves could be opened in 2 positions. The first position allowed for the gas to pass through the soil column and proceed to the detector. Before reaching the detector the gas then passed through a column of magnesium perchlorate to remove any remaining moisture. The second position

allowed for the gas to bypass the soil column and proceed to the detector without any interaction with the soil column. The voltage signal was then converted into ppm H₂ hydrogen using the standard curve for H₂ concentration described in section 2.2.1. The difference between the ppm H₂ measured when the column was bypassed and the ppm H₂ measured when passed through the soil was used to calculate the H₂ uptake rate of the soil.

2.2.3 Soil Collection for H₂ and Air Treated Samples

Once samples reached a desired level of treatment, samples were collected. Samples were collected using a spatula into 2 ml microcentrifuge tubes and labelled. H₂ flow was maintained during sample collection by flowing H₂ at the treatment rate of 1000 ppm through one end of the soil column and collecting from the other. Tubes were immediately frozen upon collection using liquid nitrogen. The continued flow of H₂ and freezing with liquid nitrogen was done to reduce the chances of the degradation of RNA. Once frozen, the samples were stored at -80 °C until needed.

Figure M1 – Diagram of controlled H₂ and air treatment system (Dong and Layzell, 2001)

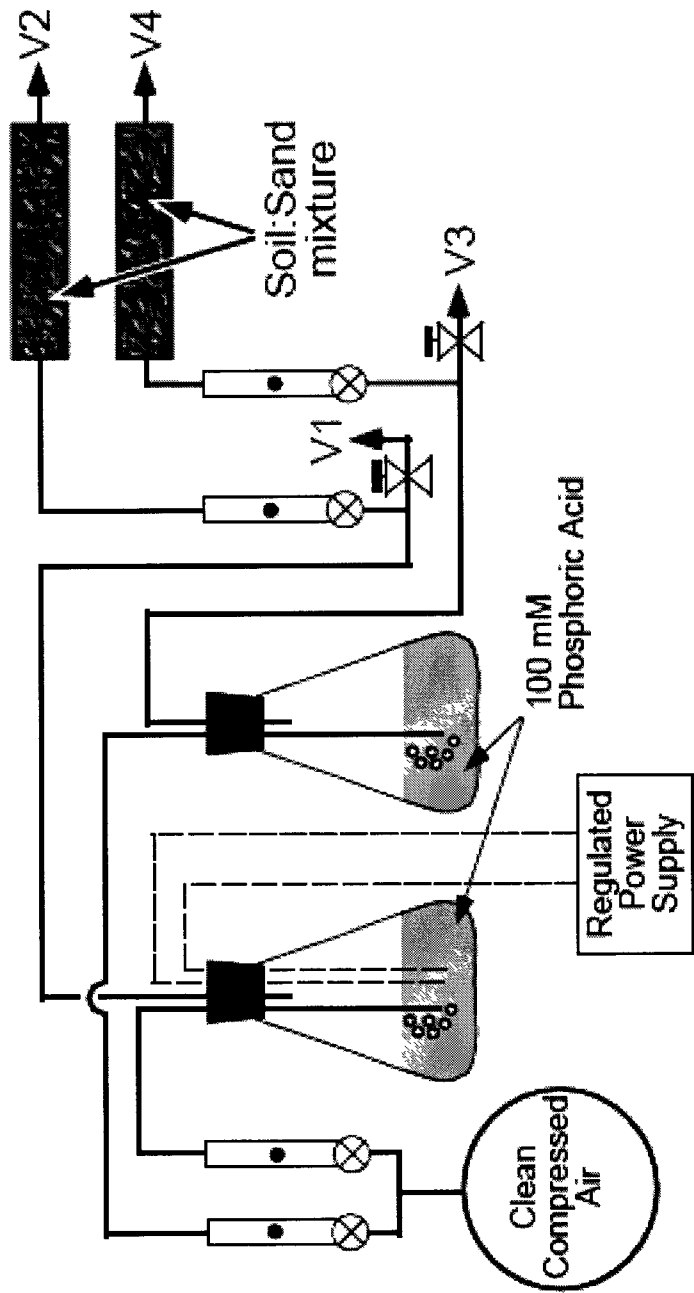
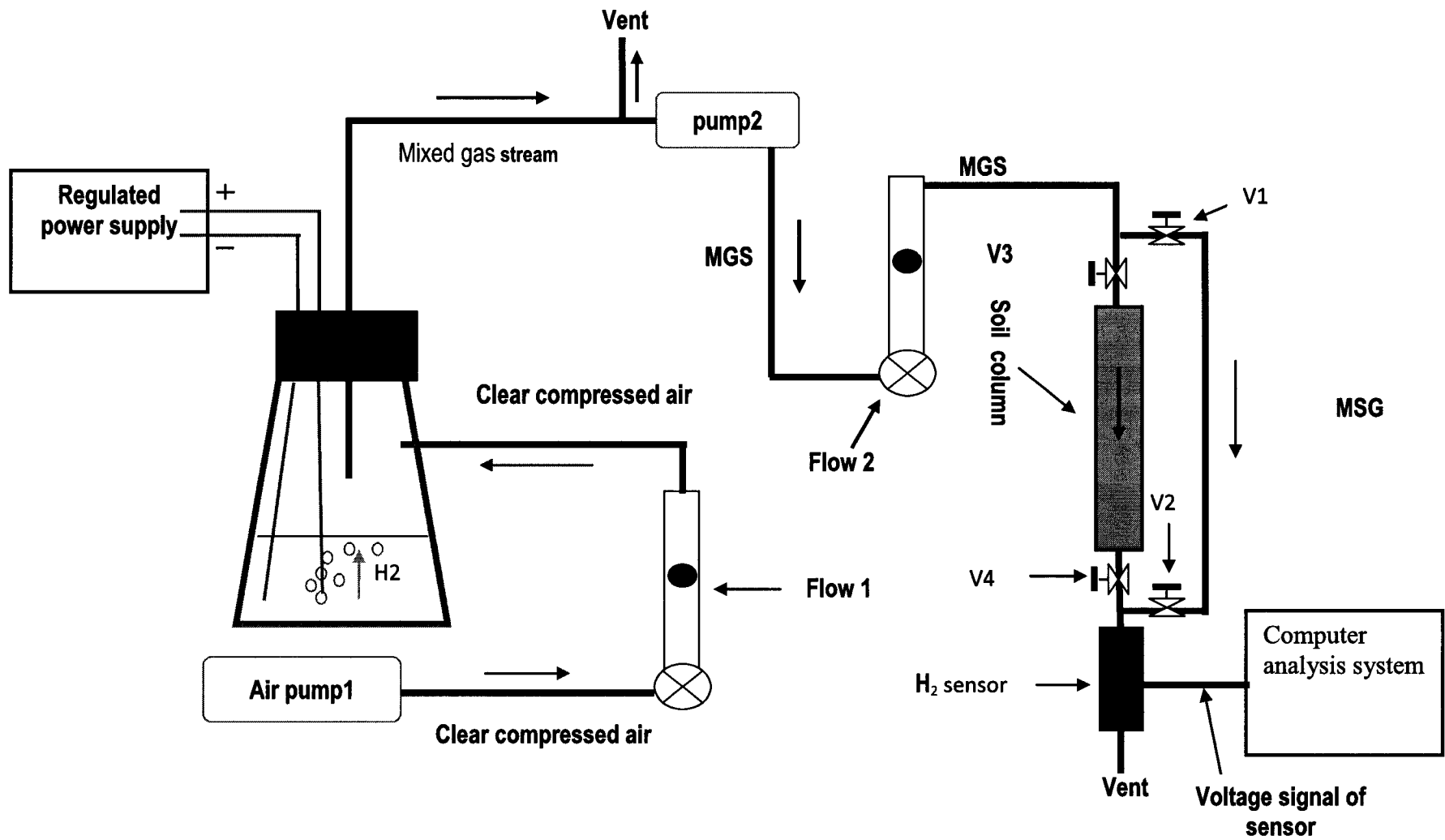


Figure M2 – Setup for H₂ uptake measurements using controlled gas flow and Qubit H₂ sensor. (He, 2009)



2.3 Soybean Rhizosphere Soil Preparation

Soybeans (*Glycine max*) were used as a model legume plant in order to test the effects of nodule type on the *cbbL* gene copy numbers and expression in adjacent soil.

2.3.1 Surface Sterilization of Seeds

Before inoculating and planting soybeans it was necessary to surface sterilize the soybean seeds in order to remove any bacterial contamination that may interfere with the formation of desired nodules. Two separate methods for the surface sterilization of seeds were used. One method involved the use of 70% ethanol. Seeds were placed in a breaker and immersed in a solution of 70% percent ethanol for 15 minutes. Ethanol was poured off the seeds and the seeds were then rinsed three times using de-ionized water. Seeds were then dried under a flow bench to avoid contamination. Seeds sterilized with ethanol failed to germinate as desired, and sodium hypochlorite (bleach) was used as an alternative sterilization method. Seeds were surface sterilized by immersing in a 5% solution of sodium hypochlorite (bleach) for 5 minutes. Again, seeds were rinsed at least three times with water and allowed to air dry under a flow bench.

2.3.2 Inoculation with Rhizobia Bacteria

In order to obtain the desired nodulation on the soybean plants the soybeans were inoculated using a peat moss containing rhizobia bacteria. Two types of bacterial inoculants were used. The bacterial inoculants were isogenic strains of *Bradyrhizobium japonicum*. The strains used were JH and JH47. JH *B. Japonicum* contains the uptake

hydrogenase gene to produce H₂ conserving (Hup⁺) nodules. JH47 *B. Japonicum* contained a knockout uptake hydrogenase gene, making it non-functional, giving rise to H₂ releasing (Hup⁻) nodules (Hom *et al.*, 1988). As a control, surface sterilized seeds were planted without inoculation so that soil could be collected from the area adjacent to non-nodulated roots. Inoculation of the seeds was performed in three different ways in order to improve nodulation. This study only investigated the soil surrounding the nodules and not the abundance of nodules, so different inoculation techniques were used in attempt to improve nodulation so that more soil could be collected from an individual plant. The first group of plants were inoculated by shaking the seeds with inoculated peat to coat the seeds. The seeds were then planted. For the second group of soybean plants, seeds were sterilized and planted in vermiculite. After several days of growth the seedlings were removed from the vermiculite the roots of the plants were dipped in a solution of inoculated peat and water. Seedlings were then planted. Finally, the third group of soybean plants were again planted in vermiculite and allowed to grow for several days. Seedlings were then carefully transferred to soil pots and inoculated by adding 1 ml of JH or JH47 bacteria culture broth to the base of the root.

2.3.3 Soybean Growth

Soybeans were grown in 9 inch pots containing a sandy clay loam (using the same sand to clay ratio as with the controlled H₂ treatments). Soybeans were monitored and watered as needed using a nutrient solution. The nutrient solution was mixed by combining the following 1000x stock solutions.

Solution A: 17.48757g KH_2PO_4 , 4.9641g K_2HPO_4 , 500 ml H_2O

Solution B: 43.7418g K_2SO_4 , 500 ml H_2O

Solution C: 29.9472g $\text{MgSO}_4 \times 7\text{H}_2\text{O}$, 25.0071g $\text{MgCl}_2 \cdot 6\text{H}_2\text{O}$, 500 ml H_2O

Solution D: 54.9855g $\text{CaCl}_2 \times 2\text{H}_2\text{O}$, 500 ml H_2O

Solution E: 5.1361g $\text{FeCl}_4 \times 6\text{H}_2\text{O}$, 500 ml H_2O

Solution F: 0.8451g $\text{MnSO}_4 \times \text{H}_2\text{O}$, 0.1248g $\text{CuSO}_4 \cdot 5\text{H}_2\text{O}$, 0.1438g $\text{ZnSO}_4 \times 7\text{H}_2\text{O}$,

0.9584g H_3BO_3 , 0.0605g $\text{Na}_2\text{MoO}_4 \times 2\text{H}_2\text{O}$, 0.0281g $\text{CoSO}_4 \times 7\text{H}_2\text{O}$, 500 ml H_2O

Solution N: 5.0552g KNO_3 , 100 ml H_2O

For a working solution, 1 ml of each stock solution was added to 1 L of water.

Solution N contained nitrogen and was used in the working solution for the first week of watering to promote the initial growth of the seedling. The first two trials of soybeans were grown in the greenhouse at Saint Mary's University. Due to problems with pests and temperature control in the greenhouse, the third trial of soybeans was grown in the growth chambers in the science building at Saint Mary's University. Soybeans were grown until signs of maturity were evident, at which point soil samples were collected from the rhizosphere.

2.3.4 Soil Collection from Rhizosphere

Soil was collected from the area adjacent to the nodule for inoculated plants, and from the area adjacent to roots for non-inoculated plants. Plants were cut at the stem and removed from the pot. A spatula was used to dig through soil surrounding the roots; when a nodule was found the soil adjacent to the nodule was collected into a 2 ml microcentrifuge tube. From the soybean trials there were three sample sets collected; JH samples collected from the soil adjacent to HUP⁺ nodules of JH inoculated plants, JH47 samples collected from the soil adjacent to HUP⁻ nodules of JH47 inoculated plants and Root samples collected from the soil adjacent to roots of non-inoculated plants.

2.3.5 Testing HUP Status

The HUP status of the nodules was tested using a methylene blue assay. After soil was collected from the area around a nodule the nodule was then removed from the roots and cleaned using water. The collected nodules were then placed on a filter paper containing methylene blue reduction assay. Nodules were crushed using the flat end of a spatula and placed in a vacuum chamber. All air was removed from the chamber and replaced with H₂. After 48 hours the nodules were removed from the chamber and photographed. The reduction assay acts as an electron acceptor when H₂ is oxidized by Hup⁺ nodules, and turns from blue to clear (Lambert *et al.*, 1985). A positive result indicates that a nodule is Hup⁺ due to the presence of uptake hydrogenase activity.

2.4 DNA Extraction from Soil Samples

Soil samples remained frozen at -80°C until they were needed for extraction. Samples were removed from -80°C and were transferred on ice. Samples were immediately weighed after being placed on ice. Soil samples were extracted using a protocol modified from Griffith *et al.* published in 2000 (Griffith *et al.*, 2000). For more information on the protocol, contact Dr. Michael Schloter at the German Research Center for Environmental Health.

2.5 RNA Extraction from Soil Samples

The protocol described above was designed for the co-extraction of DNA and RNA from environmental soil samples. However, after much optimization it was not possible to get a detectable concentration of RNA extracted from soils; due to this, RNA was extracted from soil samples using the MoBio RNA PowerSoil Extraction Kit (Medicorp, Inc., Montreal, QC). MoBio Ultraclean RNase Free Gloves (Medicorp, Inc., Montreal, QC) were worn during all steps of the protocol. Work surfaces were cleaned using Ambion RNaseZap (Applied Biosystems Canada, Streetsville, ON) to avoid contamination with environmental RNase that would degrade extracted RNA. Soil samples were removed from the -80°C freezer and immediately 1 g of soil was weighed into a 15 ml bead tube. 2.5 ml of Bead Solution was added and vortexed to mix. 0.25 ml of Solution SR1 was added and vortexed to mix. 0.8 ml of Solution SR2 was added to the tube which was then vortexed at maximum speed for 5 minutes; tape was used to

secure the tubes the vortex and provide more even vortexing. 3.5 ml of Phenol:Chloroform:Isoamyl Alcohol 25:24:1 Saturated with 10 mM Tris, pH 8.0, 1 mM EDTA was added to the tube and then vortexed briefly to mix followed by vortexing at maximum speed for 10 minutes. Following centrifugation for 10 minutes at 2500 x g at room temperature the top aqueous phase was removed and transferred to a new 15 ml collection tube. 1.5 ml of Solution SR3 was added to the tube followed by incubation at 4°C for 10 minutes and then centrifugation for 10 minutes at 2500 x g at room temperature. The supernatant was transferred to a new 15 ml collection tube. 5 ml of Solution SR4 was added to the supernatant and vortexed briefly to mix followed by incubation at room temperature with gentle shaking for 45-60 minutes. The sample was then centrifuged for 30 minutes at 2500 x g at room temperature. The supernatant was poured off the pellet and the pellets were air dried by inverting the tube on paper towel. The pellets were then resuspended in 1 ml of Solution SR5; the resuspension required incubation for 10 minutes at 45°C followed by vortexing. RNA Capture Columns were prepared by placing the RNA Capture Column into a 15 ml collection tube and passing 2 ml of Solution SR5 through the column. Once Solution SR5 has passed through the column the resuspended RNA sample was then added to the column. When the RNA sample finished running through, the column was then washed using 1 ml of Solution SR5. Once Solution SR5 finished flowing through the column, the RNA Capture Columns were transferred to new 15 ml collection tubes. 1 ml of Solution SR6 was added to the column and allowed to flow through to elute the RNA bound to the column. The eluted

RNA was transferred to a 2.2 ml collection tube and 1 ml of Solution SR4 was added and mixed by inverting. The sample was then incubated for 10 minutes at -20°C to precipitate the RNA followed by centrifugation at 13,000 x g for 15 minutes at room temperature. The supernatant was decanted off the pellet which was then air dried by inverting on paper towel. The RNA pellet was then resuspended in 100 µl of solution SR7. RNA samples were stored at -20°C until needed.

2.6 cDNA Preparation

2.6.1 RNA Purification

After the extraction of RNA from soil samples it is necessary to check for the presence of DNA contamination. RNA purity was tested by performing a 16S PCR; a positive result for the 16S PCR would suggest that RNA is contaminated with DNA. The 25µl 16S reaction mixture contained: 1 µl each of 16S primers (BSF8/20, BSR534/18), 2.5µl of 10x Buffer, 2.5 µl of 2mM dNTP, 2 µl of 25mM MgCl₂, 0.2 µl of 5U/µl Taq enzyme (Fermentas, Burlington, ON), 0.5 µl of RNA template and 15.3 µl of DPEC treated or Sigma water. Conditions for the PCR were 3 minutes at 95°C for denaturation, 30 cycles of 95°C for 30 seconds, 55°C for 30 seconds and 72°C for 30 seconds, and a final hold of 72°C for 10 minutes. PCR products were checked on an agarose gel for the presence of the 16S band.

RNA samples were purified of DNA by performing a DNA digestion with DNase I (Applied Biosystems Canada, Streetsville, ON). The DNase reaction mixture contained:

12.5 µl of 10x DNase buffer, 2.5 µl of 2U/µl DNase I, 98.5 µl of RNA sample and 12 µl of RNase-free water. Samples were incubated for 30-45 minutes at 37°C. After incubation 200 µl of Phenol:Chloroform:Isoamyl Alcohol 25:24:1 Saturated with 10 mM Tris, pH 8.0, 1 mM EDTA was added to the samples, followed by incubation for 5 minutes at room temperature and centrifuging for 5 minutes at 10,000g. The top aqueous layer was removed and transferred to a new microcentrifuge tube. RNA was precipitated by adding 1/10 volume (20 µl) of 5M NaCl and 2 volumes (400 µl) of 100% EtOH followed by incubation at -20°C for 30 minutes. Precipitated RNA was pelleted by centrifuging for 10 minutes at 10,000g. After drying pellets were resuspended in 100 µl of RNase-free water.

2.6.2 Reverse Transcription of RNA to cDNA

RNA was reverse transcribed using the High Capacity cDNA Reverse Transcription Kit (Applied Biosystems Canada, Streetsville, ON). The reverse transcription reaction mixture contained: 2 µl of 10x RT buffer, 0.8 µl of 25mM dNTP, 2 µl of 10x RT random primers, 1 µl of 50 U/µl Multiscribe Reverse Transcriptase, 1 µl of 20 U/µl RNase inhibitor, 3.2 µl of RNase-free water and 10 µl of RNA sample.

For quantitative study, each RNA sample required a minus reverse transcriptase control in order to control for the effects of residual DNA in the RNA sample. A minus RT control contains the same reagents as reverse transcription but lacks the reverse transcriptase enzyme. The minus RT control mixture contained: 2 µl of 10x RT buffer, 0.8

μl of 25mM dNTP, 2 μl of 10x RT random primers, 1 μl of 20U/ μl RNase inhibitor, 4.2 μl of RNase-free water and 10 μl of RNA sample.

The conditions for the reverse transcription reaction were 10 minutes at 25°C, 2 hours at 37°C, and 5 minutes at 85°C. cDNA obtained from the reverse transcription was then purified using the QIAquick PCR Purification Kit (Qiagen, Mississauga, ON). Purified cDNA was then ready for quantitative and qualitative molecular work.

2.7 PCR for RubisCO Large Sub-unit Genes

Primers for the detection of the red-like and green-like RubisCO large sub-unit genes were obtained from Selesi *et al.*, (2005). *cbbLR1F* (AAGGAYGACGAGAACATC) and *cbbLR1R* (TCGGTCGGSGTG TAGTTGAA) were used for the detection of the red-like RubisCO large sub-unit gene while *cbbLG1F* (GGCAACGTGTTCCGGSTTCAA) and *cbbLG1R* (TTGATCTCTTCCACGTTTCC) were used for the detection of the green-like RubisCO large sub-unit gene.

The 25 μl *cbbL* gene PCR reaction mixture contained: 2.5 μl of 10 μM of each of the *cbbL* primers (*cbbLR1F*/*cbbLR1R* or *cbbLG1F*/*cbbLG1R*), 2.5 μl of 10x reaction buffer, 2.5 μl of 2mM dNTP, 1.5 μl of 25mM MgCl₂, 1.25 μl of DMSO, 1.25 μl of 3% BSA, 0.2 μl of 5U/ μl Taq enzyme, 1 μl of DNA template and 9.75 μl of RNase-free water. Conditions for the PCR were 4 minutes at 95°C for denaturation, 30 cycles of 95°C for 1 minute, 58°C for 1 minute and 72°C for 1 minute for red-like *cbbL* or 40 cycles of 95°C for 1 minute, 57°C for 1 minute and 72°C for 1 minute for green-like *cbbL*, and a final hold of 72°C for

10 minutes. PCR products were checked on an agarose gel for the presence of the red-like *cbbL* (~800 bp) or green-like *cbbL* (~1100 bp) bands.

2.8 Primer Design for Green-like *cbbL* Real Time PCR

Sequences for the *cbbL* gene were obtained from the National Center for Biotechnology Information website. The NCBI database does not differentiate between the red-like and green-like sequences for the *cbbL* gene. To obtain the green-like *cbbL* sequences the deduced amino acid sequences for the DNA sequences were obtained. Amino acid sequences were aligned using Clustalx2.0.12 (Conway Institute UCD, Dublin). The aligned amino acid sequences were then saved as a FASTA file and a phylogenetic tree was produced using Geneious (Biomatters Ltd, Auckland, New Zealand) to show the grouping of the sequences. The results showed two main groupings for the amino acid sequences which were cross-referenced with results from Selesi *et al.*, (2005). Due to the relative diversity of green-like DNA sequences it was not possible to create an effective primer set using all sequences available. The sequences were grouped based on similarity and closely related groups were used to develop primers for real time PCR.

Sequences obtained from cloning of the *cbbLG1F/cbbLG1R* fragment were combined with the sequences from *N. winogradskii* (2 strains), *M. capsulatus*, *N. vulgaris*, and *T. denitrificans* along with several sequences obtained from primer set *cbbLG1F/cbbLG1R* to develop the primer set. Using these sequences it was possible to develop the reverse primer CTYGTCGTCCTTSGGTGAA, given the name *cbbLG2R1* and

when combined with the primer *cbbLG1F* (Selsi *et al.*, 2005) produced a fragment of 250 bp.

2.9 Quantification of *cbbL* Gene Copies and Expression

The quantification of gene copies and gene expression from treated samples was performed using absolute quantification with SYBR Green fluorescence. Two separate primer sets were used for the detection of red-like and green-like *cbbL* genes. Table M1 below describes all primers used for the quantification of *cbbL* genes.

Table M1 – Real time PCR primers used in this study

Primer Name	Sequence	Gene	Reference
<i>cbbLR1F</i>	AAGGAYGACGAGAACATC	Red-like <i>cbbL</i>	Selesi <i>et al.</i> , 2005
<i>cbbLR1intR</i>	TGCAGSATCATGTCRTT	Red-like <i>cbbL</i>	Selesi <i>et al.</i> , 2007
<i>cbbLG1F</i>	GGCAACGTGTTCCGGSTTCAA	Green-like <i>cbbL</i>	Selesi <i>et al.</i> , 2005
<i>cbbLG2R1</i>	CTYGTCGTCCTTSGGTGAA	Green-like <i>cbbL</i>	This Study

2.9.1 Preparation of Standards

2.9.1.1 Internal vs. External Standards

Quantification using real time PCR required that a known control is used for reference in calculating unknown samples (Heid *et al.*, 1996). Internal controls known as house-keeping genes are commonly used quantification standards since their quantities should not vary in the tissues or cells being investigated (Vandesompele *et al.*, 2002). Common housekeeping genes include *ACTB*, *B2M*, *GAPD*, *HMBS* and *RPL13A*.

External controls utilize a standard curve of known amount of copies of a standard. In this study linear plasmid DNA was used as an external standard to create a standard curve for the calculation of the unknown samples. The equation of standard curve of the known standards allows for the calculation of the unknown copies. Due to its simplicity, the standard curve method was used for this study.

2.9.1.2 Amplification for Cloning

Primers for the quantification of the red-like RubisCO large sub-unit genes were obtained from Selesi *et al.*, (2007). *cbbLR1F* (AAGGAYGACGAGAACATC) and *cbbLR1intR* (TGCAGSATCATGTCRTT) were used for the quantification of the red-like RubisCO large sub-unit gene. The forward primer for the quantification of green-like *cbbL* was obtained from Selesi *et al.*, (2005); the reverse primer was designed for this study. *cbbLG1F* (GGCAACGTGTTCCGGSTTCAA) and *cbbLG2R1* (CTYGTCGTCCTTSGGTGAA) were used for the quantification of green-like *cbbL*.

The 25µl *cbbL* gene PCR reaction mixture contained: 2.5 µl each of the 10 µM *cbbL* primers (*cbbLR1F/ cbbLR1intR*), 2.5µl of 10x reaction buffer, 2.5 µl of 2mM dNTP, 1.5 µl of 25mM MgCl₂, 1.25 µl of DMSO, 1.25 µl of 3% BSA, 0.2 µl of 5U/µl Taq enzyme, 1 µl of DNA template and 9.75 µl of RNase free water. Conditions for the PCR were 4 minutes at 95°C for denaturation, 30 cycles of 95°C for 1 minute, 58°C (red-like) or 54°C (green-like) for 1 minute and 72°C for 1 minute, and a final hold of 72°C for 10 minutes.

PCR products were checked on an agarose gel for the presence of the red-like *cbbL* gene fragments (~274 bp) or green-like *cbbL* gene fragment (~250 bp).

2.9.1.3 Purification of PCR Product

PCR product from the *cbbLR1F/cbbLR1intR* was purified using the QIAquick PCR Purification Kit. All centrifugation steps are at 13,000 rpm. 5 volumes (100 µl) of Buffer PBI were added to 20 µl of PCR product. Sample was added to a QIAquick spin column and DNA was bound to the column by centrifuging for 1 minute and discarding the flow-through. To wash 0.75 ml of Buffer PE was added to the column and centrifuged for 1 minute. The flow-through was discarded and the column was centrifuged for an additional 1 minute to remove any residual Buffer PE. The column was placed in a new 1.5 ml microcentrifuge tube and 50 µl of Buffer EB was added to the spin column membrane. DNA was eluted by centrifuging for 1 minute.

2.9.2 Cloning

2.9.2.1 Ligation and Transformation

The *cbbL* genes were cloned using the pGEM-T Easy Vector (Promega, Madison, USA). The vector was ligated and the *cbbL* gene inserted by mixing 5 µl of 2x Rapid Ligation Buffer, 0.5 µl of pGEM-T Easy Vector, 1 µl of T4 DNA Ligase and 3.5 µl of the PCR product. The ligation reaction was mixed and incubated overnight at 4°C.

The vectors were transformed using JM109 competent cells (Promega, Madison, USA). After incubation 3 μ l of the ligation reaction was added to a 1.5 ml microcentrifuge tube on ice. 20 μ l of the JM109 competent cells were added to the ligation reaction and allowed to incubate on ice for 20 minutes. Following incubation the cells were heat shocked by placing in a 42°C water bath for 45 seconds and immediately placed on ice for 2 minutes. Cells were removed from ice and 100 μ l of room temperature SOC medium was added. Cells were then incubated for 2 hours at 37°C with shaking at 225 rpm.

LB-ampicillin plates were made by mixing 12.5 g of LB broth, 7.5 g of granulated agar and 500 ml of distilled water. After autoclaving the agar was left to cool to 50-60°C just before plating, 500 μ l of 50 mg/ml ampicillin was added to give a final concentration of 0.5 mg/ml ampicillin. Before adding transformed cells to plates, 100 μ l of 100 mM IPTG and 20 μ l of 50 mg/ml X-Gal were added to the plates and allowed to absorb for 30 minutes at 37°C. 100 ml of the cell culture was added to the plate and spread using a Lazy-L-Spreader™. Plates were incubated overnight at 37°C.

Plates were screened for white colonies. White colonies were picked using sterile 10 μ l pipette tips or sterile toothpicks and transferred to a fresh LB-ampicillin plate. Plates were incubated overnight at 37°C. Colonies were again picked using a sterile pipette tip or sterile toothpick and mixed with 5 μ l of Sigma water then used to inoculate a test tube containing 2 ml of LB-ampicillin broth. Tubes were incubated for 16-18 hours at 37°C with shaking at 225 rpm.

Bacteria cultures were transferred to 1.5 ml microcentrifuge tubes and centrifuged to pellet cells. Plasmids were purified using Miniprep Plasmid Purification Kit (Fermentas, Burlington, ON). Plasmid DNA samples which were positive for the *cbbL* gene were sent for sequencing (Macrogen, Seoul, Korea). The resulting sequences were then identified using BLAST and screened manually for primer sequences, length and restriction enzyme cutting sites.

2.9.2.2 Plasmid Linearization

To perform real-time PCR the plasmid should first be linear. 1 µg of each plasmid was digested using 60 units of Sall at 37°C for 2 hours. The reaction was ended using QIAquick Gel Extraction Kit (Qiagen, Mississauga, ON). Products were checked on 1 % agarose gel with ethidium bromide staining.

2.9.3 Generation of Standard Curve

For the standard curve 3 unique *cbbL* sequences were chosen for both primer sets. Real-time PCR reactions were carried out using the ABI Prism 7000 Sequence Detection System (Applied Biosystems Canada, Streetsville, ON). The 25 µl PCR reaction mixture contained 0.5mM primers (*cbbLR1F/cbbLR1intR* or *cbbLG1F/cbbLG2R1*), 1 µl of linear plasmid DNA, and 12.5 µl of Power SYBR Green PCR Master Mix (Applied Biosystems Canada, Streetsville, ON). Conditions for the PCR for the *cbbLR1F/cbbLR1intR* pair were 2 minutes at 50°C, 10 minutes at 95°C, the 40 cycles of 95°C for 1 minute, 58°C for 1 minute and 72°C for 1 minute, then a final elongation for

10 minutes at 72°C followed by a final dissociation step. Conditions for the PCR for the *cbbLG1F/cbbLG2R1* pair were 2 minutes at 50°C, 10 minutes at 95°C, the 40 cycles of 95°C for 1 minute, 54°C for 1 minute and 72°C for 1 minute, then a final elongation for 10 minutes at 72°C followed by a final dissociation step. Data collection occurred each cycle at the 72°C for 1 minute elongation step. Linear plasmid DNA was diluted to 10^9 copies then a dilution series of 10^8 to 10^3 was mixed. After completion of the run the threshold cycle (C_t) was plotted against the log of the concentration of *cbbL* controls to produce the standard curve.

2.10 Quantity of *cbbL* genes in Unknown Samples

2.10.1 Preparation of Unknown Samples

The concentration of unknown samples was determined using the Thermo Scientific Nanodrop 2000 Spectrophotometer (Qiagen, Mississauga, ON). Using the nucleotide concentration obtained from the Spectrophotometer the samples were diluted to 1 ng of DNA per μ l by adding 1 μ l of sample to $x - 1$ μ l of RNase-free water; where x was equal to total concentration of DNA (ng/ μ l). For RNA samples, 10 μ l of total RNA was added to the reverse transcription reaction. cDNA was diluted to 1 ng/ μ l and 1 μ l was added to each reaction; this volume was used to calculate back to the amount of initial RNA added. The cDNA and –RT samples were then diluted to between 1 and 0.1 ng of initial RNA.

Standards were quantified along with unknown samples to provide reference. Standards chosen for each run ranged from 10^8 copies to 10^3 copies. The PCR protocols for red-like and green-like *cbbL* from section 2.9.3 was used for quantification.

It is possible that inhibitory substances may have been co-extracted during the extraction procedure. The presence of PCR inhibitors would result in under calculating the initial number of gene copies. To control for these inhibitory substances samples were spiked using 10^5 or 10^4 copies of the standard for the *cbbL* gene. These spiked samples were used in comparison with the standards to determine if inhibitory substances were present in the unknown sample.

2.10.2 Calculating Quantity of *cbbL* in Unknowns

After running the real time PCR, the C_t (threshold cycle) values for the unknown samples were determined using the auto baseline and auto C_t functions included in the ABI Prism SDS 7000 software. In subsequent runs being compared the baseline was set automatically by program software and the threshold for determining C_t was set to match for all runs.

The C_t values obtained from unknown samples were plugged into the equation of the standard curve that was created using standards quantified along with each run; this resulted in the number of genes present in 1 ng of unknown DNA/cDNA sample. Using the concentration of extracted DNA/RNA for a sample (ng/g soil); the initial number of *cbbL* genes per gram soil was calculated.

2.10.3 Limit Detection, Quantification Limit and Undetected Expression

A working definition for the detection limit of a PCR system is 3 standard deviations above the average quantification for a negative control, while the quantification limit is defined as 10 standard deviations above the average quantification for a negative control (Vaerman, *et al.*, 2006). However, in practice the detection limit for a PCR reaction can be set at 10 copies of analyte per reaction while the quantification limit may be set at 100 copies of analyte per reaction; under this limit, coefficients of variation for Ct values will increase (Vaerman, *et al.*, 2006). The quantification limit for this experiment was set at 100 copies per reaction; quantities under 100 copies per reaction were considered undetected.

To determine the amount of analyte to be added to each reaction a dilution series for several samples was created using 10, 1, 0.1, 0.01, 0.001 and 0.0001 ng of analyte per reaction. Due to the low quantity of copies and expression in certain samples, the amount of analyte used for detection was set between 1 and 0.1 ng per reaction. Dilution of the samples also helped to reduce effects of inhibitory substances from the soil (proteins, humic acids) since dilution of the sample would also dilute the inhibitory effect.

Each cDNA sample quantified had a corresponding -RT control which was used to control for residual DNA left over after the DNase digestion. The actual copies per ng cDNA was calculated by subtracting the copies per ng RNA added for the -RT control

from the copies per ng RNA added for the cDNA sample. In cases where the -RT control had more copies than the cDNA sample, the sample was reported as undetected.

For statistical calculations all samples that were reported as undetected were counted as 0. These cases only occurred during the quantification of RNA samples; undetected expression was treated as no expression of the *cbbL* gene in the sample.

2.11 *cbbL* Sequencing

Sequencing was used in order to determine the range of coverage of both the primer pairs used in this study. The following steps were performed for both the *cbbLR1F/cbbLR1intR* and *cbbLG1F/cbbLG2R1* primer pairs. PCR reactions were performed using the protocols mentioned previously, for each primer pair. PCR products were combined in triplicate and purified using the QIAquick PCR Purification Kit. The cloning procedure described previously in section 2.8.2 was used to isolate unique copies of the *cbbL* gene. Sequencing was performed by Promega (Promega, Nepean, ON) and Macrogen (Macrogen, Seoul, Korea). Primers were located within the resulting sequence and the *cbbL* gene fragment was identified using BLAST (NCBI, Bethesda, USA) to find the nearest match.

3 Results

3.1 Controlled Gas Treatment

3.1.1 Standard Curve

A standard curve was created in order to calculate the concentration of H₂ gas in ppm from the voltage output reading from the Qubit H₂ sensor. Standard measurements used to create the curve can be found in Table 1. The calculated H₂ concentration was plotted against the voltage output. Using a power function, the equation for the standard curve was calculated to be $y = 7.8912 * e^{1.269x}$, where x is equal to the voltage output reading and e is the natural number (2.71828) (Figure 1). This equation was used to calculate H₂ uptake rates for controlled gas treated samples.

3.1.2 H₂ Treated Soil Samples

The semi-daily H₂ uptake rate record for long term H₂ treatment (H₂T1) and midterm H₂ treatment (H₂T2) can be found in Table 2 and Table 3 respectively. These recordings correspond to a 77 day H₂ exposure of treatment H₂T1 (Table 2) and a 47 day H₂ exposure of treatment H₂T2 (Table 3). The CO₂ exchange rate measurements for treatments H₂T1 and H₂T2 can be found in Table 4 and Table 5 respectively. Figure 2 and Figure 3 show the H₂ uptake rate vs. time for treatments H₂T1 and H₂T2 respectively and Figure 4 and Figure 6 show the CO₂ exchange rate vs. the H₂ uptake rates for treatments H₂T1 and H₂T2 respectively. Figure 5 and Figure 7 show the CO₂ exchange rate vs. time for treatments H₂T1 and H₂T2 respectively

The highest H₂ uptake rate reached for sample H₂T2 was measured on day 47 when the H₂ uptake rate was calculated to be 0.201 μmol hr⁻¹ g⁻¹. This was also the point at which soil samples for this treatment were collected as it was evident that a relative maximum in the H₂ uptake rate was reached.

The highest H₂ uptake rate reached for sample H₂T1 was measured on day 54 when the H₂ uptake rate was calculated to be 0.219 μmol hr⁻¹ g⁻¹. However, a first relative maximum was reached between 28 and 40 days of treatment. As the H₂ treatment progressed beyond this point the uptake rate began to fluctuate. Soil samples were collected on day 77 of treatment when the uptake rate stabilized at 0.101 μmol hr⁻¹ g⁻¹.

Short term H₂ treatment (H₂T3) was obtained from Sarah Hall; soil was collected during the initial increase in H₂ uptake. H₂T3 data was combined from two treatments each lasting 32 days. H₂ uptake data for treatment H₂T3 can be found in Table 6 and CO₂ exchange data can be found in Table 7. Figure 8 displays the H₂ uptake rate vs. time for treatment H₂T3. Figure 9 displays the CO₂ exchange rate vs. H₂ uptake rate for treatments H₂T3, while Figure 10 displays the CO₂ exchange rate vs. time. The H₂ uptake rates for the short-term H₂ treatments at the time of collection were 0.076 μmol hr⁻¹ g⁻¹ and 0.0614 μmol hr⁻¹ g⁻¹, and the corresponding CO₂ exchange rates for the treatments were 0.0073 μmol hr⁻¹ g⁻¹ and 0.0367 μmol hr⁻¹ g⁻¹ respectively.

3.1.3 Air Treated Soil Samples

The H₂ uptake log for two air treated soil treatments can be found in Table 8 and Table 9. These recordings correspond to 47 day air exposure of treatment AT1 (Table 8) and for the 77 day air exposure of treatment AT2 (Table 9). The CO₂ exchange rate measurements for samples AT1 and AT2 can be found in Table 10 and Table 11 respectively. These logs contain less data entry points as little to no change was expected in the rates of H₂ uptake and CO₂ exchange. Figure 11 and Figure 12 show the H₂ uptake rate vs. time for treatments AT1 and AT2 respectively. Figure 13 and Figure 14 show the CO₂ exchange rate vs. time for treatments AT1 and AT2 respectively.

Soil samples were collected from treatment AT1 on day 47 when the H₂ uptake rate was 0.014 $\mu\text{mol hr}^{-1} \text{g}^{-1}$ and the soil samples were collected from treatment AT2 on day 77 when the H₂ uptake rate was 0.013 $\mu\text{mol hr}^{-1} \text{g}^{-1}$.

For reference, a comparison of H₂ uptake rates for gas treatments can be found in Figure 15. Figure 15 also shows comparison for time of collection for treatments H₂T1, H₂T2, H₂T3, AT1 and AT2. A reference table for general trends in H₂ uptake and CO₂ exchange for all treatments can be found in Table 12.

3.2 Rhizosphere Soil Samples

Soil samples were collected from the rhizosphere of soybean plants grown individually in pots. After sample collection the soybean nodules were tested using a methylene blue assay in a H₂ chamber. The methylene blue assay was used to

determine the Hup status of the nodules. Methylene blue assay pictures for JH47 nodules can be found in Figure 16, assay pictures for JH nodules can be found in Figure 17 and assay pictures for volunteer nodules from control soybean plants can be found in Figure 18. A positive result for the nodule assay in JH nodules demonstrates the presence of uptake hydrogenase activity within the nodules. A negative result for the nodule assay in JH47 nodules demonstrates the absence of uptake hydrogenase activity within the nodule; likewise there is a negative result for uptake hydrogenase activity in the volunteer nodules found in control plants. Soil collected from around these nodules was treated as HUP⁻ soil.

3.3 Nucleotide Extraction

3.3.1 DNA Extraction

DNA was extracted using a modified Griffith's protocol. Using this protocol it was possible to extract a wide range of bacterial DNA from differently treated soils. DNA extraction data for all treatments can be found in Table 13. The treatment with the highest average extracted DNA was the midterm H₂ treatment (H₂T2) with 5.09×10^3 ng per g soil, while the treatment with the lowest average extracted DNA was air treatment AT1 with 0.711×10^3 ng per g soil. Data was transformed using the equation $y = \log(x)$ to achieve normality and equal variances among treatments. An ANOVA was used to detect variance in total DNA extracted from the different treatments. The ANOVA showed a significant variation among samples. A Tukey's Honestly-Significant-Difference test

showed that both long term H₂ treatment (H₂T1) and midterm H₂ treatment (H₂T2) had significantly higher DNA per g soil than short term H₂ treatment (H₂T3) and air treatments ($p < 0.01$). There was also no significant difference in DNA extracted per g soil detected among the rhizosphere samples.

3.3.2 RNA Extraction

RNA was extracted using the RNA PowerSoil kit. After the purification of RNA using DNase treatment we were able to calculate the amount of RNA extracted per gram soil. RNA extraction data for all treatments can be found in Table 14. The treatment with the highest average extracted RNA was JH47 with 2.03×10^3 ng per g soil. The treatment with the lowest average RNA extracted was AT (AT1 and AT2 combined) with 0.424×10^3 ng per g soil. AT1 and AT2 were combined since they had the same level of H₂ treatment, 0 days, and to limit the number of RNA extractions required. An ANOVA showed that there was no significant difference in RNA extracted per g soil among the H₂ treatments and air treatments. There was also no significant difference in RNA extracted per g soil among the rhizosphere samples.

Figure 19 shows a comparison of the average extracted RNA and DNA for all treatments. It can be seen that for most soils there is a greater concentration of DNA than RNA per g soil.

3.4 Detection and Quantification of RubisCO *cbbL* Genes

Two primer sets were used to detect the presence of RubisCO large subunit genes in soil samples. Figure 20 shows the results of a RubisCO large subunit PCR using the primer sets *cbbLR1F/cbbLR1R* for red-like *cbbL* and *cbbLG1F/cbbLG1R* for green-like PCR. Bands of the expected size were amplified with PCR with *cbbLR1F/cbbLR1R* producing a band size of ~800 bp and *cbbLG1F/cbbLG1R* producing a band of ~1100 bp. With sequencing, it was possible to confirm the identity of these fragments as being amplified from the RubisCO large subunit gene.

3.4.1 Real Time PCR Primer Testing

For the detection and quantification of red-like RubisCO genes in soil, the primer set *cbbLR1F/cbbLR1intR* was used. Figure 21 shows the PCR result for the *cbbLR1F/cbbLR1intR* primer set producing a fragment of ~272 bp. Sequencing of the cloned PCR product was used in order to confirm the size and identity of the amplified fragment as originating from the red-like RubisCO large subunit gene.

PCR was used in order to test the primer set designed for this experiment. Figure 22 shows the PCR result for the *cbbLG1F/cbbLG2R1* primer set. A fragment of the expected size of ~250 bp was amplified. Sequencing of the cloned PCR product showed that the fragments were of the right size, however, a large number of the fragments amplified did not have close sequence matches on BLAST for identification.

3.4.2 Quantification of RubisCO Genes from Gas Treated Soils

3.4.2.1 Primer Set *cbbLR1F/cbbLR1intR*

The quantity of RubisCO large subunit genes detected in controlled gas treated soil samples varied greatly within treatments leading to large standard deviations for each treatment. H₂ treatments had higher measured copies per ng DNA than air treatments. Long term H₂ treatment had the highest average copies per ng DNA with an average of 12.7×10^4 (+/- 1.51×10^4), followed by midterm H₂ treatment with 6.97×10^4 (+/- 6.93×10^4), followed by short term H₂ treatment with 2.04×10^4 (+/- 2.29×10^4). Air treatments had the lowest copies per ng DNA with 1.25×10^4 (+/- 0.646×10^4) and 0.972×10^4 (+/- 0.337×10^4) for treatments AT1 and AT2 respectively; both treatments received 0 days of H₂ treatment.

Both long term (H₂T1) and midterm (H₂T2) H₂ treated soils had significantly higher DNA yields than air treated soils (see Table 13/Figure 19); due to this, the increase in *cbbL* copies detected per ng DNA in H₂ treated soils is multiple times greater per g soil. Long term H₂ treatment (H₂T1) had the highest copies per g soil, followed by midterm H₂ treatment (H₂T2) followed by short term H₂ treatment (H₂T3). Again, air treatments had the lowest measured copies per g soil.

Summary of gene copy data per ng DNA and per g soil for primer set *cbbLR1F/cbbLR1intR* can be found in Table 15a and Table 15b respectively. Comparison between quantified gene copies and gene expression of *cbbL* can be found in Figure 23a

and Figure 23b. An example of a real time PCR amplification plot can be seen in Figure 25. Figure 25 shows amplification plots for control standards, unknown samples and inhibition controls.

3.4.2.2 Primer Set *cbbLG1F/cbbLG2R1*

Both long term H₂ treatment (H₂T1) and midterm H₂ treatment had higher measured copies per ng DNA than air treatments. Midterm H₂ treatment had the highest average copies per ng DNA with an average of 19.2×10^4 ($\pm 1.57 \times 10^4$), followed by long term H₂ treatment with 11.2×10^4 ($\pm 8.39 \times 10^4$), followed by air treatments with 3.38×10^4 ($\pm 3.97 \times 10^4$). Short term H₂ treatment (H₂T3) had the lowest measured copies per ng DNA with 1.03×10^4 ($\pm 0.856 \times 10^4$).

As previously mentioned, both long term (H₂T1) and midterm (H₂T2) H₂ treated soils had significantly higher DNA yields than air treated soils (see Table 13/Figure 19). Again, the increase in *cbbL* copies detected per ng DNA in these H₂ treated soils is multiple times greater per g soil. Midterm H₂ treatment (H₂T2) had the highest copies per g soil, followed by long term H₂ treatment (H₂T1) followed by air treatments. Again, short term H₂ treatment had the lowest measured copies per g soil. A summary of gene copy data per ng DNA and per g soil for primer set *cbbLG1F/cbbLG2R1* can be found in Table 16a and Table 16b, respectively. Comparison between quantified gene copies and gene expression of *cbbL* can be found in Figure 24a and Figure 24b.

3.4.3 Quantification of RubisCO Genes from Rhizosphere Soil

3.4.3.1 Primer Set cbbLR1F/cbbLR1intR

Soil adjacent to the non-nodulated roots of soybeans had the highest measured copies per ng DNA with 24.4×10^4 ($\pm 6.66 \times 10^4$), followed by soil adjacent to Hup⁻ nodules (JH47) with 8.47×10^4 ($\pm 4.93 \times 10^4$), followed by soil adjacent to Hup⁺ nodules (JH) with 7.67×10^4 ($\pm 2.90 \times 10^4$).

Soil adjacent to the non-nodulated roots of soybeans also had the highest measured copies per g soil, followed by JH47 soil, followed by JH soil.

3.4.3.2 Primer Set cbbLG1F/cbbLG2R1

Soil adjacent to HUP⁻ nodules (JH47) measured 1.08×10^4 ($\pm 0.472 \times 10^4$) copies per ng DNA, which was slightly higher than soil adjacent to Hup⁺ nodules (JH) with 0.732×10^4 ($\pm 0.0863 \times 10^4$).

Soil adjacent to Hup⁻ nodules had slightly higher copies per g soil than soil adjacent to Hup⁺ nodules.

3.4.4 Statistical Variation in Gene Copies

3.4.4.1 Primer Set cbbLR1F/cbbLR1intR

Data was transformed using the equation $y = \log_{10}(x)$ in order to normalize data and achieve equal variances. A multivariate analysis of variance (MANOVA) was used to detect variance in the copies per ng DNA and copies per g soil data. The transformed data showed that there were significant differences between treatments for gene copies per ng DNA, and gene copies per g soil. A Tukey's Honestly-Significant-Difference test was used for pair-wise comparisons between treatments. Long term H₂ (H₂T1) and midterm H₂ (H₂T2) treatments had significantly higher copies per ng DNA than air treatments and short term H₂ treatment (H₂T3) ($p < 0.05$). Soil adjacent to soybean roots had significantly higher copies per ng DNA than soil adjacent to both Hup⁺ (JH) and Hup⁻ (JH47) nodules ($p < 0.05$).

Long term H₂ treatment and midterm H₂ treatment had significantly higher copies per g soil than both air treatments and short term H₂ treatment ($p < 0.05$). There was no significant difference between soil adjacent to nodules and soil adjacent to roots. Figure 23a shows the average copies/ng measured for all treatments with the standard error about the mean, and Figure 23b shows the average copies/g soil for all treatments with the standard error about the mean.

3.4.4.2 Primer Set cbbLG1F/cbbLG2R1

The data set could not be normalized using transformation so a Kruskal-Wallis One-way analysis of variance for non parametric data was used to detect variance. The test found that there was a significant variation among treatments at the copies per ng DNA level ($p < 0.01$) and at the copies per g soil level ($p < 0.01$). Figure 24a shows the average copies/ng measured for all treatments with the standard error about the mean and Figure 24b shows the average copies/g soil for all treatments with the standard error about the mean.

3.4.5 Quantification of RubisCO Gene Expression from Gas

Treated Soils

3.4.5.1 Primer Set cbbLR1F/cbbLR1intR

The RubisCO large subunit gene expression detected varied greatly within treatments leading to large standard deviations for each treatment. Long term H₂ treatment had the highest measured copies per ng RNA with 60.3×10^4 ($\pm 37.6 \times 10^4$), followed by short term H₂ treatment (H₂T3) with 18.4×10^4 ($\pm 9.24 \times 10^4$), followed by air treatments with 17.0×10^4 ($\pm 22.7 \times 10^4$). Midterm H₂ treatment (H₂T2) had the lowest copies per ng RNA with 7.28×10^4 ($\pm 5.02 \times 10^4$).

All H₂ treatments had higher expression (RNA copies) per g soil than air treatments. Long term H₂ treatment had the highest expression per g soil, followed by

short term H₂ treatment, followed by midterm H₂ treatment. Air treatments had the lowest expression per g soil.

Summary of gene expression data per ng RNA and per g soil for primer set cbbLR1F/cbbLR1intR can be found in Table 17a and Table 17b respectively.

3.4.5.2 Primer Set cbbLG1F/cbbLG2R1

Soils treated with H₂ had higher expression (RNA copies) per ng RNA than air treatments. Midterm H₂ treatment had the highest measure expression per ng RNA with 12.6×10^5 (+/- 10.2×10^5), followed by long term H₂ treatment with 7.19×10^4 (+/- 2.45×10^4). Air treatments had the lowest expression per ng RNA with 4.05×10^4 (+/- 4.98×10^4).

The same trend mentioned previously was found when expression per g soil was calculated. Midterm H₂ treatment had the highest expression, followed by long term H₂ treatment followed by air treatments.

Summary of gene expression data per ng RNA and per g soil for primer set cbbLG1F/cbbLG2R1 can be found in Table 18a and Table 18b respectively.

3.4.6 Quantification of RubisCO Gene Expression from Rhizosphere

3.4.6.1 Primer Set cbbLR1F/cbbLR1intR

Soil adjacent to the Hup⁻ nodules (JH47) had the highest measured expression (RNA copies) per ng RNA with 21.1×10^4 (+/- 12.2×10^4), followed by soil adjacent to Hup⁺ nodules (JH) with 4.46×10^4 (+/- 8.79×10^4). Soil adjacent to non-nodulated roots (Root) had the lowest expression per ng RNA with 2.34×10^4 (+/- 2.67×10^4).

The same trend mentioned previously was found when expression per g soil was calculated. Soil adjacent to Hup⁻ nodules (JH47) had the highest expression, followed by soil adjacent to Hup⁺ nodules (JH), followed by soil adjacent to non-nodulated roots (Root).

3.4.6.2 Primer Set cbbLG1F/cbbLG2R1

There was little difference in the expression (RNA copies) per ng RNA for rhizosphere samples. Soil adjacent to Hup⁺ nodules (JH) had the highest copies per ng RNA with 1.90×10^4 (+/- 1.48×10^4), followed by soil adjacent to non-nodulated roots with 1.66×10^4 (+/- 0.949×10^4). Soil adjacent to Hup⁻ nodules (JH47) had the lowest measured expression per ng RNA with 1.48×10^4 (+/- 1.54×10^4).

Soil adjacent to non-nodulated roots had the highest calculated expression per g soil, followed by soils adjacent to Hup⁺ nodules (JH), followed by soil adjacent to Hup⁻ nodules (JH47).

3.4.7 Statistical Variation in Gene Expression

3.4.7.1 Primer Set cbbLR1F/cbbLR1intR

Expression data was transformed in order to normalize the data and achieve equal variances: the equation $y = \log_{10}(x)$ was used to transform copies per ng cDNA data, and the equation $y = \sqrt{x}$ was used to transform cDNA copies per g soil data. A multivariate analysis of variance (MANOVA) was used on the transformed data to detect variance between treatments for expression (RNA copies) per ng RNA and expression per g soil. A Tukey's Honestly-Significant-Difference test showed that long term H₂ treatment (H₂T1) had significantly higher expression per ng RNA than midterm H₂ treatment (H₂T2) and air treatments ($p < 0.05$).

Soil adjacent to Hup⁻ nodules (JH47) had significantly higher expression per ng RNA than soil adjacent to Hup⁺ nodules (JH) ($p < 0.05$).

A MANOVA showed that there were significant differences in the expression per g soil between treatments. A Tukey's Honestly-Significant-Differences test showed that all H₂ treatments had significantly higher expression (RNA copies) per g soil than air

treatments ($p < 0.05$). There was no significant difference in expression per g soil among the rhizosphere samples.

3.4.7.2 Primer Set cbbLG1F/cbbLG2R1

Data could not be transformed in order to achieve normality and equal variances between treatments, so a Kruskal-Wallis one way analysis of variance for non-parametric data was used. The Kruskal-Wallis test showed that there was no significant difference in expression (RNA copies) per ng RNA among H₂ and air treatments. There was a significant difference detected in expression per g soil among the H₂ and air treatments ($p < 0.05$). There was no significant difference detected in expression per ng RNA or expression per g soil for rhizosphere samples.

3.5 Sequencing Results for Real-time Primers

Sequencing was performed in order to observe the species coverage of the two primer sets (cbbLR1F/cbbLR1intR and cbbLG1F/cbbLG2R1) to understand and deduce the species of bacteria being quantified by the experiment.

3.5.1 Cloning for Primer Set cbbLR1F/cbbLR1intR

A total of 186 clones were sequenced from the real time PCR primer set cbbLR1F/cbbLR1intR. Clones were isolated from the combined DNA of various soil treatments (H₂T1, H₂T2, AT1, AT2, JH and JH47). BLAST results from the cloned sequences can be found in Table 19 below. A total of 25 unique species matches were

obtained from the primer set. However, the vast majority of these clones had the closest match with a single species of uncultured bacterium classified as *Uncultured bacterium clone HKOR7 ribulose-1,5-bisphosphate carboxylase/oxygenase*, with a total of 66.13% of the 186 clones. The next most abundant nearest match was *Starkeya novella DSM 506*, with only 9.14% of the 186 clones.

3.5.2 Cloning for Primer Set cbbLG1F/cbbLG2R1

A total of 74 clones were sequences from the real time PCR primer set cbbLG1F/cbbLG2R1. Again clones were isolated from the combined DNA of all soil treatments. BLAST results from the cloned sequences can be found in Table 20. A total of 9 unique species matches were obtained from the primer set. The most abundant nearest match was with *Mycobacterium sp. DSM 3803 ribulose-1,5-bisphosphate carboxylase/oxygenase*, with 31.08% of the 74 clones. The next most abundant nearest match was again *Starkeya novella DSM 506*, with 24.32% of the 74 clones.

3.5.3 Cloning for H₂ vs. Air treated Soils

To further investigate the effects of hydrogen treatment on the CO₂ fixing bacterial community separate cloning was done for Air treated and H₂ treated soils using primer set cbbLR1F/cbbLR1intR as part of the above mentioned cloning. A total of 54 clones were isolated and sequenced from air treated soils and 59 clones were isolated from H₂ treated soils. BLAST results from the isolated sequences can be found in Table 21. A total of 10 unique matches were found for air treated soils and of these the

majority of the sequences had their nearest match with *Uncultured bacterium clone HKOR7 ribulose-1,5-bisphosphate carboxylase/oxygenase*, with a total of 79.63% of the 54 clones while the next most abundant nearest match had only 3.70%. A total of 7 unique matches were found for H₂ treated soils and again the majority of the sequences had their nearest match with *Uncultured bacterium clone HKOR7 ribulose-1,5-bisphosphate carboxylase/oxygenase* with 67.80% of the 59 clones while the next most abundant nearest match was *Starkeya novella DSM 506*, with 22.03%.

Table 1 – Standard curve data for H₂ uptake calculations from controlled gas treated soils

Target [H ₂] (ppm)	mA Used	Actual [H ₂] (ppm)	V Detected	Calculated [H ₂] (ppm)*
25	0.76	17.8	0.82	26.0
50	2.01	46.99	1.3	46.2
75	2.8	65.46	1.65	70.3
100	4.18	97.88	1.87	91.4
200	8.47	197.87	2.5	194
500	20.26	474.42	3.31	512
1000	44.4	1037.94	3.86	990

*Calculated using standard curve derived from Actual [H₂] vs. V Detected (See Figure 1)

Figure 1 – Standard curve for [H₂] calculations showing [H₂] in ppm vs. voltage output detected (V). Equation of the exponential trend line was found to be $y = 7.8912e^{1.269x}$, where x is the voltage detected and e is the natural number.

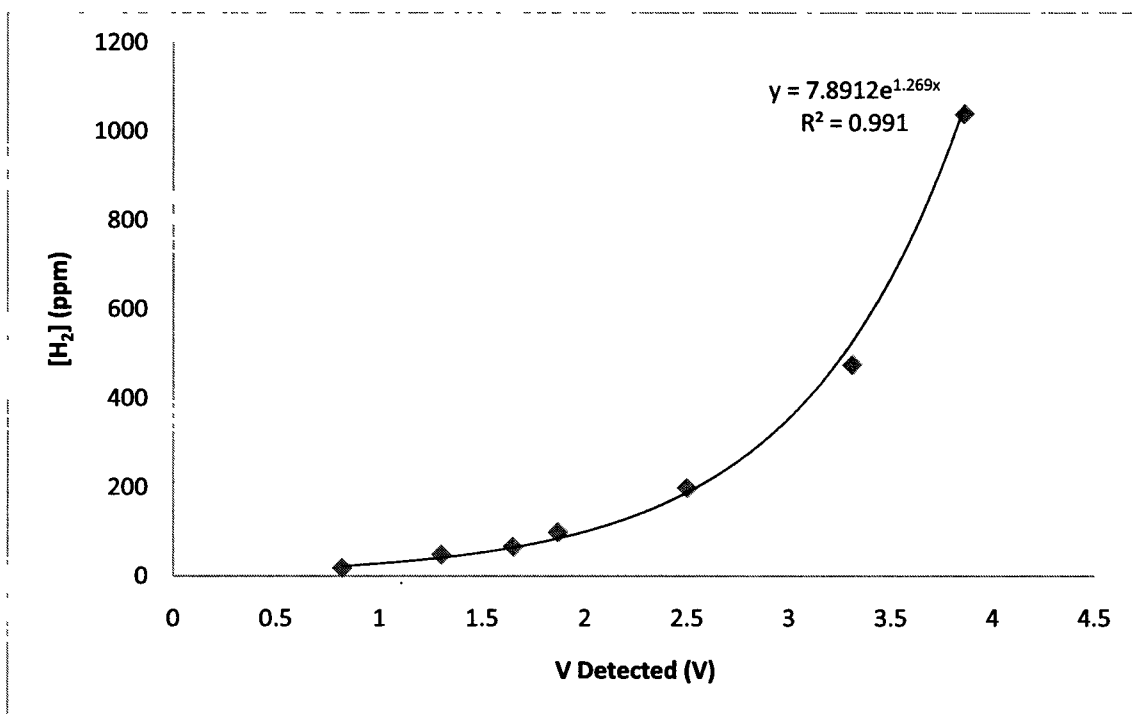


Table 2 – H₂ uptake data for treatment H₂T1.

Day	mA	H ₂ In (V)	H ₂ In (ppm)	H ₂ Out (V)	H ₂ Out (ppm)	H ₂ Absorbed (ppm)	Uptake Rate ($\mu\text{mol h}^{-1}\text{g}^{-1}$)
6	4.20	1.92	90.2	1.92	90.2	0	0
8	4.26	1.94	92.5	1.92	90.2	2.32	0.00340
11	4.28	2.04	105	1.99	98.6	6.46	0.00947
13	4.20	2.04	105	2.00	99.9	5.20	0.00762
15	4.24	2.09	112	2.03	104	8.21	0.0120
18	4.24	1.92	90.2	1.66	64.9	25.4	0.0372
19	4.29	2.01	101	1.70	68.2	32.9	0.0482
20	4.27	2.03	104	1.56	57.1	46.6	0.0683
21	4.29	2.03	104	1.43	48.4	55.3	0.0811
22	4.29	2.17	124	1.16	34.4	89.5	0.131
25	4.29	2.16	122	0.78	21.2	101	0.148
26	4.29	2.17	124	0.62	17.3	107	0.156
27	4.29	2.23	134	0.56	16.1	118	0.172
28	4.25	2.24	135	0.44	13.8	122	0.178
29	4.24	2.20	129	0.32	11.8	117	0.171
32	4.28	2.24	135	0.20	10.2	125	0.184
33	4.23	2.17	124	0.14	9.43	114	0.168
34	4.26	2.19	127	0.10	8.96	118	0.173
35	4.29	2.18	125	0.08	8.73	117	0.171
36	4.30	2.19	127	0.06	8.52	119	0.174
40	4.21	2.27	141	0.41	13.3	127	0.187
47	4.26	2.37	160	1.62	61.7	98.0	0.144
48	4.22	2.34	154	1.61	60.9	92.9	0.136
49	4.28	2.37	160	1.54	55.7	104	0.152
50	4.22	2.34	154	1.46	50.3	103	0.152
54	4.28	2.58	208	1.59	59.4	149	0.219
55	4.15	2.51	191	1.64	63.24	128	0.187
58	4.18	2.49	186	1.74	71.8	114	0.167
59	4.20	2.50	188	1.72	70.0	118	0.174
60	4.28	2.52	193	1.71	69.1	124	0.182
64	4.21	2.15	121	1.46	50.3	70.5	0.103
67	4.26	2.01	101	1.31	41.6	59.5	0.0873
68	4.20	2.13	118	1.51	53.6	64.1	0.0941
69	4.25	2.24	135	1.51	53.6	81.8	0.120
70	4.26	2.21	130	1.62	61.7	68.7	0.101
71	4.25	2.18	125	1.61	60.9	64.6	0.0947
74	4.25	2.28	142	1.76	73.6	68.8	0.101
75	4.25	2.34	154	1.77	74.6	79.2	0.116
76	4.21	2.30	146	1.8	77.5	68.6	0.101
77	4.25	2.30	146	1.8	77.5	68.6	0.101

Figure 2 – H₂ uptake plot for treatment H₂T1. Treatment lasted for 77 days. Y-axis shows H₂ uptake rate in μmol absorbed per hour per gram soil and X-axis shows number of days of treatment at time of measurement

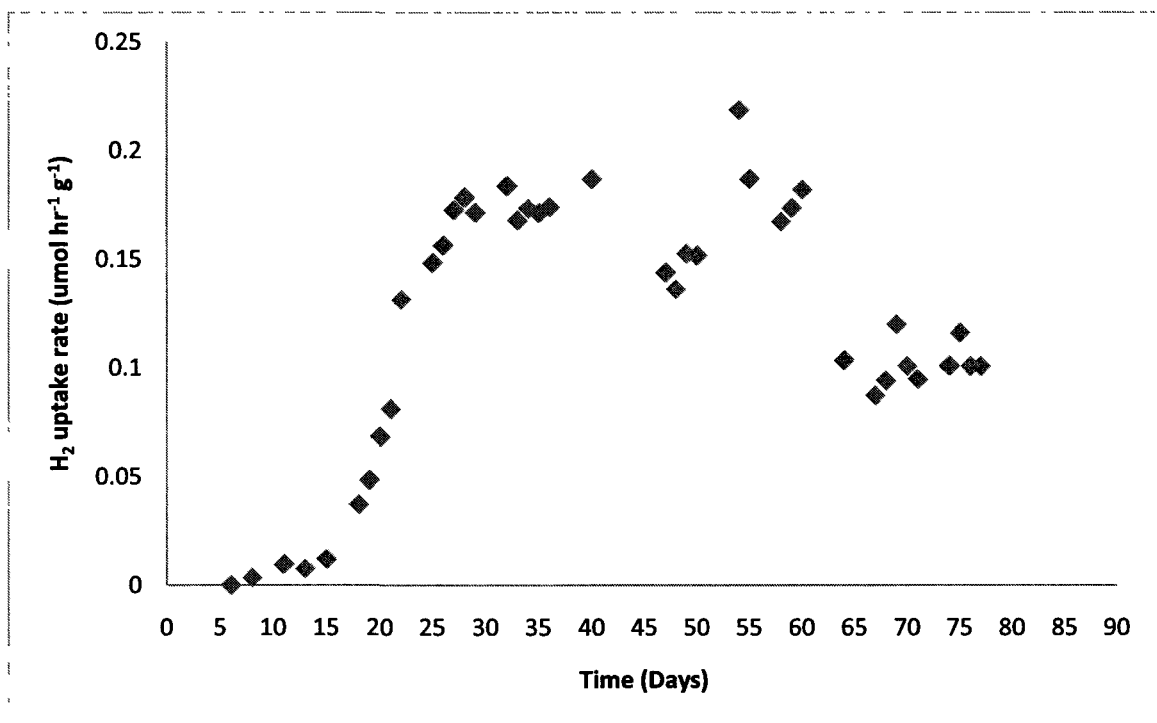


Table 3 – H₂ uptake data for treatment H₂T2.

Day	mA	H ₂ In (V)	H ₂ In (ppm)	H ₂ Out (V)	H ₂ Out (ppm)	H ₂ Absorbed (ppm)	Uptake Rate ($\mu\text{mol h}^{-1}\text{g}^{-1}$)
6	4.26	1.93	91.3	1.91	89.1	2.29	0.00323
8	4.27	1.95	93.7	1.93	91.4	2.35	0.00331
11	4.28	2.07	109	2.01	101	8.00	0.0113
13	4.24	2	99.9	1.95	93.7	6.14	0.00866
15	4.25	2.05	106	1.95	93.7	12.7	0.0179
18	4.29	2.03	104	1.71	69.1	34.6	0.0488
19	4.29	2.02	102	1.61	60.9	41.5	0.0586
20	4.26	2.07	109	1.56	57.1	52.0	0.0733
21	4.25	2.07	109	1.43	48.4	60.7	0.0856
22	4.57	2.22	132	1.25	38.6	93.5	0.132
25	4.28	2.18	125	0.87	23.8	102	0.143
26	4.32	2.23	134	0.75	20.4	113	0.160
27	4.27	2.24	135	0.63	17.6	118	0.166
28	4.24	2.22	132	0.56	16.1	116	0.163
29	4.25	2.23	134	0.41	13.3	120	0.169
32	4.29	2.25	137	0.28	11.3	126	0.177
33	4.22	2.16	122	0.20	10.2	112	0.158
34	4.27	2.18	125	0.09	8.85	117	0.164
35	4.3	2.22	132	0.05	8.41	124	0.174
36	4.36	2.24	135	0.04	8.30	127	0.180
40	4.31	2.32	1501	0.04	8.30	142	0.200
47	4.26	2.33	152	0.13	9.31	142	0.201

Figure 3 – H₂ uptake plot for treatment H₂T2. Treatment lasted for 47 days. Y-axis shows H₂ uptake rate in μmol absorbed per hour per gram soil and X-axis shows number of days of treatment at time of measurement.

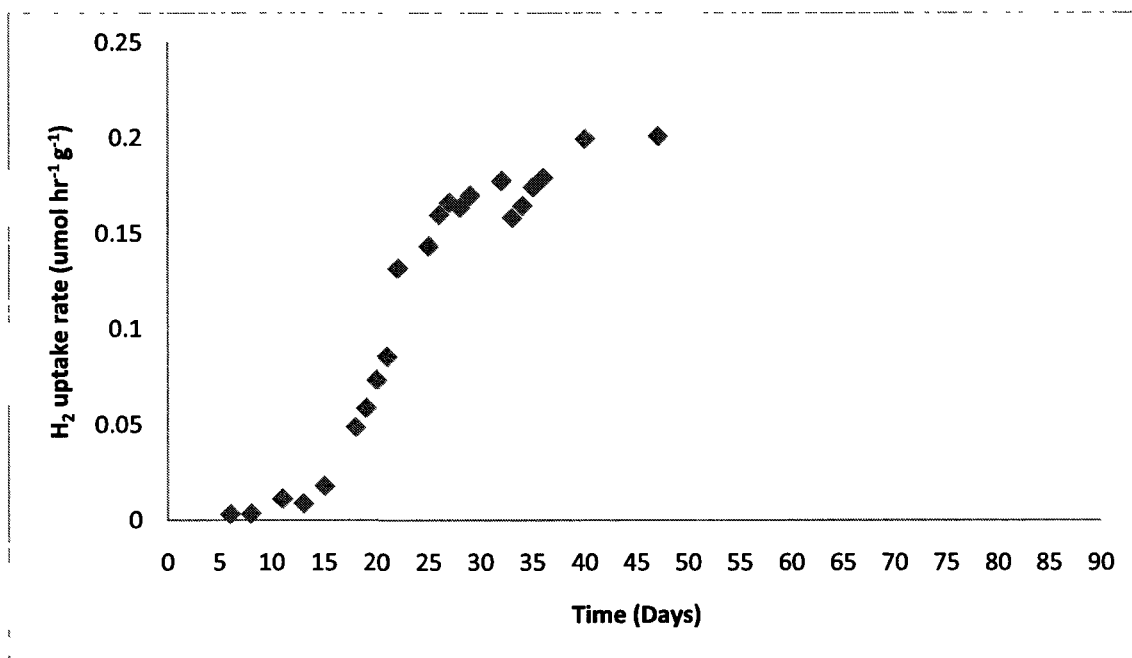


Table 4 – CO₂ exchange data for treatment H₂T1.

Day	CO ₂ In (ppm)	CO ₂ Out (ppm)	Difference (ppm)	umol*hr ⁻¹ *g ⁻¹
15	380	400	20	0.0282
18	380	405	25	0.0352
19	380	395	15	0.0211
20	380	390	10	0.0141
21	385	380	-5	0.00705
22	385	375	-10	0.0141
28	390	408	18	0.0254
29	380	390	10	0.0141
33	370	340	-30	0.116
34	405	365	-40	0.154
35	384	360	-24	0.0926
36	405	375	-30	0.116
40	370	360	-10	0.0386
47	360	400	40	0.160
48	371	411	40	0.160
49	350	375	25	0.100
50	369	388	19	0.0762
60	370	390	20	0.0802
64	390	407	17	0.0682
67	370	380	10	0.0401
68	367	375	8	0.0321
69	355	368	13	0.0522
70	381	390	9	0.0361
71	372	390	18	0.0722
74	381	390	9	0.0361
75	370	389	19	0.0762
76	380	400	20	0.0802
77	375	389	14	0.0562

Figure 4 – CO₂ exchange plot for treatment H₂T1. Treatment lasted for 77 days. Y-axis shows CO₂ exchange rate in μmol per hour per gram soil and X-axis shows H₂ uptake rate in μmol absorbed per hour per gram soil.

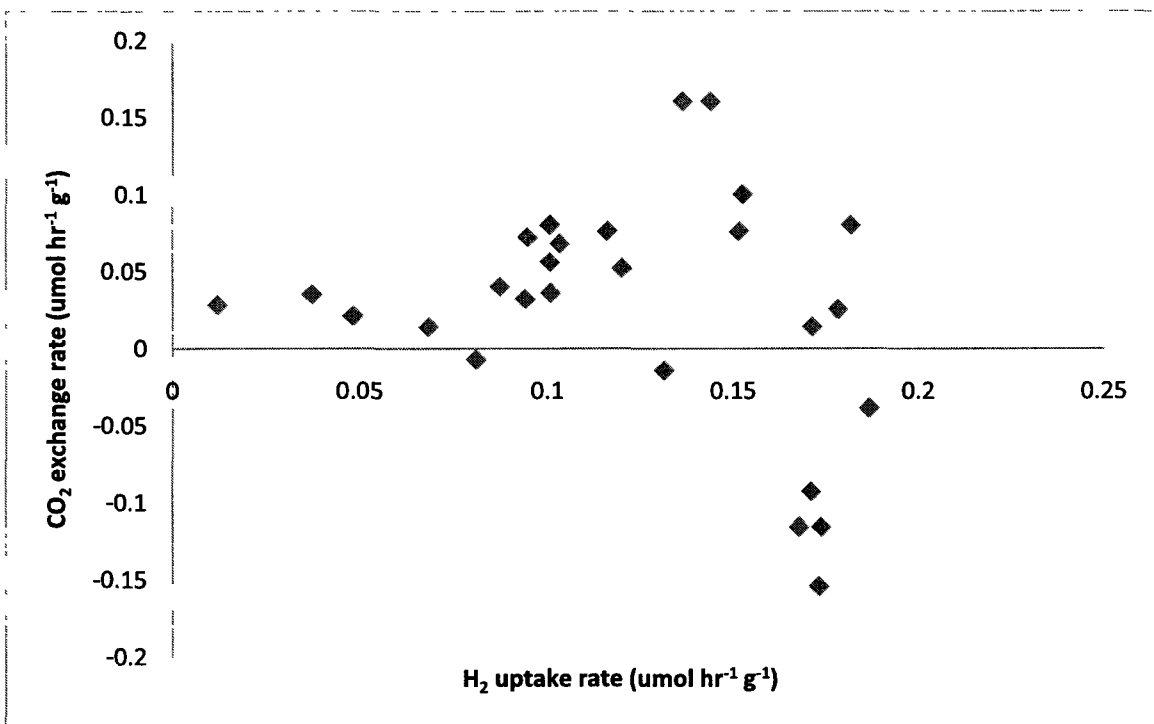


Figure 5 – CO₂ exchange plot for treatment H₂T1. Treatment lasted for 77 days. Y-axis shows CO₂ exchange rate in μmol per hour per gram soil and X-axis shows number of days of treatment at time of measurement

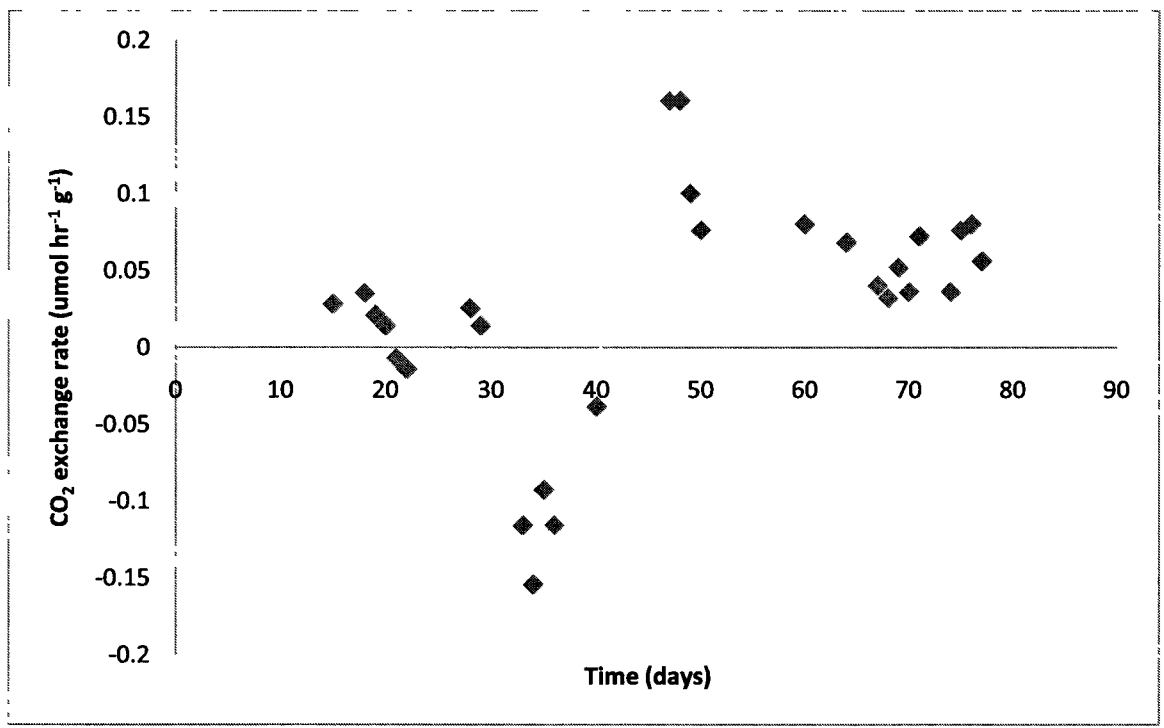


Table 5 – CO₂ exchange data for treatment H₂T2.

Day	CO ₂ In (ppm)	CO ₂ Out (ppm)	Difference (ppm)	μmol*hr ⁻¹ *g ⁻¹
15	380	400	20	0.0282
18	380	395	15	0.0211
19	380	395	15	0.0211
20	380	385	5	0.00705
21	390	395	5	0.00705
22	385	370	-15	-0.0211
28	390	400	10	0.0141
29	378	389	11	0.0155
33	373	340	-33	-0.127
34	393	350	-43	-0.166
35	380	345	-35	-0.135
36	365	338	-27	-0.104
40	375	340	-35	-0.135
47	360	340	-20	-0.0802

Figure 6 – CO₂ exchange plot for treatment H₂T2. Treatment lasted for 47 days. Y-axis shows CO₂ exchange rate in μmol per hour per gram soil and X-axis shows H₂ uptake rate in μmol absorbed per hour per gram soil.

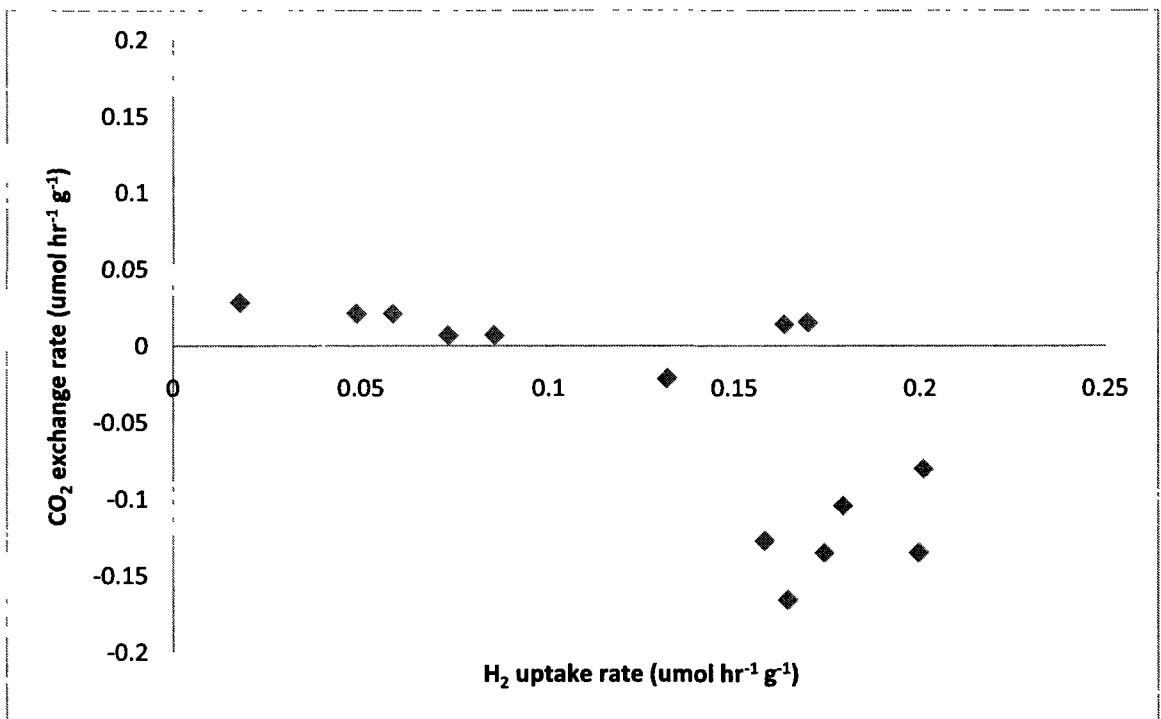


Figure 7 – CO₂ exchange plot for treatment H₂T2. Treatment lasted for 47 days. Y-axis shows CO₂ exchange rate in μmol per hour per gram soil and X-axis shows number of days of treatment at time of measurement

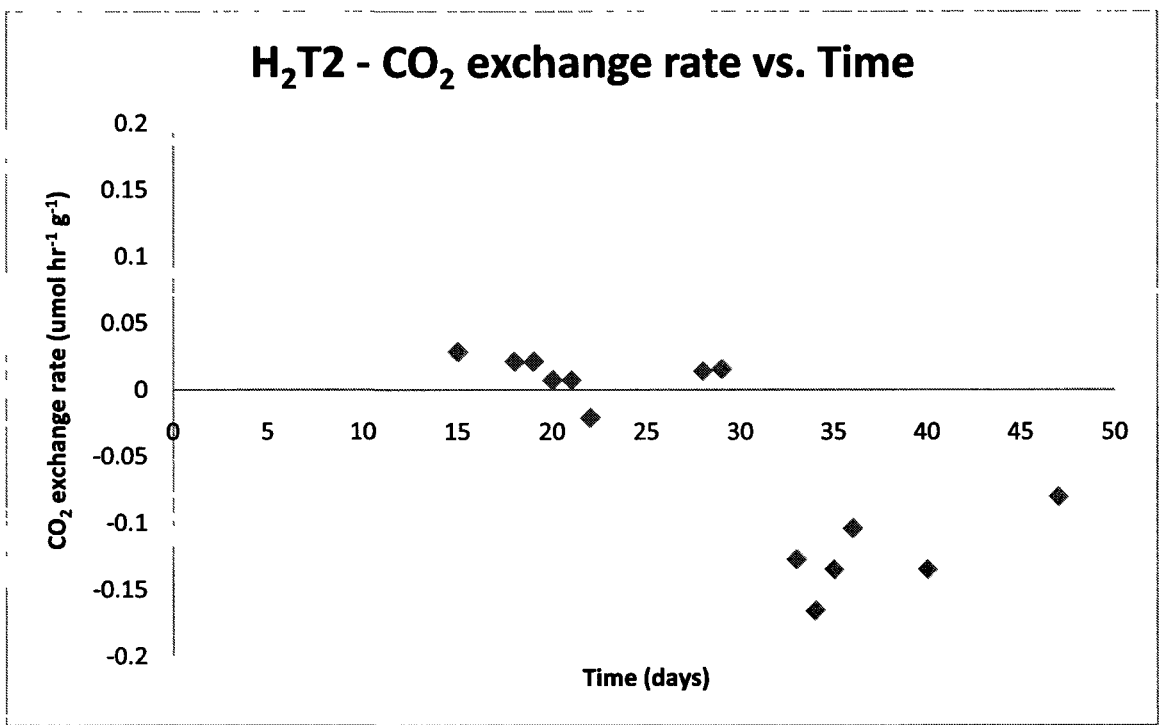


Table 6 – H₂ uptake data for two treatments, H₂T3

day	H ₂ in	ppm in	H ₂ out	ppm out	H ₂ absorbed (ppm)	μmolxhr ⁻¹ xg ⁻¹
0	2.41	196	2.34	180.	16.2	0.0197
1	1.73	85.3	1.66	78.3	7.02	0.00858
5	1.48	62.8	1.46	61.3	1.52	0.00186
6	1.69	81.3	1.61	73.7	7.6	0.00928
7	1.71	83.3	1.69	81.3	2.02	0.00247
8	1.64	76.4	1.58	71.0	5.42	0.00662
11	1.7	82.3	1.66	78.3	3.94	0.00481
12	1.62	74.6	1.58	71.0	3.57	0.00436
13	1.60	72.8	1.56	69.3	3.48	0.00426
15	1.61	73.7	1.54	67.6	6.06	0.00740
19	1.78	90.7	1.64	76.4	14.3	0.0175
21	1.92	108	1.63	75.5	32.2	0.0394
22	1.57	70.0	1.30	50.4	19.8	0.0242
25	1.58	71.0	1.15	41.9	29.1	0.0356
26	1.71	83.3	1.15	41.9	41.4	0.0505
27	1.66	78.3	1.02	35.7	42.6	0.0520
28	1.70	82.3	0.94	32.4	49.9	0.0609
29	1.73	85.3	0.90	30.9	54.5	0.0666
32	1.71	83.3	0.59	21.1	62.2	0.0760
0	2.35	183	2.34	180	2.22	0.00272
1	1.66	78.3	1.67	79.31	-0.966	-0.00118
5	1.49	63.6	1.47	62.1	1.54	0.00188
6	1.65	77.4	1.62	74.6	2.79	0.00341
7	1.69	81.3	1.65	77.4	3.89	0.00475
8	1.64	76.4	1.60	72.8	3.66	0.00447
11	1.70	82.3	1.65	77.4	4.89	0.00598
12	1.66	78.3	1.62	74.6	3.75	0.00458
13	1.60	72.8	1.54	67.6	5.16	0.00631
15	1.60	72.8	1.57	70.1	2.63	0.00321
19	1.77	89.6	1.64	76.4	13.2	0.0161
21	1.85	98.9	1.66	78.3	20.5	0.0251
22	1.64	76.4	1.40	56.9	19.5	0.0238
25	1.61	73.7	1.29	49.8	23.9	0.0292
26	1.70	82.3	1.27	48.6	33.7	0.0412
27	1.67	79.3	1.17	43.0	36.3	0.0444
28	1.64	76.4	1.10	39.4	37.0	0.0452
29	1.69	81.3	1.04	36.6	44.6	0.0545
32	1.67	79.3	0.85	29.0	50.3	0.0614

Table 7 – CO₂ exchange data for two treatments, H₂T3

	Co ₂ in	Co ₂ out	Difference (ppm)	
0	370	425	55	0.0672
1	380	400	20	0.0244
5	386	416	30	0.0367
6	378	395	17	0.0208
7	380	404	24	0.0293
8	384	407	23	0.0281
11	382	413	31	0.0379
12	370	396	26	0.0318
15	394	413	19	0.0232
19	386	423	37	0.0452
21	368	393	25	0.0305
22	368	393	25	0.0305
25	380	420	40	0.0489
26	380	400	20	0.0244
27	380	402	22	0.0269
28	378	407	29	0.0354
29	373	396	23	0.0281
32	380	386	6	0.00733
0	374	417	43	0.0525
1	359	386	27	0.0330
5	391	420	29	0.0354
6	380	401	21	0.0257
7	380	399	19	0.0232
8	348	371	23	0.0281
11	375	398	23	0.0281
12	368	398	30	0.0367
15	367	387	20	0.0244
19	385	412	27	0.03301
21	369	399	30	0.0367
22	369	399	30	0.0367
25	380	420	40	0.0489
26	380	409	29	0.0354
27	380	418	38	0.0464
28	378	414	36	0.0440
29	374	408	34	0.0415
32	389	419	30	0.0367

Figure 8 - H₂ uptake plot for treatments H₂T3. Treatment lasted for 32 days. Y-axis shows H₂ uptake rate in μmol absorbed per hour per gram soil and X-axis shows number of days of treatment at time of measurement.

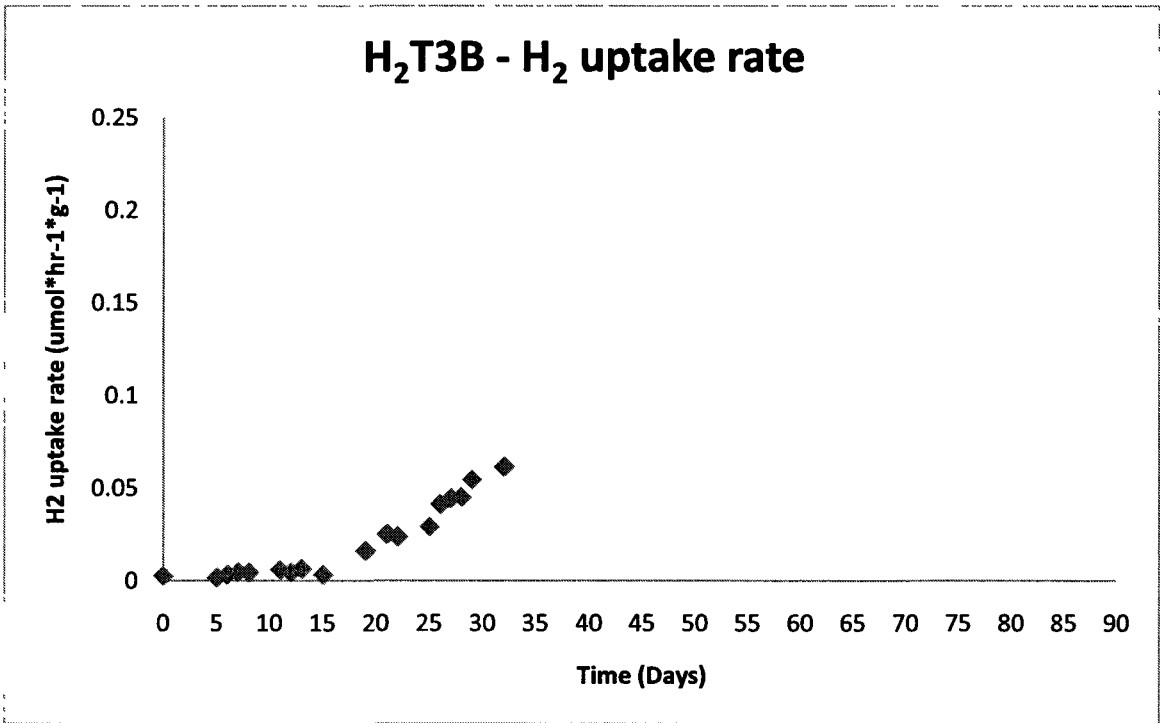
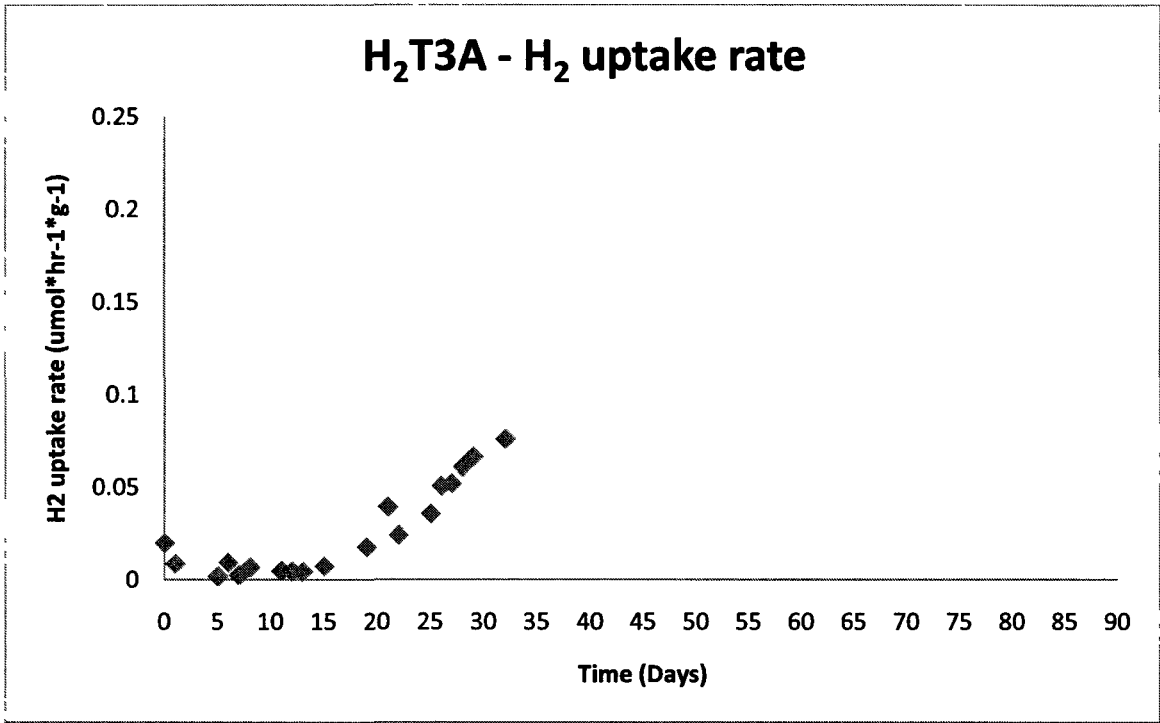


Figure 9 – CO₂ exchange plot for treatments H₂T3. Treatment lasted for 47 days. Y-axis shows CO₂ exchange rate in μmol per hour per gram soil and X-axis shows H₂ uptake rate in μmol absorbed per hour per gram soil.

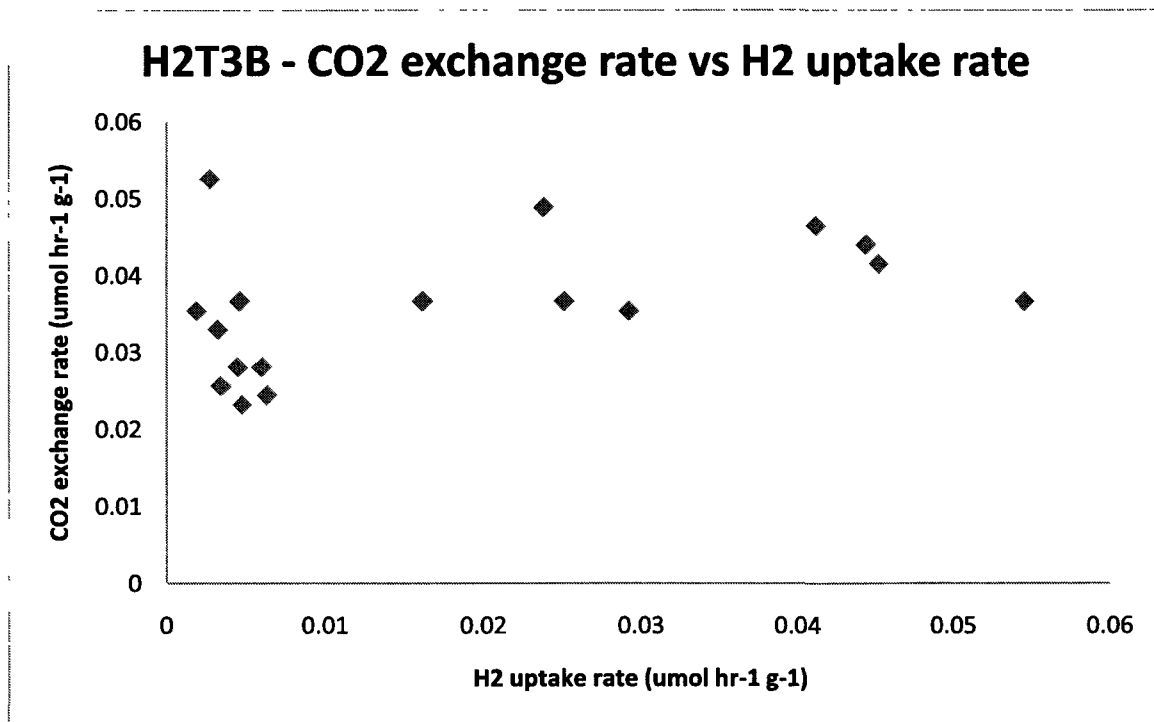
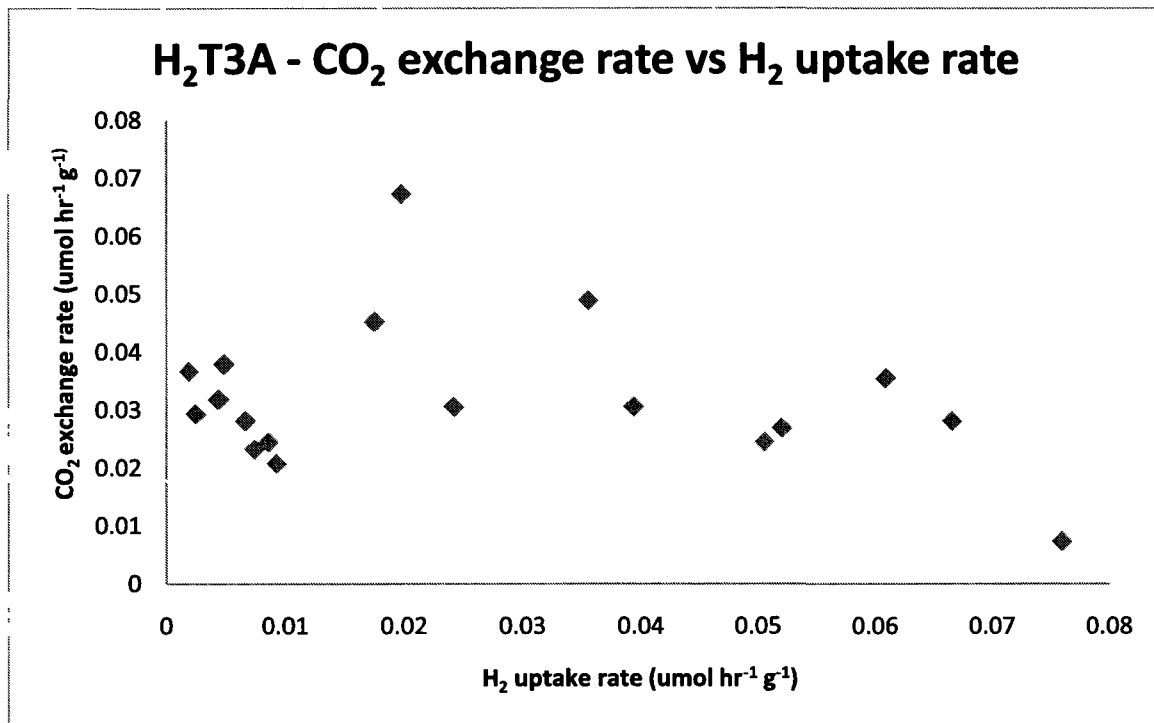


Figure 10 – CO₂ exchange plot for treatments H₂T3. Treatment lasted for 47 days. Y-axis shows CO₂ exchange rate in μmol per hour per gram soil and X-axis shows number of days of treatment at time of measurement

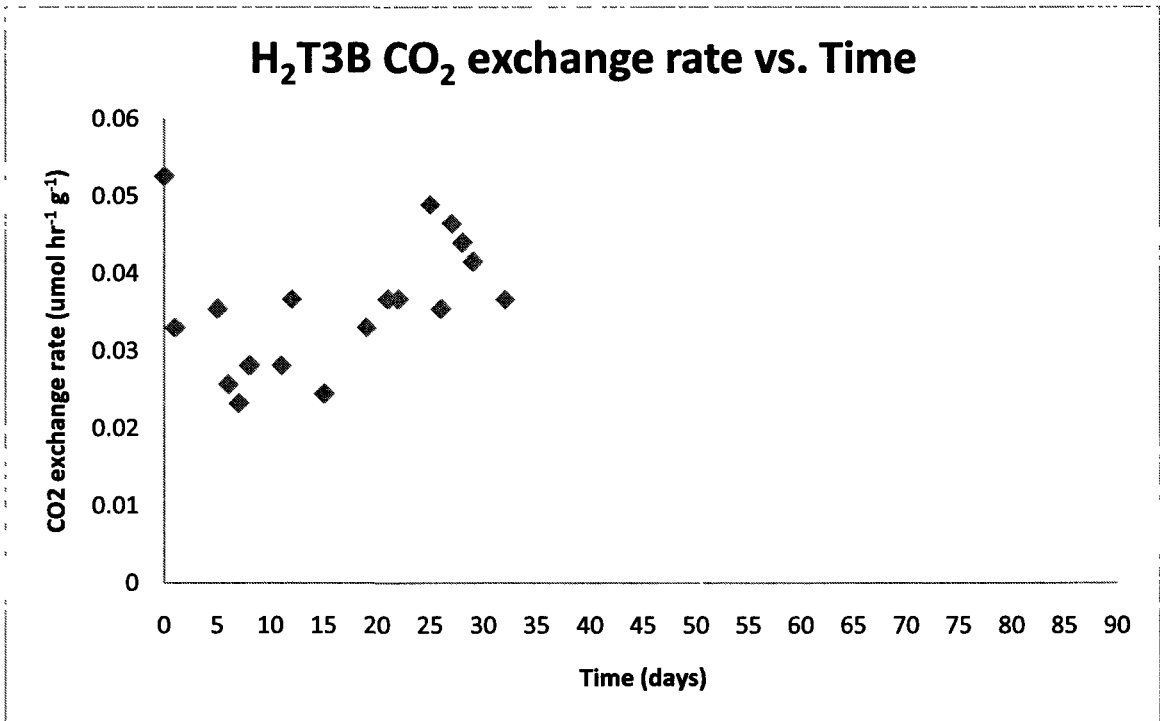
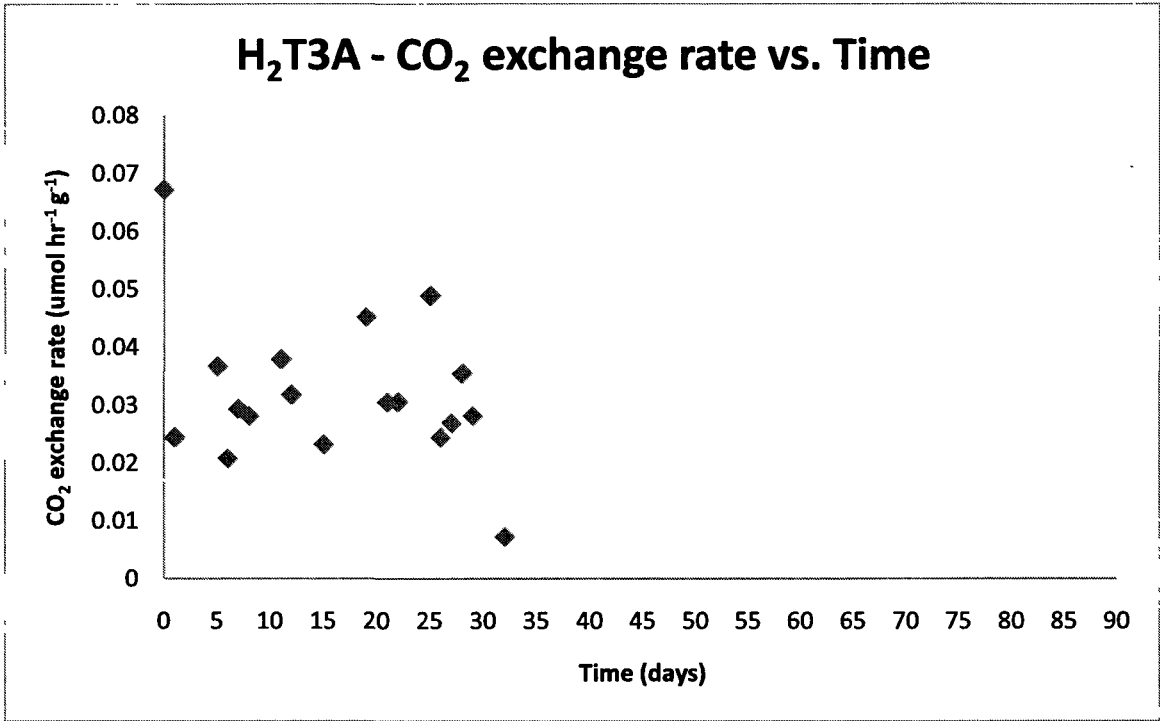


Table 8 – H₂ uptake data for treatment AT1.

Day	mA	H ₂ In (V)	H ₂ In (ppm)	H ₂ Out (V)	H ₂ Out (ppm)	H ₂ Absorbed (ppm)	Uptake Rate ($\mu\text{mol h}^{-1}\text{g}^{-1}$)
6	4.25	1.94	92.5	1.89	86.8	5.69	0.00834
8	4.26	2.02	102	2.00	99.9	2.57	0.00376
21	4.27	2.08	111	2.05	106	4.13	0.00605
47	4.28	2.33	152	2.28	142	9.33	0.0137

Figure 11 – H₂ uptake plot for treatment AT1. Treatment lasted for 47 days. Y-axis shows H₂ uptake rate in μmol absorbed per hour per gram soil and X-axis shows number of days of treatment at time of measurement

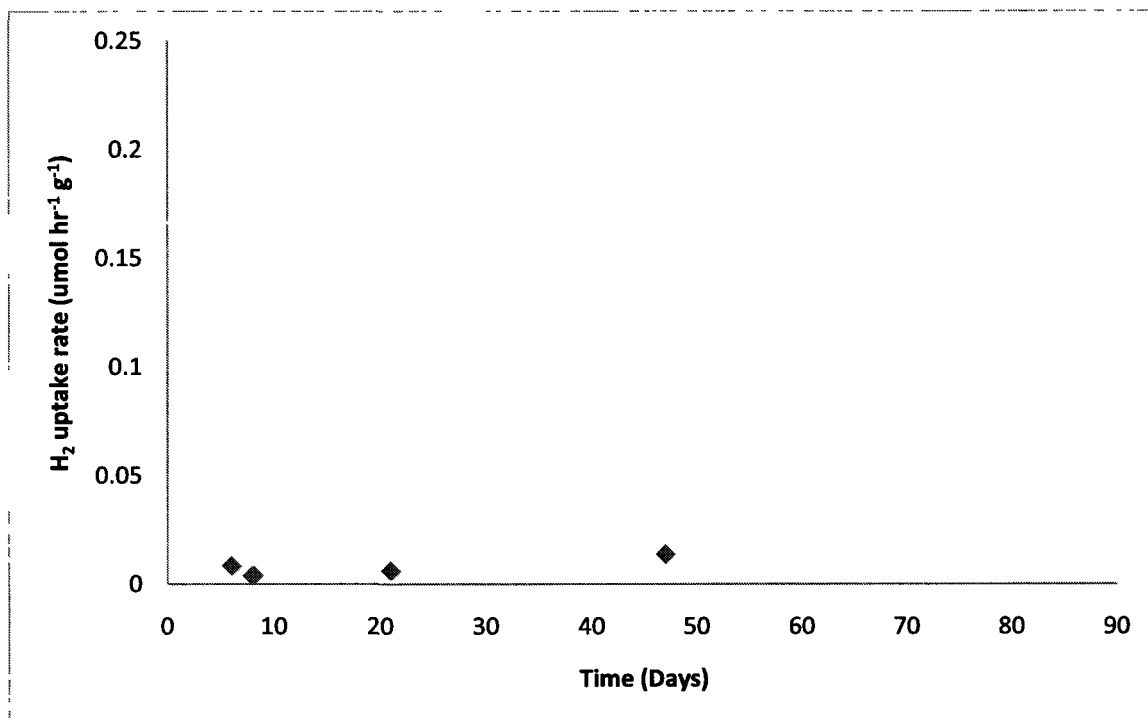


Table 9 – H₂ uptake data for treatment AT2.

Day	mA	H ₂ In (V)	H ₂ In (ppm)	H ₂ Out (V)	H ₂ Out (ppm)	H ₂ Absorbed (ppm)	Uptake Rate ($\mu\text{mol h}^{-1}\text{g}^{-1}$)
6	4.22	1.94	92.5	1.89	86.8	5.69	0.00772
8	4.25	2.03	104	1.99	98.6	5.13	0.00697
21	4.3	2.08	111	2.04	105	5.47	0.00743
48	4.24	2.40	166	2.34	154	12.2	0.0165
50	4.32	2.39	164	2.34	154	10.1	0.0137
58	4.33	2.57	206	2.53	196	10.2	0.0138
64	4.22	2.20	129	2.14	119	9.44	0.0128
67	4.25	2.02	102	1.93	91.4	11.1	0.0150
68	4.26	2.19	127	2.13	118	9.32	0.0126
69	4.25	2.21	130	2.15	121	9.56	0.0130
70	4.26	2.25	137	2.20	129	8.43	0.0114
71	4.23	2.24	135	2.17	124	11.5	0.0156
74	4.26	2.31	148	2.27	141	7.32	0.00994
75	4.27	2.34	154	2.27	141	13.1	0.0177
76	4.22	2.35	156	2.29	144	11.4	0.0155
77	4.22	2.34	154	2.29	144	9.45	0.0128

Figure 12 – H₂ uptake plot for treatment AT2. Treatment lasted for 77 days. Y-axis shows H₂ uptake rate in μmol absorbed per hour per gram soil and X-axis shows number of days of treatment at time of measurement.

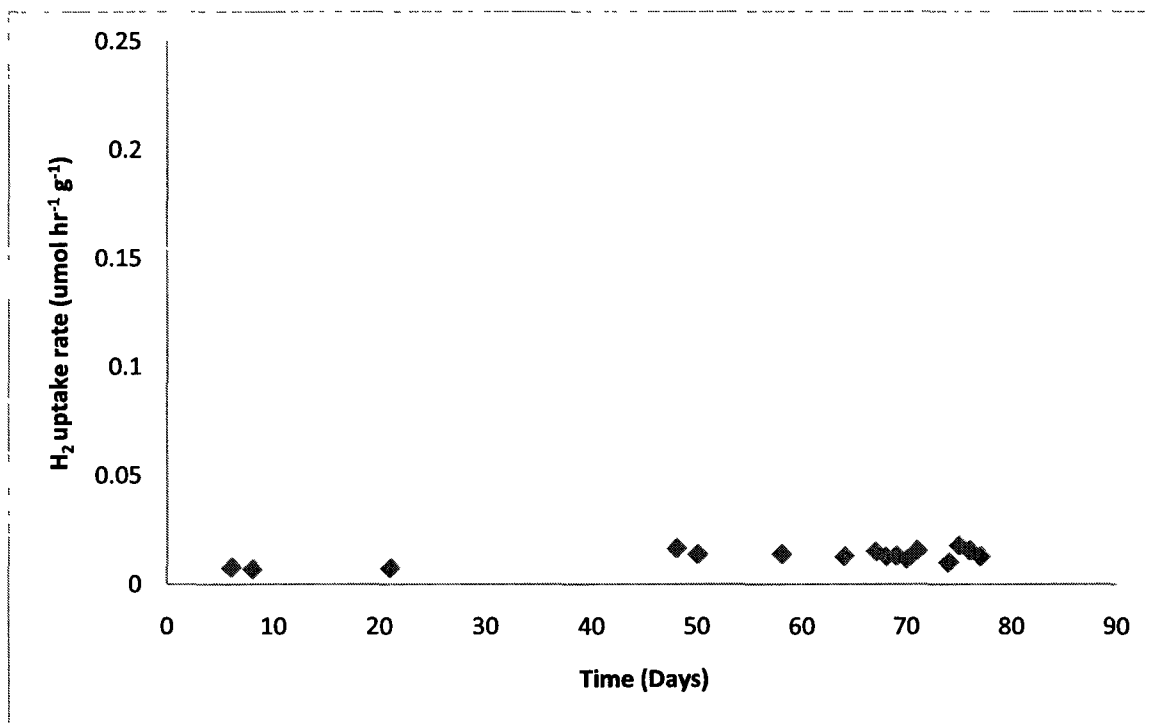


Table 10 – CO₂ exchange data for treatment AT1.

Day	CO ₂ In (ppm)	CO ₂ Out (ppm)	Difference (ppm)	μmol*hr ⁻¹ *g ⁻¹
32	390	418	28	0.0395
35	370	382	12	0.0170
47	369	380	11	0.0155

Figure 13 – CO₂ exchange plot for treatment AT1. Treatment lasted for 47 days. Y-axis shows CO₂ exchange rate in μmol per hour per gram soil and X-axis shows number of days of treatment at time of measurement

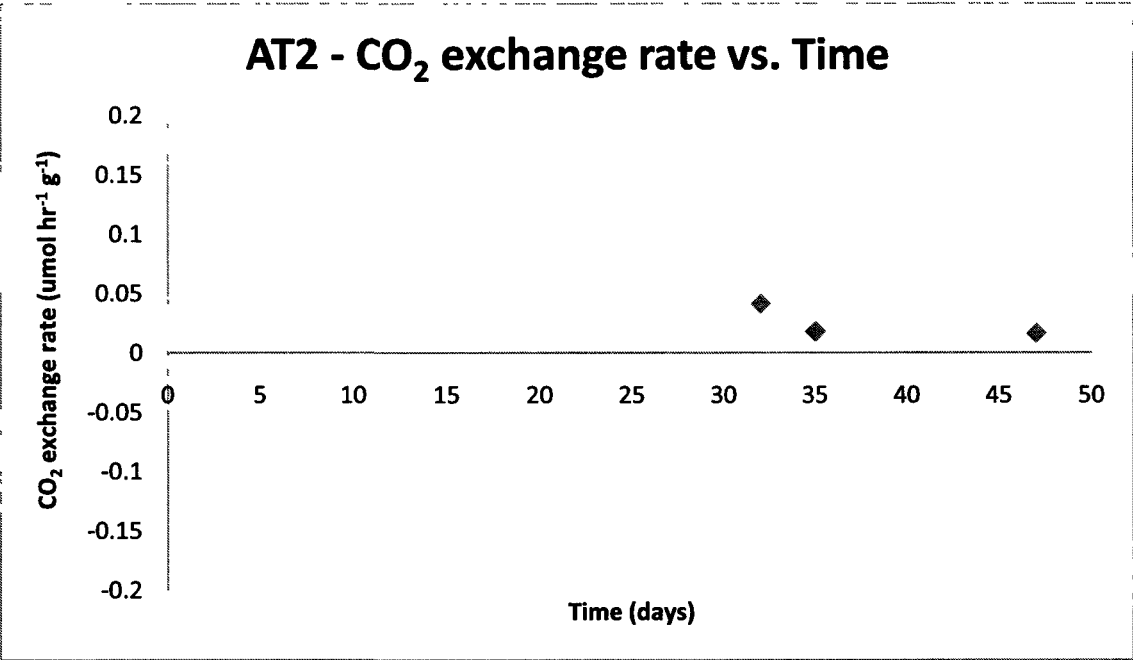


Table 11 – CO₂ exchange data for treatment AT2.

Day	CO ₂ In (ppm)	CO ₂ Out (ppm)	Difference (ppm)	μmol*hr ⁻¹ *g ⁻¹
32	390	500	110	0.149
35	355	372	17	0.0231
48	374	385	11	0.0149
50	358	370	12	0.0163
60	360	370	10	0.0136
67	367	375	8	0.0109
68	370	382	12	0.0163
69	375	390	15	0.0204
70	385	390	5	0.00679
71	375	388	13	0.0176
74	381	390	9	0.0122
75	380	390	10	0.0136
77	390	395	5	0.00679

Figure 14 – CO₂ exchange plot for treatment AT2. Treatment lasted for 77 days. Y-axis shows CO₂ exchange rate in μmol per hour per gram soil and X-axis shows number of days of treatment at time of measurement

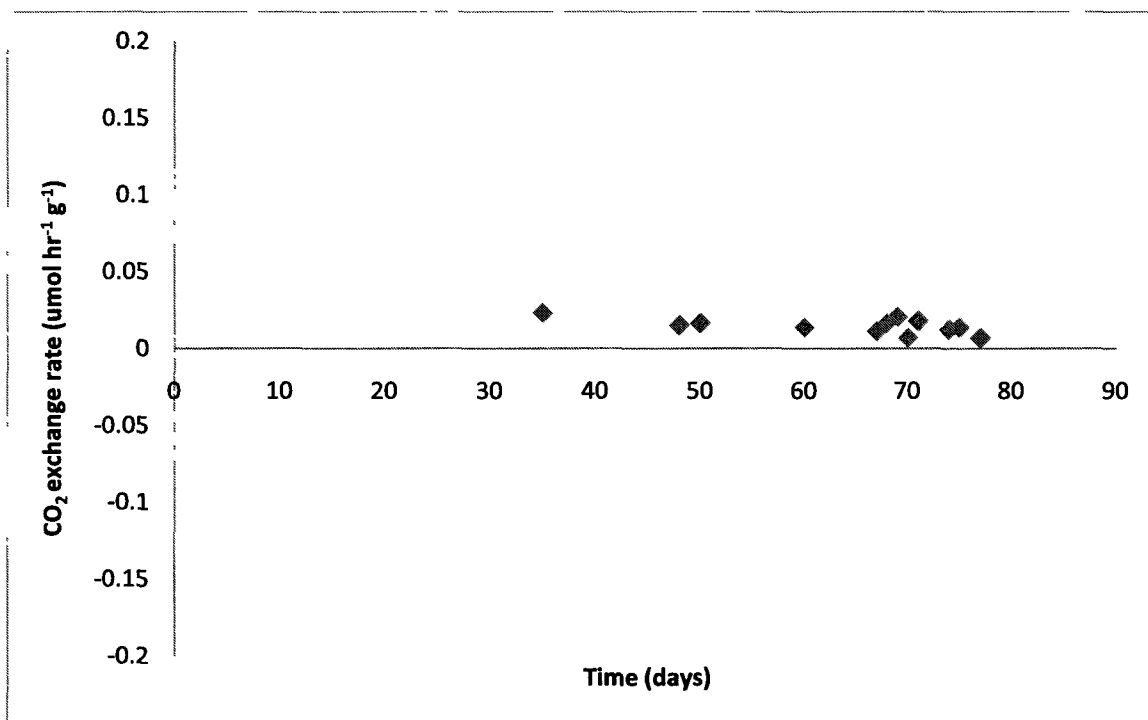


Figure 15 – Reference for comparison of H₂ uptake rates of treatments at time of collection

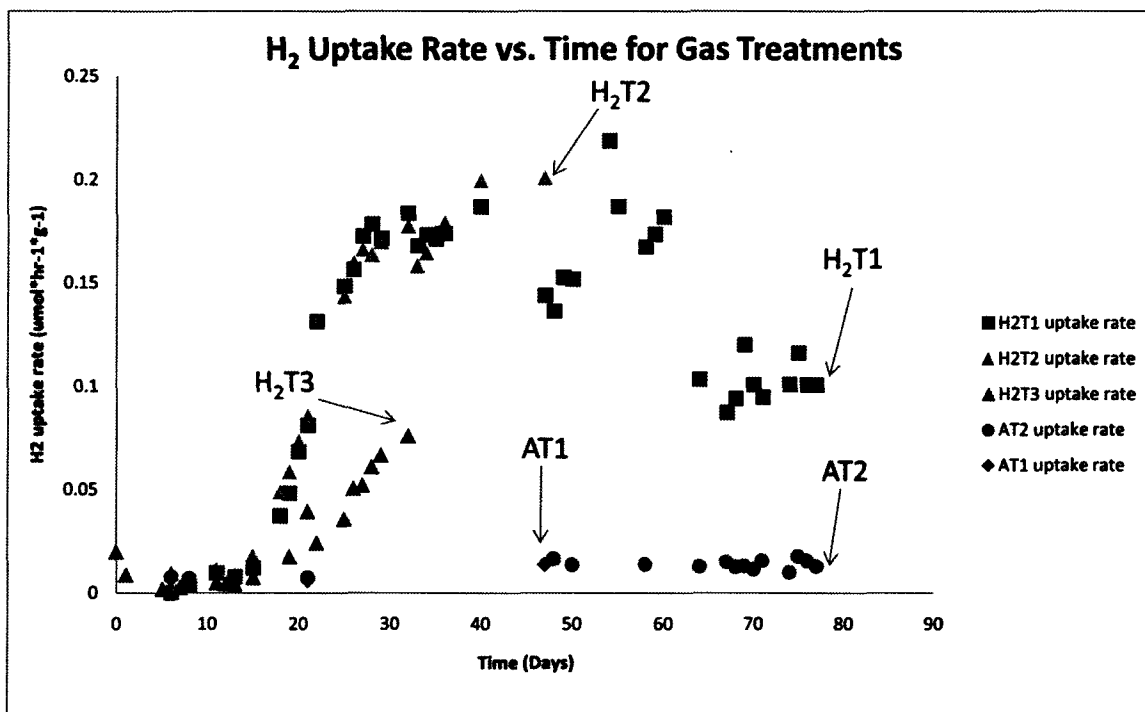


Table 12 – Reference table for general trends in H₂ uptake rate and CO₂ exchange rate in gas treated samples

Name	Treatment	Duration	H ₂ Exposure	Relative H ₂ Uptake rate	Net CO ₂ exchange (μmol hr ⁻¹ g ⁻¹)	Production/ Fixation
H ₂ T1	1000 ppm H ₂	77 days	Long	Mid	0.0562	Production
H ₂ T2	1000 ppm H ₂	47 days	Mid	High	-0.0802	Fixation
H ₂ T3	1000 ppm H ₂	32 days	Short	Mid-Low	0.0220 ⁺	Production
AT1	Room air	47 days	None	Low	0.0161	Production
AT2	Room air	77 days	None	Low	0.00679	Production

⁺Average of two short term treatments

Figure 16 – Methylene blue assays for nodules of soybean plants inoculated with JH47

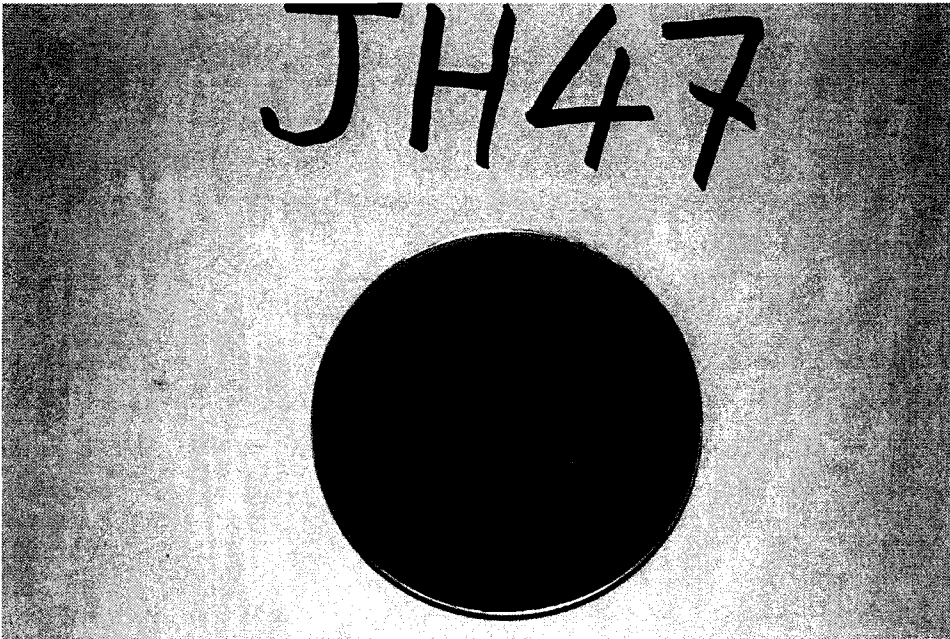
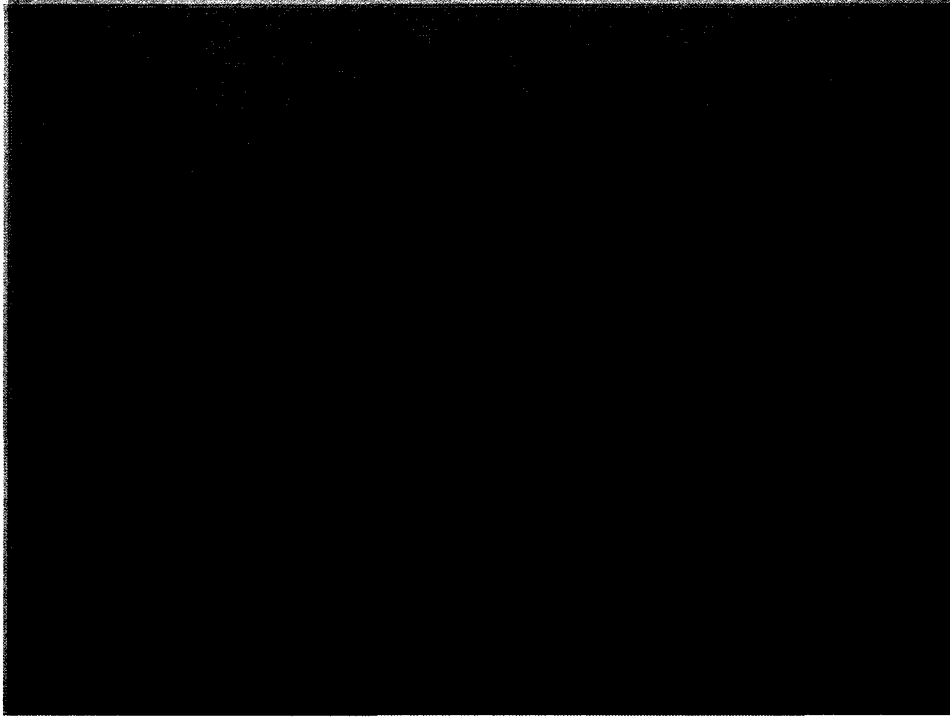


Figure 17 – Methylene blue assays for nodules of soybean plants inoculated with JH

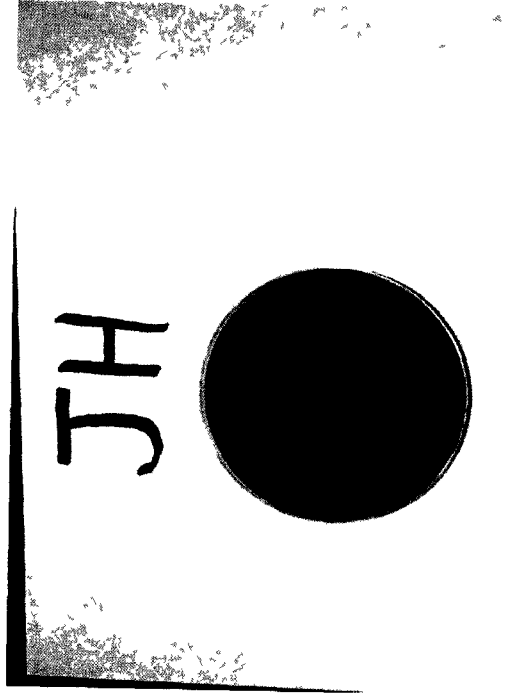
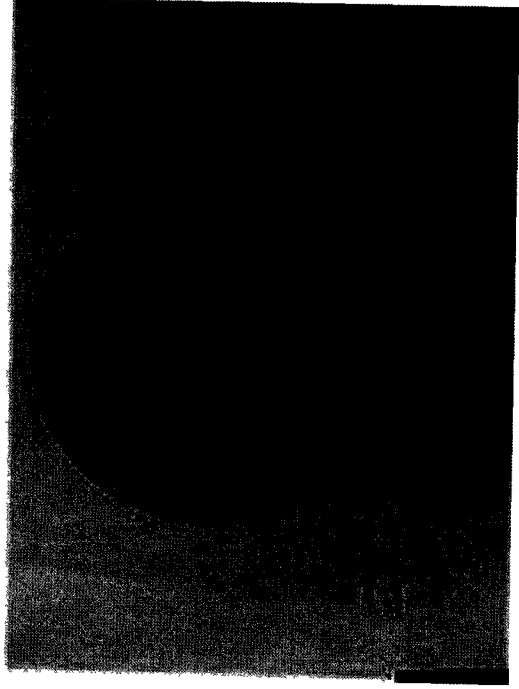
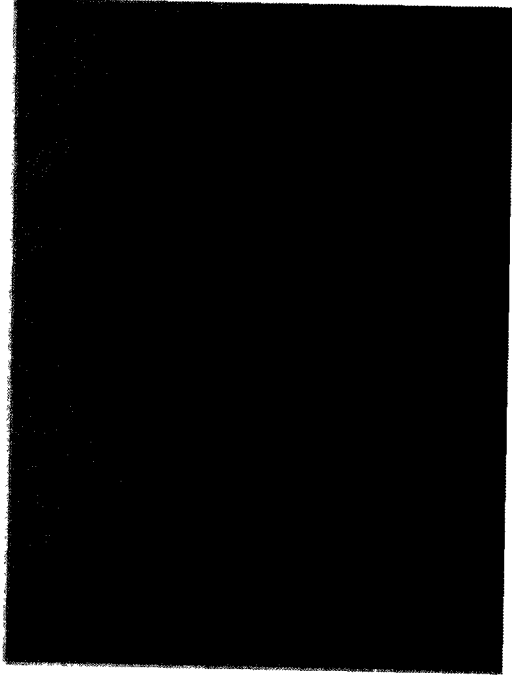


Figure 18 – Methylene blue assays for nodules of soybean plants inoculated with volunteer nodules. Nodules were treated as Hup⁻



control

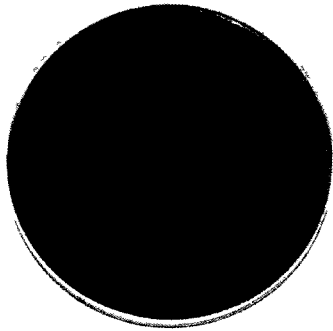


Table 13 – DNA extraction data for all treatments. Data includes maximum, minimum and mean DNA extracted for all treatments. Measured in ng DNA per g soil.

Treatment	Minimum (ng/g)	Maximum (ng/g)	Mean (ng/g)	S.D. (ng/g)
H ₂ T1	2.77x10 ³	6.60x10 ³	4.49x10 ³	1.22x10 ³
H ₂ T2	2.88x10 ³	6.87x10 ³	5.09x10 ³	1.68x10 ³
H ₂ T3	0.703x10 ³	1.03x10 ³	0.906x10 ³	0.144x10 ³
AT1	0.375x10 ³	0.994x10 ³	0.711x10 ³	0.285x10 ³
AT2	0.326x10 ³	1.20x10 ³	7.44x10 ³	0.339x10 ³
JH	1.89x10 ³	5.88x10 ³	3.48x10 ³	1.43x10 ³
JH47	2.27x10 ³	6.72x10 ³	3.83x10 ³	1.61x10 ³
Root	1.80x10 ³	2.58x10 ³	2.05x10 ³	0.368x10 ³

Table 14 – RNA extraction data for all treatments. Data includes maximum, minimum and mean DNA extracted for all treatments. Measured in ng RNA per g soil.

Treatment	Minimum (ng/g)	Maximum (ng/g)	Mean (ng/g)	S.D. (ng/g)
H ₂ T1	4.45x10 ²	17,1 x10 ²	9.73x10 ²	5.29x10 ²
H ₂ T2	8.49x10 ²	23.2x10 ²	13.2 x10 ²	6.78x10 ²
H ₂ T3	9.91x10 ²	13.4x10 ²	11.5 x10 ²	1.70x10 ²
AT	0.933x10 ²	9.08x10 ²	4.24x10 ²	2.97x10 ²
JH	1.68x10 ²	26.3 x10 ²	10.0 x10 ²	10.3 x10 ²
JH47	2.09x10 ²	33.8 x10 ²	20.4 x10 ²	12.4x10 ²

Figure 19 –DNA/RNA extracted from all soil treatments. Chart displays calculated mean with standard error bars.

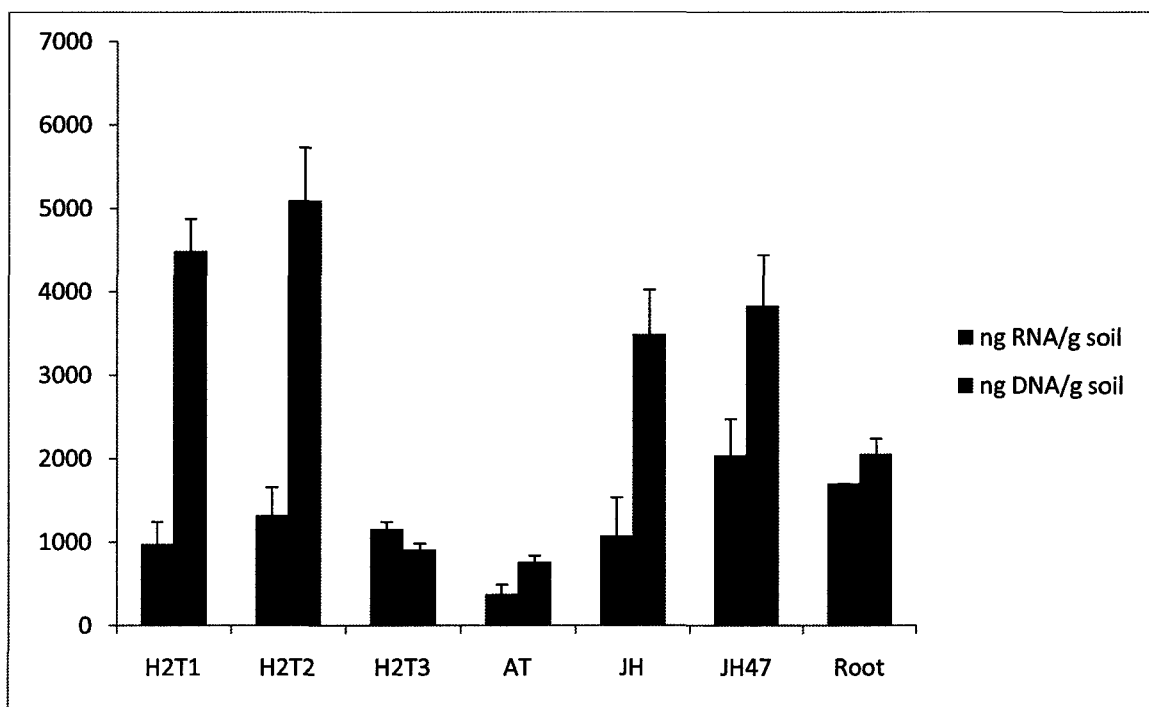


Figure 20 –PCR result for *cbbLR1F/cbbLR1R* for red-like *cbbL* (wells 2-5) and *cbbLG1F/cbbLG1R* for green-like (wells 8-11). Wells 2, 3, 8 and 9 contain DNA from Air treated soil and 4,5,10 and 11 contain DNA from H₂ treated soil.

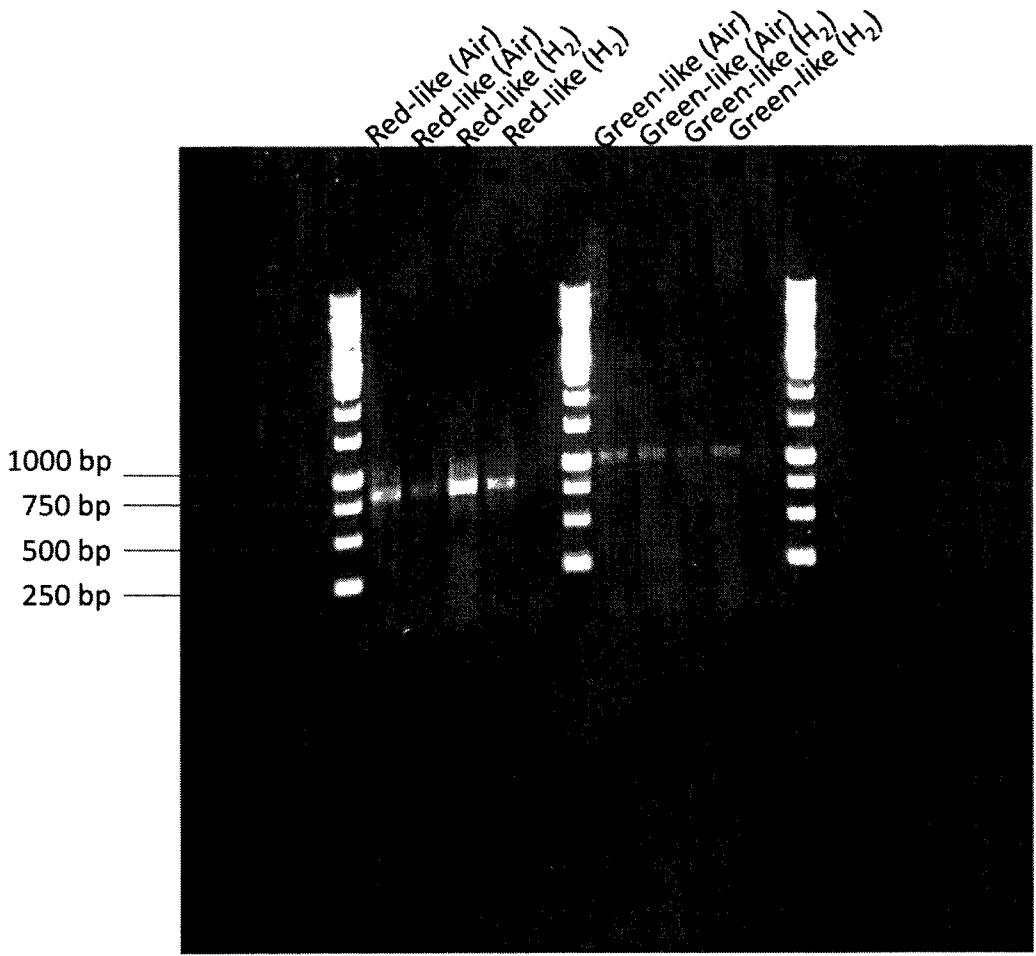


Figure 21—Example of PCR result for cbbLR1F/cbbLR1intR. Shows cDNA result for air treated soil (wells 2, 3), rhizosphere soils (wells 4, 5, 6) and plasmid control (well 7). Bottom band of ladder = 250 bp.

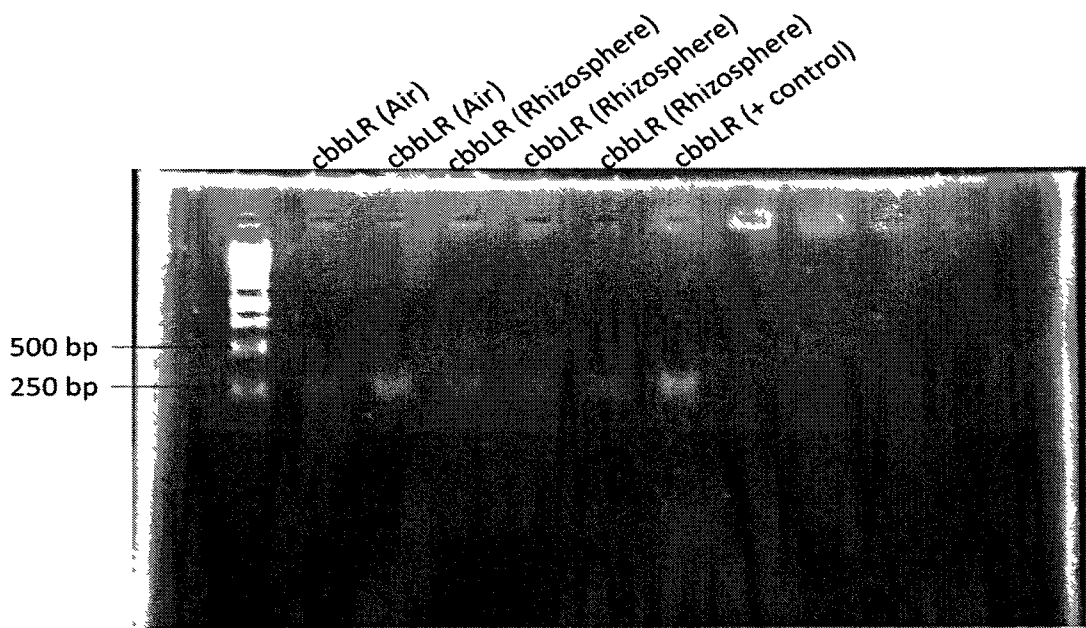


Figure 22 –Example of PCR result for cbbLG1F/cbbLG2R1. Shows DNA results for H₂ treated soil (wells 2-5), rhizosphere (wells 6-9) and negative control (well 10).

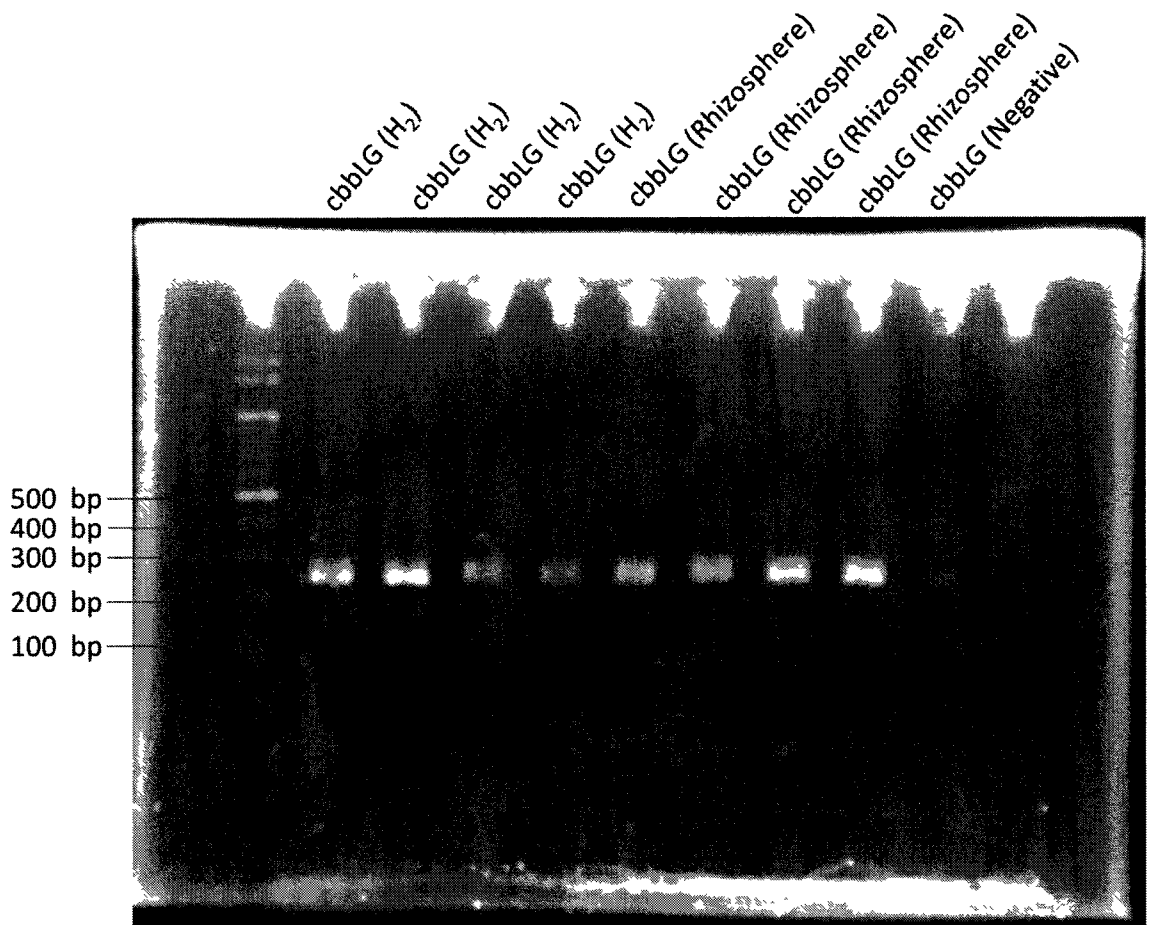


Table 15 – cbbLR1F/cbbLR1intR gene copy data for all treatments. Includes copies per ng DNA and copies per g soil. Table 15a shows copies per ng DNA and Table 15b shows copies per g soil. Note: subscript letters with means show significant groupings ($p < 0.05$).

Table 15a - Copies per ng DNA

Treatment	Minimum	Maximum	Mean ⁺	S.D.	N
Gas treated					
H ₂ T1	1.94 x10 ⁴	26.7x10 ⁴	12.7 x10 ⁴ _a	6.24 x10 ⁴	17
H ₂ T2	0.785 x10 ⁴	31.1 x10 ⁴	6.97 x10 ⁴ _b	6.93 x10 ⁴	20
H ₂ T3	0.790 x10 ⁴	5.47 x10 ⁴	2.04 x10 ⁴ _c	2.29 x10 ⁴	4
AT1	0.351 x10 ⁴	2.24 x10 ⁴	1.25 x10 ⁴ _c	0.646 x10 ⁴	7
AT2	0.382 x10 ⁴	1.33 x10 ⁴	0.972 x10 ⁴ _c	0.337 x10 ⁴	8

Rhizosphere					
JH	2.73 x10 ⁴	10.9 x10 ⁴	7.67 x10 ⁴ _d	2.90 x10 ⁴	15
JH47	2.07 x10 ⁴	21.8 x10 ⁴	8.47 x10 ⁴ _d	4.93 x10 ⁴	15
Root	17.1x10 ⁴	34.1x10 ⁴	24.4x10 ⁴ _e	6.66 x10 ⁴	6

Table 15b - Copies per g Soil

Treatment	Minimum	Maximum	Mean ⁺	S.D.	N
Gas treated					
H ₂ T1	12.8 x10 ⁶	176 x10 ⁶	55.3 x10 ⁶ _a	40.2 x10 ⁶	17
H ₂ T2	4.40 x10 ⁶	213 x10 ⁶	41.8 x10 ⁶ _b	51.0 x10 ⁶	20
H ₂ T3	0.556 x10 ⁶	5.37 x10 ⁶	1.94 x10 ⁶ _c	2.29 x10 ⁶	4
AT1	0.311 x10 ⁶	2.19 x10 ⁶	1.22 x10 ⁶ _c	0.637 x10 ⁶	8
AT2	0.384 x10 ⁶	1.40 x10 ⁶	1.04 x10 ⁶ _c	0.329 x10 ⁶	8

Rhizosphere					
JH	6.37 x10 ⁶	50.5 x10 ⁶	30.2 x10 ⁶	15.6 x10 ⁶	15
JH47	8.71 x10 ⁶	147 x10 ⁶	43.1 x10 ⁶	35.4 x10 ⁶	15
Root	31.1 x10 ⁶	75.2 x10 ⁶	53.1 x10 ⁶	16.3 x10 ⁶	6

⁺ a, b and c denote statistically significant grouping (p < 0.05); d and e denote significant groups for rhizosphere samples (p < 0.05)

Table 16 – cbbLG1F/cbbLG2R1 gene copy data for all treatments. Includes copies per ng DNA and copies per g soil. Table 16a shows copies per ng DNA and Table 16b shows copies per g soil.

Table 16a - Copies per ng DNA

Treatment	Minimum	Maximum	Mean	S.D.	N
Gas Treated					
H ₂ T1	3.79 x10 ⁴	18.7 x10 ⁴	11.3 x10 ⁴	8.39 x10 ⁴	4
H ₂ T2	17.3 x10 ⁴	20.7 x10 ⁴	19.2 x10 ⁴	1.57 x10 ⁴	4
H ₂ T3	0.304 x10 ⁴	2.14 x10 ⁴	1.03 x10 ⁴	0.856 x10 ⁴	4
AT	0.170 x10 ⁴	9.76 x10 ⁴	3.38 x10 ⁴	3.97 x10 ⁴	6
Rhizosphere					
JH	0.629 x10 ⁴	0.840 x10 ⁴	0.731 x10 ⁴	0.0863 x10 ⁴	4
JH47	0.779 x10 ⁴	1.62 x10 ⁴	1.08 x10 ⁴	0.472 x10 ⁴	3

Table 13b - Copies per g Soil

Treatment	Minimum	Maximum	Mean	S.D.	N
Gas Treated					
H ₂ T1	14.3 x10 ⁶	76.8 x10 ⁶	45.6 x10 ⁶	35.2 x10 ⁶	4
H ₂ T2	64.9 x10 ⁶	141 x10 ⁶	102 x10 ⁶	37.3 x10 ⁶	4
H ₂ T3	0.313 x10 ⁶	2.10 x10 ⁶	1.02 x10 ⁶	0.831 x10 ⁶	4
AT1	0.111 x10 ⁶	9.81 x10 ⁶	3.31 x10 ⁶	4.04 x10 ⁶	6
Rhizosphere					
JH	1.82 x10 ⁶	2.82 x10 ⁶	2.29 x10 ⁶	0.436 x10 ⁶	4
JH47	1.88 x10 ⁶	10.8 x10 ⁶	6.00 x10 ⁶	4.55 x10 ⁶	3

Table 17 – cbbLR1F/cbbLR1intR gene expression data for all treatments. Includes copies per ng RNA and RNA copies per g soil. Table 17a shows copies per ng RNA and Table 17b shows copies per g soil Note: subscript letters with means show significant groupings (p<0.05)

Table 17a - Copies per ng RNA

Treatment	Minimum	Maximum	Mean ⁺	S.D.	N
Gas treated					
H ₂ T1	6.79 x10 ⁴	105 x10 ⁴	60.4 x10 ⁴ _{a c}	37.6x10 ⁴	9
H ₂ T2	1.40 x10 ⁴	13.5 x10 ⁴	7.28 x10 ⁴ _b	5.02x10 ⁴	8
H ₂ T3	5.89 x10 ⁴	33.4x10 ⁴	18.4x10 ⁴ _{b c}	9.24x10 ⁴	8
AT1	1.28 x10 ⁴	55.7 x10 ⁴	17.0 x10 ⁴ _b	22.7x10 ⁴	10

Rhizosphere					
JH	0.000	23.2 x10 ⁴	4.46 x10 ⁴ _d	8.79x10 ⁴	7
JH47	0.000	37.1 x10 ⁴	21.1 x10 ⁴ _e	12.2 x10 ⁴	7
Root	0.450 x10 ⁴	4.23 x10 ⁴	2.34 x10 ⁴	2.67 x10 ⁴	2

Table 17b - RNA Copies per g Soil

Treatment	Minimum	Maximum	Mean ⁺	S.D.	N
Gas treated					
H ₂ T1	11.6 x10 ⁶	91.0 x10 ⁶	53.7 x10 ⁶ _a	30.2 x10 ⁶	9
H ₂ T2	2.56 x10 ⁶	13.9 x10 ⁶	7.94 x10 ⁶ _b	4.68 x10 ⁶	8
H ₂ T3	7.92 x10 ⁶	34.4 x10 ⁶	20.5 x10 ⁶ _{a c}	9.22 x10 ⁶	8
AT	0.285 x10 ⁶	6.33 x10 ⁶	2.78x10 ⁶ _c	2.28 x10 ⁶	10

Rhizosphere					
JH	0.000	61.1 x10 ⁶	11.8x10 ⁶	23.1 x10 ⁶	7
JH47	0.000	80.0 x10 ⁶	25.0 x10 ⁶	28.9 x10 ⁶	7
Root	0.764 x10 ⁶	7.18 x10 ⁶	3.97 x10 ⁶	4.54 x10 ⁶	2

⁺ a, b and c denote significant groups for gas treated samples; d and e denote significant groups for rhizosphere samples (p < 0.05)

Table 18 – cbbLG1F/cbbLG2R1 gene expression data for all treatments. Includes copies per ng DNA and copies per g soil. Table 18a shows copies per ng RNA and Table 18b shows RNA copies per g soil

Table 18a - Copies per ng RNA

Treatment	Minimum	Maximum	Mean	S.D.	N
Gas treated					
H ₂ T1	4.75 x10 ⁴	9.30 x10 ⁴	7.20 x10 ⁴	2.45 x10 ⁴	4
H ₂ T2	4.61 x10 ⁴	26.4 x10 ⁴	12.6 x10 ⁴	10.2 x10 ⁴	4
AT1	0.000	12.5 x10 ⁴	4.05 x10 ⁴	4.98 x10 ⁴	6
Rhizosphere					
JH	0.000	4.16 x10 ⁴	19.0 x10 ⁴	1.48 x10 ⁴	8
JH47	0.000	3.91 x10 ⁴	1.48 x10 ⁴	1.54 x10 ⁴	7
Root	0.985 x10 ⁴	2.33 x10 ⁴	1.66 x10 ⁴	0.949 x10 ⁴	2

Table 18b - RNA Copies per g Soil

Treatment	Minimum	Maximum	Mean	S.D.	N
Gas treated					
H ₂ T1	4.10 x10 ⁶	15.9 x10 ⁶	10.1 x10 ⁶	6.63 x10 ⁶	4
H ₂ T2	4.73 x10 ⁶	47.3 x10 ⁶	26.1 x10 ⁶	26.9 x10 ⁶	4
AT	0.000	6.24 x10 ⁶	1.94 x10 ⁶	2.51 x10 ⁶	6
Rhizosphere					
JH	0.000	6.64 x10 ⁶	1.94 x10 ⁶	2.51 x10 ⁶	8
JH47	0.000	6.86 x10 ⁶	1.85 x10 ⁶	2.32 x10 ⁶	7
Root	1.67 x10 ⁶	3.95 x10 ⁶	2.81 x10 ⁶	1.61 x10 ⁶	2

Figure 23 – Average gene copy number and gene expression for primer set cbbLR1F/cbbLR1intR. Figures show average quantification with standard error bars. Figure 23a shows copies per ng DNA/RNA. Figure 23b shows DNA/RNA copies per g soil

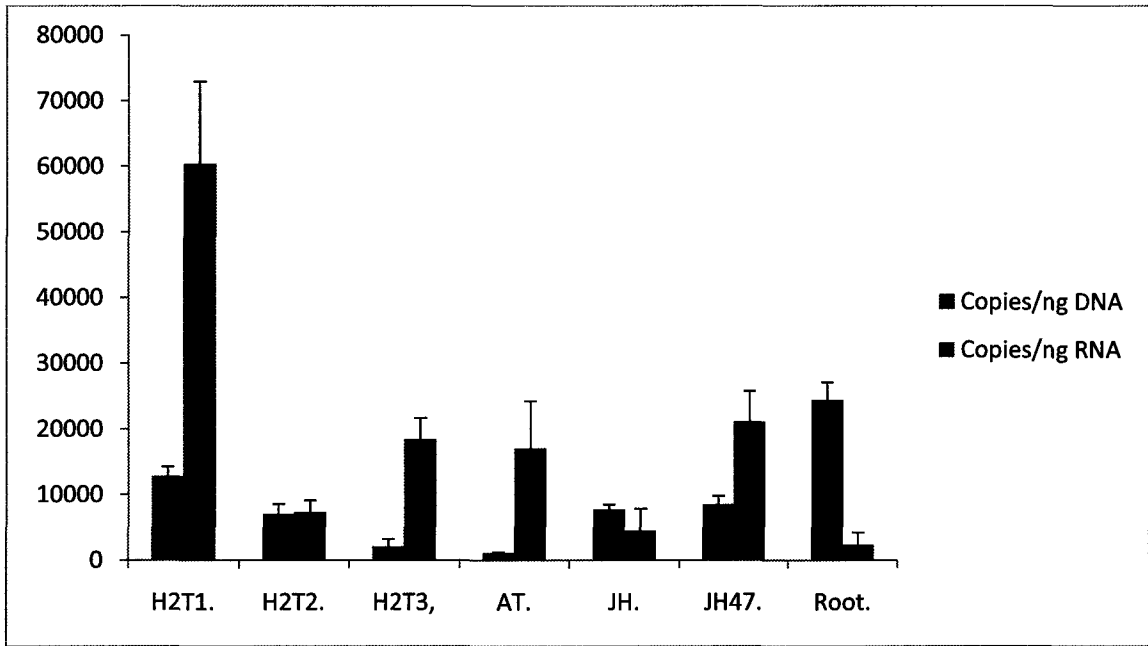


Figure 23a - Copies per ng DNA/RNA

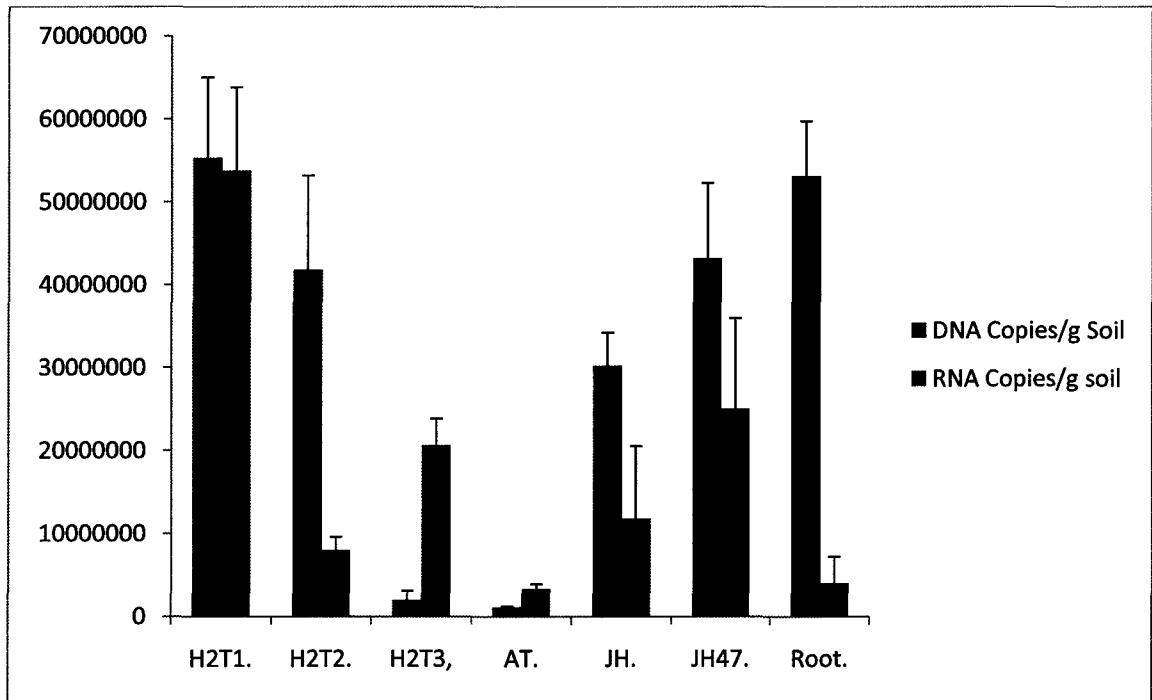


Figure 23b – DNA/RNA copies per g soil

Figure 24 – Average gene copy number and gene expression for primer set cbbLG1F/cbbLG2R1. Figures show average quantification with standard error bars. Figure 24a shows copies per ng DNA/RNA. Figure 24b shows DNA/RNA copies per g soil

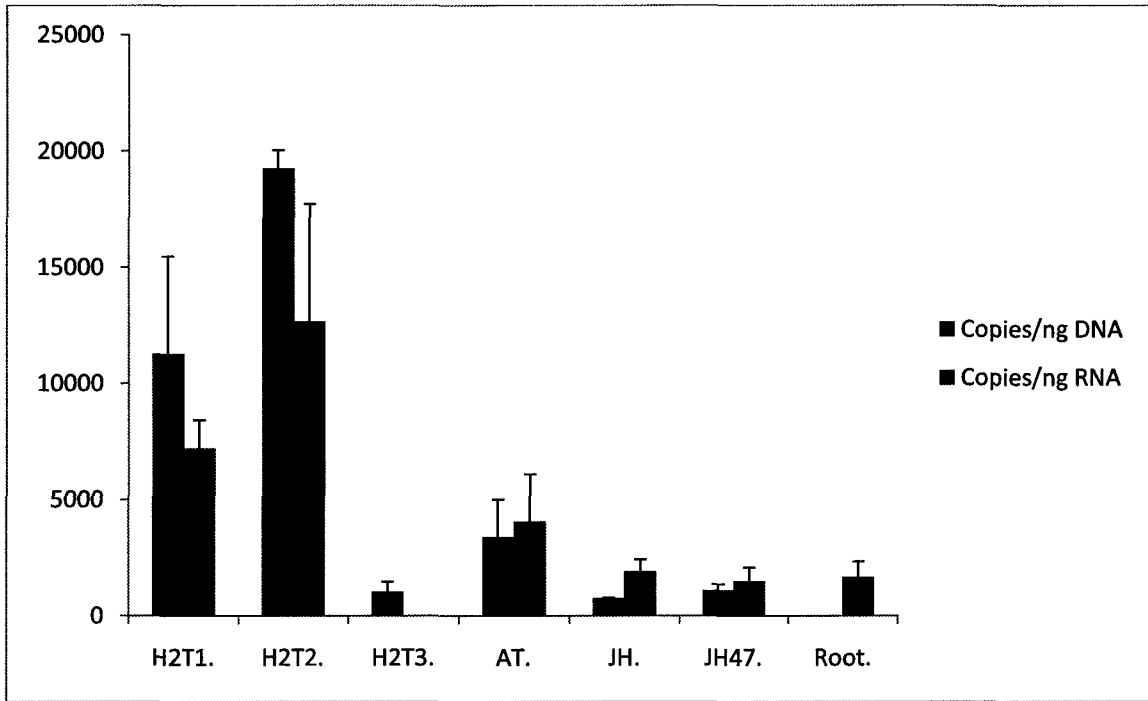


Figure 24a - copies per ng DNA/RNA.

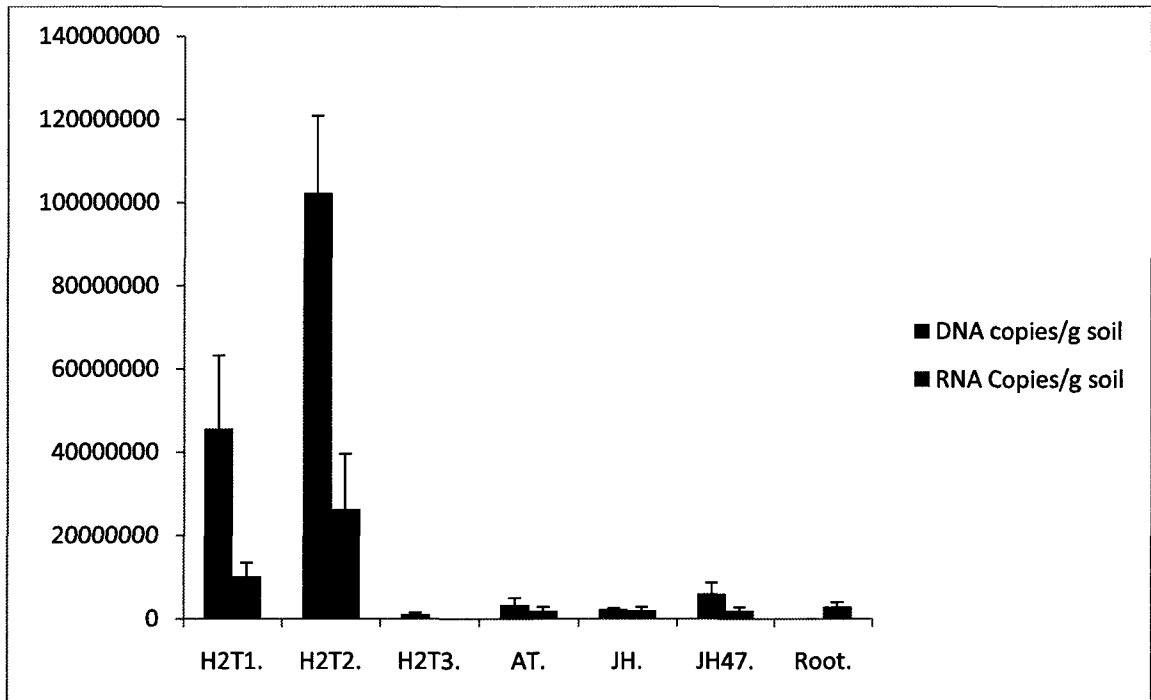


Figure 24b - DNA/RNA copies per g soil

Figure 25 – Example of real time PCR results. Labels include standards (10^8 , 10^6 , 10^4 and 10^3), unknown sample, inhibition control (unknown+ 10^4) and negative control

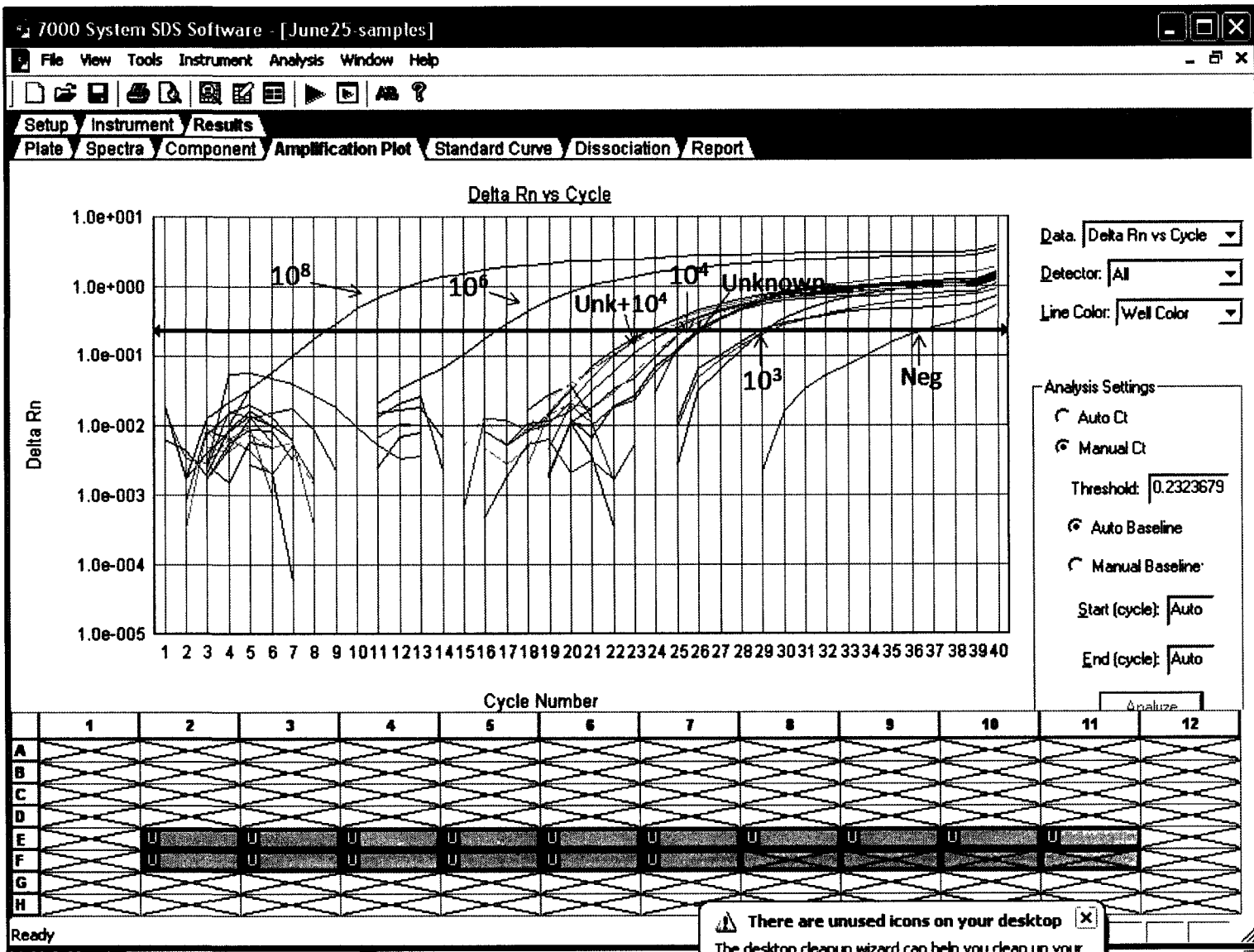


Table 19 – Sequencing results for primer set cbbLR1F/cbbLR1intR. 186 Cases

Nearest Match	#	%
<i>Uncultured bacterium clone HKOR7 ribulose-1,5-bisphosphate carboxylase/oxygenase</i>	123	66.1
<i>Starkeya novella DSM 506</i>	17	9.14
<i>Bradyrhizobium japonicum strain USDA 6 ribulose 1,5-bisphosphate</i>	7	3.76
<i>Oligotropha carboxidovorans strain OM5 ribulose 1,5-bisphosphate carboxylase/oxygenase large subunit (rbcl) gene</i>	5	2.69
<i>Uncultured bacterium clone HKOR8 ribulose-1,5-bisphosphate carboxylase/oxygenase</i>	5	2.69
<i>Variovorax paradoxus S110 chromosome 1</i>	3	1.61
<i>Uncultured soil bacterium clone CT5.23 ribulose-1,5-bisphosphate carboxylase/oxygenase large subunit (cbbL) gene</i>	2	1.08
<i>Bradyrhizobium japonicum USDA 110</i>	2	1.08
<i>Uncultured proteobacterium clone F36 ribulose-1,5-bisphosphate carboxylase/oxygenase large subunit (rbcl) gene</i>	2	1.08
<i>Uncultured bacterium clone L5 ribulose-1,5-bisphosphate carboxylase/oxygenase large subunit (cbbL) gene, partial cds</i>	2	1.08
<i>Bradyrhizobium sp. CPP ribulose 1,5-bisphosphate carboxylase/oxygenase</i>	2	1.08
<i>Uncultured proteobacterium clone F24 ribulose-1,5-bisphosphate</i>	2	1.08
<i>Uncultured soil bacterium clone GP5.178 ribulose-1,5-bisphosphate</i>	2	1.08
<i>Nitrobacter winogradskyi Nb-255</i>	1	0.538
<i>Uncultured bacterium clone H33 ribulose-1,5-bisphosphate carboxylase/oxygenase large subunit (cbbL) gene</i>	1	0.538
<i>Rhizobium leguminosarum bv. trifolii strain ATCC 53912 ribulose-1,5-bisphosphate carboxylase/oxygenase large subunit (cbbL) gene</i>	1	0.538
<i>Uncultured bacterium gene for ribulose-1,5-bisphosphate carboxylase/oxygenase large subunit, partial cds, clone: OY04C1cbbL-073</i>	1	0.538
<i>Methylibium petroleiphilum PM1</i>	1	0.538
<i>Uncultured proteobacterium clone F30 ribulose-1,5-bisphosphate</i>	1	0.538
<i>Uncultured bacterium clone R39c ribulose-1,5-bisphosphate carboxylase/oxygenase</i>	1	0.538
<i>Uncultured soil bacterium clone CT5.13 ribulose-1,5-bisphosphate carboxylase/oxygenase large subunit (cbbL) gene</i>	1	0.538
<i>Uncultured soil bacterium clone GP5.178 ribulose-1,5-bisphosphate</i>	1	0.538
<i>Uncultured soil bacterium clone CT5.93 ribulose-1,5-bisphosphate carboxylase/oxygenase large subunit (cbbL) gene</i>	1	0.538
<i>Rhodopseudomonas palustris BisA53, complete genome</i>	1	0.538
<i>Uncultured bacterium clone D12r132 ribulose-1,5-bisphosphate</i>	1	0.538
Total	186	

Table 20 – Sequencing results for primer set cbbLG1F/cbbLG2R1. 74 Cases

Nearest Match	#	%
<i>Mycobacterium</i> sp. DSM 3803 ribulose-1,5-bisphosphate carboxylase/oxygenase	23	31.1
<i>Starkeya novella</i> DSM 506	18	24.3
<i>Bradyrhizobium japonicum</i> USDA 110	7	9.46
<i>Thermomonospora curvata</i> DSM 43183	6	8.11
<i>Rhodopseudomonas palustris</i> TIE-1	6	8.11
<i>Pirellula staley</i> DSM 6068, complete genome	6	8.11
<i>Rhodopseudomonas palustris</i> BisB18	4	5.41
<i>Bradyrhizobium</i> sp. BTAi1, complete genome	3	4.05
<i>Bradyrhizobium</i> sp. ORS278	1	1.35
Total	74	

Table 21 – Sequencing results for primer set cbbLR1F/cbbLR1intR comparing species found in Air and H₂ treated soils

Air Treated	#	%	H₂ Treated	#	%
<i>Uncultured bacterium clone HKOR7 ribulose-1,5-bisphosphate carboxylase/oxygenase</i>	43	79.6	<i>Uncultured bacterium clone HKOR7 ribulose-1,5-bisphosphate carboxylase/oxygenase</i>	40	67.8
<i>Uncultured proteobacterium clone F30 ribulose-1,5-bisphosphate</i>	1	1.85	<i>Starkeya novella DSM 506, complete genome</i>	13	22.0
<i>Uncultured bacterium clone R39c ribulose-1,5-bisphosphate carboxylase/oxygenase</i>	1	1.85	<i>Uncultured soil bacterium clone GP5.178 ribulose-1,5-bisphosphate</i>	2	3.39
<i>Uncultured proteobacterium clone F24 ribulose-1,5-bisphosphate</i>	2	3.70	<i>Rhodopseudomonas palustris BisA53, complete genome</i>	1	1.69
<i>Uncultured bacterium clone HKOR8 ribulose-1,5-bisphosphate carboxylase/oxygenase</i>	1	1.85	<i>Uncultured bacterium clone D12rl32 ribulose-1,5-bisphosphate</i>	1	1.69
<i>Uncultured soil bacterium clone GP5.178 ribulose-1,5-bisphosphate</i>	1	1.85	<i>Uncultured bacterium clone L5 ribulose-1,5-bisphosphate carboxylase/oxygenase</i>	1	1.69
Uncultured proteobacterium clone F36 ribulose-1,5-bisphosphate carboxylase/oxygenase	1	1.85	<i>Bradyrhizobium japonicum strain USDA 6 ribulose 1,5-bisphosphate</i>	1	1.69
<i>Bradyrhizobium sp. CPP ribulose 1,5-bisphosphate carboxylase/oxygenase</i>	1	1.85			
<i>Bradyrhizobium japonicum strain USDA 6 ribulose 1,5-bisphosphate</i>	2	3.70			
<i>Bradyrhizobium japonicum USDA 110 DNA, complete genome</i>	1	1.85			
Total	54			59	

4 Discussion

4.1 Controlled Gas Treatment

4.1.1 H₂ Uptake

As in past studies, it was found that treatment of soil with a controlled flow of H₂ gas led to a detectable increase in the H₂ uptake capability of soil microorganisms (Dong and Layzell, 2001, Stein et al., 2005). This increase in H₂ oxidation in soil is attributed mainly to bacteria (McLearn and Dong, 2002). It is evident that the increase in H₂ uptake in the soil is not a static occurrence but one that is in constant flux (see Figure 2); this suggests that changes are occurring to the soil bacterial community throughout treatment; this agrees with the fact H₂ treatment has been found to induce increases in the percentages certain soil bacterial groups (Stein *et al.*, 2005). The long term H₂ treatment uptake rate plot is reminiscent of one part of a predator-prey relationship in which the growing population of H₂ oxidizers in the soil are acting as food source for other organisms. It has been noted that H₂ treatment also produces an increase in springtails and small insects that may utilize bacteria as a food source (Dong and Layzell, 2001). The idea of predator-prey relationships in bacterial communities is not widely studied; prey bacteria have recently been shown to affect the community structure of predator bacteria (Chen *et al.*, 2011).

4.1.2 CO₂ Exchange

The state of flux noted in the long term H₂ uptake rate is also evident in the corresponding CO₂ exchange. The emission of CO₂ from soil decreases as the H₂ uptake rate increases to the point where there is a net flux of CO₂ into the soil (see Figure 7). However, just as the H₂ uptake rate decreases the CO₂ exchange rate also becomes more positive (emitting CO₂ from soil). In the end, the CO₂ exchange seemed to level off at a positive value (see Figure 5). It is possible that this CO₂ emission is due to decomposers and respiration more so than a lack of CO₂ fixation; this is evident in the *cbbL* activity in the soil (see Figure 23; H₂T1). This is also supported by the noted findings of other organisms in the soil that do not directly use H₂ for energy (Dong and Layzell, 2001). It has been shown that the reducing power for CO₂ fixation is provided by the oxidation of H₂ in the soil; when H₂ is oxidized in the soil 40% of the electrons produced are used for CO₂ fixation (Dong and Layzell, 2001). It would be expected that with higher H₂ oxidation in the soil there would be higher CO₂ fixation, which is the case in the initial phase of treatment, while the H₂ uptake rate is increasing. Over time the action of other organisms in the soil may outweigh the CO₂ fixation causing a net production of CO₂.

4.2 Soybean Trials and Rhizosphere Soil Samples

The soybean trials were successful in providing the desired soil samples. Nodules that formed on roots tested positive for the desired Hup status (See Figures 16-18) and

it was possible to collect soil from the rhizosphere of these nodules. A few problems did arise during the greenhouse trials. Insect pests were a constant problem during growth trials which may have diminished growth through defoliation (Todd and Morgan, 1972; Thomas *et al.*, 1974). Several treatment methods were administered in order to control pests but these were unsuccessful. Temperature was also difficult to control in the greenhouse; periods of high temperature made it difficult to maintain soil moisture. High temperature and drought stress have been shown to reduce growth in various types of plants and water stress has been shown to negatively affect nitrogenase activity in soybeans (Savin and Nicolas, 1996; Durand *et al.*, 1986). The method of growing plants in pots is also well known to restrict plant growth in many types of plants (Robbins and Pharr, 1988; Ray and Sinclair, 1998). In future studies of this nature it may be beneficial to include trials from the field in order to see the effect of improved plant growth and nodule activity on gene copy numbers and gene expression of soil bacteria.

4.3 Nucleotide Extraction Yields

4.3.1 DNA Extraction

A range of DNA yields were obtained from differently treated soils. Samples treated with mid to long term H₂ had significantly more DNA per g soil than soils treated with air. This is expected as it has been shown that treatment with H₂ gas can lead to an increase in microbial biomass over time, which intuitively would lead to an increase in DNA per g soil (La Favre and Focht, 1983). It is important to note that an increase in DNA per g soil does not necessarily mean there will be an increase in any given gene (in

this case *cbbL*); previous studies found that the bacterial biomass increase as a result of H₂ treatment occur primarily within certain groups but not all groups (Stein *et al.*, 2005).

4.3.2 RNA Extraction

The yield of RNA extracted from different soil types did not vary as much as the yield of DNA had. The only soil with any significant difference was JH47 rhizosphere soil which was significantly higher than air treated soil. As previously mentioned, an increase in DNA per g soil does not necessarily mean there will be an increase in a specific gene; likewise, an increase in total RNA does not equate to an increase in a specific gene.

4.4 *cbbL* Gene Copy Numbers

Gene copy numbers varied greatly between treatments and between individual measurements for same treatments. Differences in gene copies between treatments were expected due to the differing CO₂ exchange rates between samples at the time of collection.

For primer set *cbbLR1F/cbbLR1intR* long term H₂ treatment (H₂T1) and midterm H₂ treatment (H₂T2) had the highest abundance of gene copies per ng DNA, but there was no significant difference between the two. This was expected since these treatments showed much higher potential for CO₂ fixation activity than air treated soils due to their higher H₂ uptake activity which is directly linked to CO₂ fixation in soil (Dong and Layzell, 2001). This increase in *cbbL* copies in mid and long term H₂ treatments was

multiplied when calculating copies per g soils since both treatments had much higher DNA yields than short term H₂ or air treated samples. These differences illustrate two important points. First, it was hypothesized that there would be an increase in *cbbL* gene copies per g soil in H₂ treated soils compared to air treated soils due to greater CO₂ fixation activity in these soils. It is important to note that although long term H₂ treatment (H₂T1) displayed net CO₂ production at the time of sample collection, there is still high potential for CO₂ fixation in the soil due to the *cbbL* activity present. CO₂ exchange measurements show the net CO₂ exchange of the soil; at the time of collection a high CO₂ production (respiration/decomposition) is outweighing the CO₂ fixation taking place. Second, since there is an increase in *cbbL* copies per ng DNA (see Figure 23), it is evident that the treatment with H₂ is not only increasing the number of bacteria in the soil harbouring the *cbbL* gene, but it is also increasing the overall ratio of CO₂ fixing bacteria in the soil compared to those that do not have the *cbbL* gene. If the ratio of bacteria containing the *cbbL* gene to those who do not have it were to remain the same, it would be expected that there would be no change in the number of copies per ng DNA when comparing H₂ and air treated soil. Again, this is supported by the fact that H₂ treatment is known to increase the populations of certain bacterial groups, for instance the β-proteobacteria group, which is known to harbour the red-like *cbbL* gene (Stein *et al.*, 2005; Watson and Tabita, 1997). Although there was no significant increase in *cbbL* copies in short term H₂ treatment compared to air treatments, there was a trend in the data showing higher copies in short term H₂ treatment (H₂T3) compared to AT

even though there was not a significant difference. This may be indicative of the bacterial community structural changes that are occurring but the effects of these changes are not yet measurable.

For rhizosphere samples it was found that soil adjacent to the roots of the non-nodulated soybean plants (Root) had more copies per ng DNA of the *cbbL* gene than the soils adjacent to of both Hup⁺ (JH) and Hup⁻ (JH47) nodules. This was not expected; Hup⁻ (JH47) nodules were expected to have higher copies of *cbbL* due to the release of H₂ from the nodules, which was expected to promote higher CO₂ fixation activity. The uptake hydrogenase enzyme in Hup⁺ nodules are not necessarily 100% efficient, so there is some H₂ released from the nodules (La Favre and Focht, 1983). It is possible that there is enough H₂ released to induce CO₂ fixation. However, it is also evident that interaction with roots in the soil leads to an increase in the abundance of *cbbL* genes but there appears to be little expression in this area (see Figure 23). It is possible that a healthier plant with better growth and nodulation would have provided different results; as previously mentioned, there were problems with the growth of soybean trials in the greenhouse. There is no significant difference in the abundance of *cbbL* genes per g soil for the rhizosphere samples. Soil adjacent to both Hup⁺ and Hup⁻ nodules had higher DNA yields per g soil than soil adjacent to roots, so the three treatments measured closer copy numbers per g soil.

Primer set cbbLG1F/cbbLG2R1 provided similar results for gas treated soil samples. However, the copy numbers detected in midterm H₂ treatment (H₂T2) were

much higher. Both primer sets provided different outcomes for each treatment (see Figures 23 and 24). This is likely due to the fact that different species of bacteria are being measured by the different primer sets. Primer set cbbLR1F/cbbLR1intR was designed for the detection of red-like *cbbL* genes (Selesi, *et al.*, 2007). The primer set cbbLG1F/cbbLG2R1 was designed for the detection of green-like *cbbL* genes (Selesi *et al.*, 2005). A universal primer for the general detection of all *cbbL* genes would be difficult if not impossible to design as the sequence similarities of *cbbL* genes can be as low as 22% (Selesi *et al.*, 2005). There was no significant difference in soils adjacent to Hup⁺ and Hup⁻ nodules and roots.

The copy numbers measured for the soil samples detected in this study were similar to those found in other studies quantifying RubisCO copy numbers (Selesi *et al.*, 2007; Videmsek *et al.*, 2009). Selesi *et al.* measured red-like *cbbL* in agricultural soils (unfertilized, manure fertilized and mineral fertilized) and found that the red-like bacterial RubisCO copies per g soil ranged from an average of 6.8×10^6 to 3.4×10^7 ; this is slightly higher than the average found for air treated soil (1.08×10^6) and slightly lower than the average copies per g soils for H₂ treated samples (4.18×10^7 to 5.53×10^7). Videmsek *et al.* measured red-like *cbbL* copies in grassland soils near natural CO₂ springs and measured averages ranging from 2.2×10^6 to 8.8×10^6 copies per g soil; this again was slightly higher than the average found for air treated soil and lower than the average for H₂ treated soil. Both of these studies used Taqman real time PCR chemistry, utilizing the same red-like primer set (cbbLR1F/cbbLR1intR) used in this study with a fluorescent

probe. It is possible that slightly higher copy numbers are being observed in this study due to the removal of the probe for SYBR Green PCR; the probe was designed using specific bacterial species, so its removal may allow for wider coverage of the red-like *cbbL* primers (Selesi *et al.*, 2007).

As was mentioned in previous studies, the quantity of gene copies does not allow for the extrapolation of the quantity of gene carrying cells; some bacteria can contain a copy of the RubisCO large subunit gene in both the chromosomal DNA and plasmid DNA providing two copies in one cell (Hugendieek and Meyer, 1991; Husemann *et al.*, 1988; and Selesi *et al.*, 2007). Selesi *et al.*, also noted that the quantity of RubisCO genes is comparable to other important genes in nutrient turnover in soils including copper nitrate reductase (*nirK*), subtilisin protease (*sub*) and methane monooxygenase (*pmoA*) (Bach *et al.*, 2002; Kolb *et al.*, 2003; Henry *et al.*, 2004; and Selesi *et al.*, 2007). The increase in *cbbL* genes induced by H₂ exposure illustrates the increased importance of RubisCO and CO₂ fixation within the bacterial community.

4.5 *cbbL* Gene Expression

Gene expression data varied greatly within treatments and between treatments. Expression levels were measured using RNA. RNA is a short-lived molecule which is highly susceptible to environmental conditions (Brenner *et al.*, 1961; Deutscher, 2006). Steps were taken in order to avoid contamination and prevent the degradation of mRNA. *cbbL* expression results did not behave as expected for the treatments tested. Long term H₂ treatment (H₂T1) had significantly more *cbbL* copies per ng RNA than air

treated samples, as expected. Midterm H₂ treatment (H₂T2) had the lowest expression per ng cDNA of all treatments measured, including air treatments, despite having the highest net CO₂ fixation. Long term H₂ treatment also had significantly higher red-like *cbbL* expression than midterm H₂ treatment despite having a net CO₂ production at the time of sample collection. It is possible that this is due to a delay between the expression of the gene and the resulting enzyme activity. This would explain treatments air treatments (AT) and short term H₂ treatment (H₂T3) had higher expression levels per ng cDNA than H₂T2. Treatment H₂T3 was just beginning to show an increase in H₂ uptake and CO₂ fixation. It is possible that the higher *cbbL* expression in H₂T3 reflects an impending increase in CO₂ fixation; a delay between mRNA expression and enzyme activity was noted in diatoms and pelagophytes, but this delay was much shorter (Wawrick *et al.*, 2002). Treatment H₂T2 was collected at the peak of H₂ uptake and CO₂ fixation. The lower *cbbL* expression in H₂T2 may reflect an impending decrease in net CO₂ fixation as was seen in long term H₂ treatment (H₂T 1) (see Figure 5). Treatment H₂T1 was collected during fluctuations in both H₂ uptake and CO₂ fixation so the high *cbbL* expression may reflect that the samples were collected just before an increase in CO₂ fixation. The expression measured per g soil should more accurately reflect the overall community. All H₂ treated samples have a higher expression level per g soil than air treated samples. This was expected as the H₂ treated samples tended to have slightly higher RNA concentrations than air treated samples. Also, both long term H₂ treatment (H₂T1) and short term H₂ treatment (H₂T3) had a higher expression level per g soil than

midterm H₂ treatment (H₂T2) despite having a lower net CO₂ fixation; this supports the idea that there is a delay between the change in expression of the gene and the resulting change in enzyme activity.

For the rhizosphere samples, soil adjacent to Hup⁻ nodules (JH47) had a significantly higher expression per ng RNA than soil adjacent to Hup⁺ nodules (JH). This was as expected since JH47 nodules do release more H₂ than JH nodules. However, there was not a significant difference between the soil of either nodulated plant and the soil surrounding non-inoculated roots. It is evident that there is some interaction with the plant root that is causing some CO₂ expression activity (see Figure 23). There was no significant difference between rhizosphere samples *cbbL* expression per g soil. There was however, a trend in the data showing soil adjacent to Hup⁻ nodules (JH47) having the highest expression, followed by soil adjacent to Hup⁺ nodules (JH), followed by soil adjacent to roots (Root). Soil adjacent to roots had the lowest expression, despite having the highest copy numbers. This suggests that H₂ may be playing a role in the expression of *cbbL* genes present in the soil. Again, more ideal growth conditions for the soybean plants may have yielded different results.

Similar to copy number data, primer set *cbbLG1F/cbbLG2R1* showed higher expression for midterm H₂ treatment (H₂T2) than *cbbLR1F/cbbLR1intR* while long term H₂ treatment (H₂T1) showed lower expression. This suggests that at different stages of exposure there are bacterial community changes occurring, so that the ratios to the different species of bacteria are changing. This may explain why the two primer sets,

designed to target different species of bacteria, are showing different levels of copies and expression at given times during treatment. This again, relates to the changing bacterial community structure that results from H₂ treatment (Stein *et al.*, 2005). This can also be seen in the differing species of bacteria harbouring the red-like *cbbL* gene between air and H₂ treated soils (see Table 18). So it is possible that low expression levels of red-like *cbbL* in midterm H₂ treatment (H₂T2) is due to changing community structure during treatment; the fact that midterm H₂ treatment had the highest expression of green-like *cbbL* supports this idea (see Figure 23 and 24).

This study also looked at the net CO₂ exchange of the H₂ treated soils and not the absolute CO₂ fixation. The net CO₂ exchange is the most common measure of experimental photosynthesis (Millan-Alamaraz *et al.*, 2009). CO₂ exchange measures all CO₂ fixation and production and reflects the overall effect of the unit measured. However, since it is measuring all production and fixation at the time of collection, the measurement may not accurately reflect enzyme activity at the time of collection. As previously mentioned, later stages of H₂ treatment may have higher levels of CO₂ fixation.

Finally, the real time PCR primers used in this study were designed using select species of bacteria (see section 2.8)(Selesi *et al.*, 2005). These primers will not cover all species of bacteria containing red-like and green-like *cbbL*, so the data may not reflect the entire RubisCO CO₂ fixing community.

Little research has been done in the quantification of the expression of bacterial RubisCO, particularly in soil environments. As previously mentioned, a study quantifying RubisCO large subunit mRNA in diatoms and pelagophytes of natural phytoplankton communities found that there was a delay between the increases in measured mRNA quantity and the detected increase in CO₂ fixation (Wawrik *et al.*, 2002). As noted, a similar phenomenon may be occurring here, where there may be a delay between the increase or decrease in *cbbL* expression and the resulting change in CO₂ fixation. However, the delay in the study mentioned lasted only hours.

4.6 Inhibition

It was necessary to perform inhibition controls for the unknown samples. Inhibition was detected by adding 10⁵ or 10⁴ copies of the control standard to the unknown sample and comparing the detected quantity of the spiked unknown to the expected quantity for the spiked unknown (eg. 10⁴ + detected unknown). Under the assumption that the ratio of inhibition would remain constant, the actual quantity was recalculated using this ratio. For samples which the inhibition control was not detected, the average ratio of inhibition for like samples was used for calculation.

4.7 Why *cbbL*?

The *cbbL* gene codes for the large subunit of the RubisCO enzyme. As mentioned, RubisCO is the rate limiting enzyme of the Calvin-Benson-Bassham cycle and is made up of 16 subunits: 8 large subunits coded by *cbbL* and 8 small subunits coded by *cbbS* (Tabita, 1988). RubisCO is also the rate limiting enzyme in the Calvin cycle (Ellis, 1979).

Measuring *cbbL* copies and expression should provide a picture of the relationship between the activity of the gene and part of the CO₂ fixation within the soil.

4.8 Taqman vs. SYBR Green PCR Chemistries

Real time PCR relies on the detection of fluorescent labels in order to quantify gene copies and gene expression. Taqman PCR relies on a fluorescently labelled probe that anneals between the forward and reverse primers while SYBR Green binds to the minor grooves of the PCR product. Both chemistries had advantages and disadvantages. Taqman PCR provides higher specificity due to the added probe. SYBR Green provides less specificity allowing for wider coverage; however since SYBR Green binding is unspecific it is necessary to ensure a pure PCR product is being amplified.

Both chemistries were considered for this experiment. Taqman was unsuccessful using a primer and probe set developed by Selesi *et al.*, 2007 and in the end SYBR Green was chosen for this experiment. Since the *cbbL* gene varies greatly between species the added specificity of Taqman may not be required (Selesi *et al.*, 2005). SYBR Green was advantageous to use because it is easily incorporated into established PCR protocols and is relatively inexpensive to use and may have allowed for wider coverage of the *cbbL* sequence being detected (Bustin and Nolan, 2009).

4.9 *cbbL* Sequencing Data

Sequencing data provided good insight into the species of bacteria being detected and quantified in this study. Primer sets *cbbLR1F/cbbLR1intR* and *cbbLG1F/cbbLG2R1* were designed in order to detect red-like and green-like *cbbL*

respectively. However, there was some overlap between the sets (see Tables 16 and 17). This is likely due to the fact that the separation of red-like and green-like *cbbL* is based on phylogenetic relatedness and the two are not distinct genes so some overlap may be expected (Watson and Tabita, 1996). It has also been found that it is possible for a single species of bacteria to harbour both the red-like and green-like copies of the *cbbL* gene (Uchino and Yokota, 2003). Although some overlap did occur between the two sets, the majority of the nearest matching species detected with each set were unique. This helps to explain why each primer set yielded differing results for copy numbers and expression for each treatment.

There were some differences in the abundances and species of bacteria between H₂ and air treated samples for red-like *cbbL*, but the major species remained the same and remained at high abundance. This suggests that even though there are changes occurring in the soil there may small changes in the main CO₂ fixing bacteria in a given group.

5 General Conclusions

Previous studies have shown the relationship between H₂ exposure and the changes in CO₂ gas exchange, while others have investigated the quantification of RubisCO *cbbL* genes in soils and other media. The goal of this study was to combine the previously mentioned ideas to provide a better understanding of the molecular changes that are occurring in H₂ treated and rhizosphere soils, in order to better understand the changes in CO₂ fixation that occur.

It is evident from this study that there is a definite increase in bacterial *cbbL* copy numbers and their expression in soil as a result of H₂ treatment, and that there may be community structure changes occurring throughout treatment. Soil adjacent to roots had higher *cbbL* copies than soil adjacent to both Hup⁺ and Hup⁻ nodules; this suggests that other factors are influencing the growth of bacteria harbouring *cbbL* genes in the rhizosphere but H₂ still plays a role in their expression (see Figure 23). There was not a significant difference in expression among rhizosphere samples measured per g soil but there was a trend with red-like *cbbL* showing higher expression in soil adjacent to Hup⁻ nodules, followed by soil adjacent to Hup⁺ nodules, followed by soil adjacent to roots; it is possible that more productive and healthy legume plants may have yielded more significant results. Future studies may investigate field trials for legume plants in order to avoid the effects of heat and water stress, and pot size restrictions that occurred in the greenhouse.

There is little literature that looks at the expression of bacterial RubisCO in soils. It was noted that there may be a delay between the change in expression of the RubisCO gene and a change in the activity of the enzyme, and that this was noted in another RubisCO study as well, although this does not adequately explain differences in expression levels for the H₂ treated soils, due to the length of the delay (Wawrick *et al.*, 2002). A better explanation is that community structure changes that are occurring throughout treatment lead to differing quantification of certain groups at different times (Stein *et al.*, 2005).

Future studies may investigate the effect of changes in expression and the resulting enzyme activity by using more frequent sampling during the treatment process, particularly during the exponential increase phase of the H₂ uptake curve during which the CO₂ fixation rate is increasing (Dong and Layzell, 2001). This would provide a better understanding of how increases in expression are directly affecting the measured CO₂ exchange.

Now that gene expression and gene copy number changes have been measured in the lab and greenhouse conditions, the next step for this study would be to investigate field trials using legume crops to more accurately measure for both copy numbers and gene expression as they occur in nature and agriculture.

Finally, bacteria species containing *cbbL* genes can be investigated to see if the inoculation of soil with these bacteria has any effect on the carbon sequestration

capability of the soil. These bacteria can be screened for other beneficial effects such as the plant growth promotion effect which is seen in leguminous soils.

It is evident based on this and other studies that bacterial RubisCO is an important enzyme in the soil bacterial community. It may be worth investigating whether any manipulation to the bacterial communities in legume crops can promote the sequestration of CO₂ into the soil.

6 References

- Atomi, H. 2002. Microbial enzymes involved with carbon dioxide fixation. *Journal of Bioscience and Bioengineering*. 94(6): 497-505
- Bach, H.J., Tomanova, J., Schloter, M. and Munch, J.C. 2002. Enumeration of total bacteria and bacteria with genes for proteolytic activity in pure cultures and in environmental samples by quantitative PCR mediated amplification. *Journal of Microbiological Methods*. 49: 235–245
- Bartlett, JMS & Stirling, D (2003). A short history of the polymerase chain reaction. *Methods in Molecular Biology*. 226: 3-6.
- Bolton, EF, Dirks, VA and Aylesworth, JW (1976). Some effects of alfalfa, fertilizer and lime on corn yield in rotation on clay soil during a range of seasonal moisture conditions. *Canadian Journal of Soil Science*. 56: 21-25
- Brenner, S, Jacob, F and Meselson, M (1961). An unstable intermediate carrying information from genes to ribosomes for protein synthesis. *Nature*. 190: 576-581
- Bustin, S.A. and Nolan, T. (2009). *Chemistries*. In: *A-Z of Quantitative PCR*. International University Line. La Jolla, CA. 882 pp.
- Chen, H, Athar, R, Zheung, Guili and Williams, HN (2011). Prey bacteria shape the community structure of their predators. *The ISME Journal*. 5: 1314-1322
- Coker, GT and Schubert, KR (1981). Carbon dioxide fixation in soybean roots and nodules. *Plant Physiology*. 67: 691-696
- Conrad, R and Seiler, W (1980). Contribution of hydrogen production by biological nitrogen fixation to the global hydrogen budget. *Journal of Geophysical Research*. 85: 5493-5498
- Deutscher, M (2006). Degradation of RNA in bacteria: comparison of mRNA and stable RNA. *Nucleic Acids Research*. 34(2): 659-666
- Dong, Z and Layzell, DB (2002). Why do legumes nodules evolve hydrogen gas? In: *The 13th International Congress on Nitrogen Fixation, 2-7 July 2001, Hamilton*
- Dong, Z and Layzell, DB (2001). H₂ oxidation, O₂ uptake and CO₂ fixation in hydrogen treated soils. *Plant and Soil*. 229: 1-12

- Doran, JW and Ziess, MR (2000). Soil health and sustainability: managing the biotic component of soil quality. *Applied Soil Ecology*. 15(1): 3-11
- Durand, JL, Sheehy, JE and Minchin, FR (1986). Nitrogenase activity, photosynthesis and nodule water potential in soyabean plants experiencing water deprivation. *Journal of Experimental Botany*. 38(2): 311-321
- Eikmanns, BJ, Follettie, MT, Griot, MU and Sinsky, AJ (1989). The phosphoenolpyruvate carboxylase gene of *Corynebacterium glutamicum* : Molecular cloning, nucleotide sequence, and expression. *Molecular and General Genetics*. 218:330-339
- Emmond, G.S. and Ledingham, R.J. (1972). Effects of crop rotation on soilborne pathogens of potato. *Canadian Journal of Plant Science*. 52: 605–611.
- Ellis, RJ (1979). The most abundant protein in the world. *Trends in Biochemical Sciences*. 4: 241-244
- Filion, M., St. Arnaud, M. and Jabaji-Hare, S.H. (2003). Direct quantification of fungal DNA from soil substrate using real-time PCR. *Journal of Microbiological Methods*. 53(1): 67-76
- Frieden, E. (1972). The chemical elements of life. *Scientific American*. 227(1): 52-60
- Fyson, A and Oaks, A (1990). Growth promotion in maize by legume soils. *Plant and Soil*. 122: 259-266
- Gan, YT, Liang, C, Hamel, C, Cutforth, H, Wang, H (2011a). Strategies for reducing the carbon footprint of field crops for semiarid areas – A Review. *Agronomy for Sustainable Development*. DOI:10.1007/s13593-011-0011-7.
- Gan, YT, Liang, C, Wang, XY and McConkey, BG (2011b). Lowering carbon footprint of durum wheat through diversifying cropping systems. *Field Crops Research*. 122(3): 199-206
- Garret, R and Grisham, CM (2005). In. *Biochemistry*, Third Ed. Thomson Brooks and Cole.
- Goreau, TJ, Kaplan, WA, Wofsy, SC, McElroy, MB, Valois, FW and Watson, SW (1980). Production of NO_2^- and N_2O by nitrifying bacteria at reduced concentrations of oxygen. *Applied Environmental Microbiology*. 40(3): 5226-532
- Griffiths, RI, Whiteley, AS, O'Donnell, AG and Bailey, MJ (2000). Rapid method for the coextraction of DNA and RNA from Natural Environments for Analysis of Ribosomal DNA

and rRNA-based microbial Community Composition. *Applied and Environmental Microbiology*. 66(12) 5488-5491

Guo, LB and Gifford, RM (2002). Soil carbon stocks and land use change: a meta analysis. *Global Change Biology*. 8: 345-360

Hanson, T.E. and Tabita, F.R. (2003). Insights into the stress response and sulfur metabolism revealed by proteome analysis of a *Chlorobium tepidum* mutant lacking the Rubisco-like protein. *Photosynthesis Research*. 78: 231-248

Heid, CA, Stevens, J, Livak, KJ and Williams, PM. (1996). Real time quantitative PCR. *Genome Research*. 6: 986-994

Henry, S, Baudoin, E, Lopez-Gutierrez, JC, Martin-Laurent, F, Brauman, A and Philippot, L (2004). Quantification of denitrifying bacteria in soils by *nirK* gene targeted real-time PCR. *Journal of Microbiological methods*. 59: 327-335

Hermansson, A. and Lindgren, P. (2001). Quantification of ammonia-oxidizing bacteria in arable soil by real-time PCR. *Applied and Environmental Microbiology*. 67(2): 972-976

Houghton RA & Skole DL (1990) Carbon. In: Turner BL, Clark WC, Kates RW, Richards JF, Mathews JT & Meyer WB (Eds) *The Earth as Transformed by Human Action* (pp 393–408). Cambridge University Press, Cambridge, U.K.

Hugendieck, I. and Meyer, O. (1991). Genes encoding ribulosebisphosphatecarboxylase and phosphoribulokinase are duplicated in *Pseudomonas carboxydovorans* and conserved in carboxydrotrophic bacteria. *Archives of Microbiology*. 157(1): 92–96.

Husemann, M., Klintworth, R., Büttcher, V., Salnikow, J., Weissenborn, C. and Bowien, B. (1988). Chromosomally and plasmid-encoded gene clusters for CO₂ fixation (*cfx*) genes in *Alcaligenes eutrophus*. *Molecular and General Genetics*. 214(1): 112–120.

Innis, MA & Gelfand, DH (1994). Optimization of PCR. p. 3-12. In Innis, MA, Gelfand, DH, Sninsky, JJ and White, TJ (ed.), *PCR protocols, a guide to methods and applications*. Academic Press, San Diego, Calif.

Kaiser, EA, Kohrs, K, Kucke, M, Schnug, E, Heinemeyer, E and Much JC (1998). Nitrous oxide released from arable soil: Importance of N-fertilization, crops and temporal variation. *Soil Biology and Biochemistry*. 30(12): 1553-1563

- Kelner, DJ, Vessey, JK and Entz, MH (1997). The nitrogen dynamics of 1-, 2- and 3-year stands of alfalfa in a cropping system. *Agriculture, Ecosystems and Environment*. 64: 1-10
- Kolb, S., Knief, C., Stubner, S. and Conrad, R. (2003). Quantitative detection of methanotrophs in soil by novel *pmoA*-targeted real-time PCR assays. *Applied Environmental Microbiology* 69(5): 2423–2429.
- Kusian B and Bowien B (1997). Organization and regulation of *cbb* CO₂ assimilation genes in autotrophic bacteria. *FEMS Microbiology Reviews*. 21: 135-155
- La Favre, JS and Focht, DD (1983). Conservation in soil of H₂ liberated from N₂ fixation by Hup⁻ nodules. *Applied and Environmental Microbiology*. 46(2): 304-311
- Lal, R and Kimble, JM (1997). Conservation tillage for carbon sequestration. *Nutrient Cycling in Agroecosystems*. 49: 243-253
- Lambert, GR, Hanus, FJ, Russel, SA and Evans, HJ (1985). Determination of the hydrogenase status of individual legume nodules by a methylene blue reduction assay. *Applied and Environmental Microbiology*. 50(2): 537-539
- McLearn, N and Dong, Z (2002). Microbial nature of the hydrogen-oxidizing agent in hydrogen-treated soil. *Biology and Fertility of Soils*. 35: 465-469
- Morrison, T.B., Weis, J.J. and Wittwer, C.T. (1998). Quantification of low-copy transcripts by continuous SYBR[®] Green I monitoring during amplification. *BioTechniques*. 24(6): 954-962
- Nanba, K, King, GM and Dunfield, K (2004). Analysis of facultative lithotrophic distribution and diversity on volcanic deposits by use of the large subunit of ribulose 1,5-bisphosphate carboxylase/oxygenase. *American Society for Microbiology*. 70(4): 2245-2253
- Pfaffl, M.W. (2001). A new mathematical model for relative quantification in real-time RT-PCR. *Nucleic Acid Research*. 29(9): 2002-2007
- Pfaffl, M.W. and Hageleit, M. (2001). Validities of mRNA quantification using recombinant RNA and recombinant DNA external calibration curves in real-time RT-PCR. *Biotechnology Letters*. 23(4): 275-282

- Paustian, K, Andrén, O, Janzen, H, Lal, R, Smith, P, Tian, G, Tiessen, H, van Noordwijk, M and Woomer, P (1997). Agricultural soil as a C sink to offset CO₂ emissions. *Soil Use and Management*. 13: 230–244
- Peters, R.D., Sturz, A.V. Carter, M.R. and Sanderson, J.B. (2003). Developing disease-suppressive soils through crop rotation and tillage management practices. *Soil and Tillage Research*. 72(2): 181-192
- Popelier, F, Liessens, J and Verstraete, W (1985). Soil H₂-uptake in relation to soil properties and rhizobial H₂-production. *Plant and Soil*. 85: 85-96
- Postgate, J. 1998. *Nitrogen Fixation*, 3rd ed. Cambridge UP, Cambridge, 112 pp.
- Riecosky, DC, Dugas, WA and Torbert, HA (1997). Tillage-induced carbon dioxide loss from different cropping systems. *Soil and Tillage Research*. 41: 105-118
- Ray, JD and Sinclair, TR (1998). The effect of pot size on growth and transpiration of maize and soybean during water deficit stress. *Journal of Experimental Botany*. 49(325): 1381-1386
- Robbins, NS and Pharr, DM (1988). Effect of restricted root growth on carbohydrate metabolism and whole plant growth of *cucumis sativus L.* *Plant Physiology*. 87: 409-413
- Rosswall, T. 1976. The internal nitrogen cycle between microorganisms, vegetation and soil. *Ecological Bulletins*. 22: 157-167
- Roush, RT, Hoy, CW, Ferro, DN and Tingey, WM. (1990). Insecticide resistance in the colorado potato beetle (*Coleoptera: Chrysomelidae*): Influence of crop rotation and insecticide use. *Journal of Economic Entomology*. 83(2): 315-319
- Ruiz-Argueso, T., Maier, R.J. and Evans, H.J. 1979. Hydrogen evolution from alfalfa and clover nodules and hydrogen uptake by free-living *Rhizobium meliloti*. *Applied Environmental Microbiology*. 37(3): 582-587
- Savin, R and Nicolas, ME (1996). Effects of short periods of drought and high temperature on grain growth and starch accumulation of two malting barley cultivars. *Australian Journal of Plant Physiology*. 23(2): 201-210
- Schloter, M, Dilly, O and Munch, JC (2003). Indicators for evaluating soil quality. *Agriculture, Ecosystems and Environment*. 98: 225-262

- Schubert, KR, Engelke, JA, Russel, SA and Evans, HJ (1977). Hydrogen reactions of nodulated leguminous plants. *Plant Physiology*. 60: 651-654
- Selesi, D, Pattis, I, Schmid, M, Kandeler, E and Hartman, A (2007). Quantification of bacterial RubisCO genes in soils by cbbL targeted real-time PCR. *Journal of Microbiological Methods*. 69: 497-503
- Selesi, D, Schmid, M and Hartmann, A (2005). Diversity of green-like and red-like ribulose-1,5-bisphosphate carboxylase/oxygenase large-subunit gene (cbbL) in differently managed agricultural soils. *Applied and Environmental Microbiology*. 71(1): 175-184
- Simpson, FB, Maier, RJ and Evans, HJ (1979). Hydrogen-stimulated CO₂ fixation and coordinate induction of hydrogenase and ribulosebisphosphate carboxylase in a H₂-uptake positive strain of *Rhizobium japonicum*. *Archives of Microbiology*. 123: 1-8
- Soderlund, R. and Svenson, B.H. 1976. The global nitrogen cycle. *Ecological Bulletins*. 22: 23-73
- Sprent, JI (1989). Which steps are essential for the formation of functional legume nodules? *New Phytologist*. 111: 129-153
- Stein, S, Selesi, D, Schilling, R, Pattis, I, Schmid M and Hartmann A (2005). Microbial activity and bacterial composition of H₂-treated soils with net CO₂ fixation. *Soil Biology and Biochemistry*. 37: 1938-1945
- Tabita, F.R. (1988) Molecular and cellular regulation of autotrophic carbon dioxide fixation in microorganisms. *Microbiological Reviews*. 52(2): 155-189
- Tabita, F.R. (1990) Microbial ribulose 1,5-bisphosphate carboxylase/oxygenase: A different perspective. *Photosynthesis Research*. 60: 1-28
- Tabita, F.R., Satagopan, S., Hanson, T.E., Kreel, N.E. and Scott, S.S. (2008). Distinct form I, II, III, and IV Rubisco proteins from the three kingdoms of life provide clues about Rubisco evolution and structure/function relationships. *Journal of Environmental Botany*. 59(7): 1515-1524
- Thomas, GD, Ignoffo, CM, Biever, KD and Smith, DB (1974). Influence of defoliation and depodding on yield of soybeans. *Journal of Economic Entomology*. 67(5): 683-685
- Todd, JW and Morgan, LW (1972). Effects of hand defoliation on yield and seed weight of soybeans. *Journal of Economic Entomology*. 65(2): 567-570.

- Uchino, Y. and Yokota A. 2003. "Green-like" and "Red-like" RubisCO cbbL Genes in *Rhodobacter azotoformans*. *Molecular Biology and Evolution*. 20(5) 821-830
- Uratsu, SL, Keyser, HH, Weber, DF and Lim, ST (1982). Hydrogen uptake (HUP) activity of *Rhizobium japonicum* from major U.S. soybean production areas. *Crop Science*. 22: 600-602
- Vandesompele, J., De Preter, K., Pattyn, F., Poppe, B., Van Roy, N., De Paepe, A. and Speleman, F. 2002. Accurate normalization of real-time quantitative RT-PCR data by geometric averaging of multiple internal control genes. *Genome Biology*. 3(7): 1-12
- Vaerman, J.L., Saussoy, P. and Ingargiola, I. 2006. Evaluation of real time PCR data. *Journal of Biological Regulators and Homeostatic Agents*. 18: 212-214
- Verge, XPC, De Kimpe, C and Dejardins, RL (1997). Agricultural production, greenhouse gas emissions and mitigation potential. *Agricultural and Forest Meteorology*. 142: 255-269
- Videmsek, U., Hagn, A., Suhadolc, M., Radl, V., Knicker, H., Schloter M. and Vodnik, D. 2009. Abundance and diversity of CO₂-fixing bacteria in grassland soils close to natural carbon dioxide springs. *Microbial Ecology*. 58(1): 1-9
- Wang, A.M., Doyle, M.V. and Mark, D.F. 1989. Quantitation of mRNA by the polymerase chain reaction. *Proceedings of the National Academy of Science*. 86: 9717-9721
- Watson, G.M.F. and Tabita, F.R. (1996). Microbial ribulose 1,5-bisphosphate carboxylase/oxygenase: a molecule for phylogenetic and enzymological investigation. *FEMS Microbiology Letters*. 146: 13-22
- Wawrick, B, Paul, JH and Tabita, FR (2002). Real-time PCR quantification of *rbcl* (Ribulose-1,5-bisphosphate Carboxylase/Oxygenase) mRNA in diatoms and pelagophytes. *Applied and Environmental Microbiology*. 68(8): 3771-3779